Coastal and Hydraulics Laboratory

ERDC/CHL TR-00-17

US Army Corps
of Engineers®
Engineer Research and
Development Center

Model Study of Prado Spillway, California

Hydraulic Model Investigation

Ronald R. Copeland and Bobby P. Fletcher

September 2000

ERDC/CHL TR-00-17
September 2000

Model Study of Prado Spillway, California

Hydraulic Model Investigation

By Ronald R. Copeland, Bobby P. Fletcher

Coastal and Hydraulics Laboratory
U.S. Army Engineer Research and Development Center
3909 Halls Ferry Road
Vicksburg, MS 39180-6199

Final report

Prepared for U.S. Army Corps of Engineers
Washington, DC 20314-1000

Engineer Research and Development Center Cataloging-In-Publication Data

Copeland, Ronald R.
Model study of Prado Spillway, California : hydraulic model investigation / by Ronald R. Copeland, Bobby P. Fletcher ; prepared for U.S. Army Corps of Engineers.
132 p. : ill. ; 28 cm. -- (ERDC/CHL ; TR-00-17)
Includes bibliographic references.
1. Spillways -- California -- Models. 2. Flood dams and reservoirs -- California. 3. Hydraulic models -- California. I. Fletcher, Bobby P. II. United States. Army. Corps of Engineers. III. Engineer Research and Development Center (U.S.) IV. Coastal and Hydraulics Laboratory (U.S.) V. Title. VI. Series: ERDC/CHL TR ; 00-17.
TA7 E8 no.ERDC/CHL TR-00-17

Contents

List of Figures

Preface

The model investigation of Prado Dam Spillway, reported herein, was conducted at the U.S. Army Engineer Research and Development Center (ERDC) at the request of the U.S. Army Engineer District, Los Angeles.

This investigation was conducted during the period August 1992 to February 2000 in the ERDC Coastal and Hydraulics Laboratory (CHL), under the direction of Mr. Frank A. Herrmann, Jr., Director of Hydraulics Laboratory, Dr. James R. Houston, former Director, CHL, Mr. Richard Sager, Assistant Chief of the Hydraulics Laboratory, Mr. Glenn A. Pickering, Chief of the Hydraulic Structures Division, Mr. John F. George, Acting Chief of the Hydraulic Structures Division, Dr. Phil G. Combs, Chief of the Rivers and Structures Division, Mr. Noel R. Oswalt, Chief of the Spillways and Channels Branch, and Dr. Yen-Hsi Chu, Chief of the River Sedimentation Engineering Branch. The project engineers for this study and authors of this report were Mr. Bobby P. Fletcher and Dr. Ronald R. Copeland. Dr. Stephen T. Maynord reviewed this document and made helpful comments. Messrs. Kevin Pigg and Douglas White and Mrs. Dinah McComas provided technical assistance.

During the course of the model study, engineers from the Los Angeles District, South Pacific Division (SPD), and Headquarters (HQUSACE) visited ERDC to observe operation of the model and to participate in discussions about design decisions that improved cost-effectiveness and hydraulic performance of the project.

Visitors included Mr. Sam Powell (HQUSCE); Messrs. Stuart H. Brehm III, Bill Csajko, Frank Krhoun, Jaime Merino, and Jim Tanouye (SPD); Messrs. Chris Bahner, George Beams, Algis Bluiudzius, Bob Conley, Dave Cozakos, Van Crisotomo, Girish Desai, Joe Evelyn, Bill Gallegos, Bob Hall, Terry King, Bob Koplin, Rick Leifield, John Onderdonk, Tom Sage, Joan Siao, Rick Torbik, Brian Tracy, and Rene Vermeeren, the Los Angeles District; and consultants Dr. Henry Falvey and Messrs. Paul Young and Bruce Philips.

Dr. Henry T. Falvey provided consulting services relative to development of the labyrinth weir design.

Mr. Brian Tracy and Mr. Chris Bahner served as the hydraulics project engineers in the Los Angeles District, providing valuable contributions and review during the course of the study.

At the time of publication of this report, Dr. James R. Houston was Director of ERDC, and COL James S. Weller, EN, was Commander.

Conversion Factors, Non-SI to SI Units of Measurement

Non-SI units of measurement used in this report can be converted to SI units as follows:

Multiply	By	To Obtain
Acre	4,046.9	Square meters
Acre-feet	1,233.5	Cubic meters
Cubit feet	0.028317	Cubic meters
Cubic yards	0.76456	Cubic meters
Feet	0.3048	Meter
Inches	2.54	Centimeters
Miles (U.S. statute)	1.6094	Kilometers
Square miles	2.5890	Square kilometers
Pounds	4.4482	Newtons

1 Introduction

Prototype

Prado Dam is located about 40 miles[1] southeast of Los Angeles on the Santa Ana River, about 30 river miles from the Pacific Ocean (Figure 1). The dam was completed in 1941 and was designed to control the Standard Project Flood without spillway flow. The spillway was designed for a Probable Maximum Flood (PMF) discharge of 178,000 cfs. Prado Dam controls runoff from a drainage area of 2,255 square miles. About 40 percent of this drainage area consists of mountainous terrain. The remaining 60 percent is flat alluvial plain or foothills which are either fully urbanized or have the potential for development. The elevation of the drainage area varies from 470[2] at the reservoir to 11,485 at San Gorgonio Peak in the San Bernardino Mountains.

The spillway consists of a concrete ogee crest, a spillway channel, a steep chute, and a flip bucket. The ogee structure is 13 ft high with a crest at el 543 and a width of 1,000 ft. The 1,147-ft-long spillway channel has a bottom slope of 0.014 and conveys flow from the spillway crest to the spillway chute. The width of the spillway channel is 1,000 ft at the axis of the ogee crest and narrows to 660 ft at the beginning of the chute. The chute is 190 ft long, dropping from el 522.4 to 462.5 with a bottom slope of 0.503. The flip bucket has a 37.3 ft-radius of curvature and a minimum elevation of 452.5. The end sill of the flip bucket is at el 462.0. The wall heights on the spillway channel and the chute are 13 ft.

The roller-compacted earth-filled dam has a crest length of 2,280 ft and a crest at el 566. The top of the dam is about 105 ft above the streambed. The dam forms a reservoir with an area of 6,695 acres. Prado Dam is a flood-control reservoir that stores water only during storm events and is used at a limited capacity for water conservation.

The reservoir had a design capacity of 217,000 acre-ft at el 543. Of this capacity, 205,000 acre-ft was allocated for flood control and 12,000 for sediment storage over a 50-yr period. This corresponds to a sediment-filling rate of

[1] A table of factors for converting non-SI units of measurement to SI (metric) units is presented on page viii.

[2] All elevations (el) cited herein are in feet referred to the National Geodetic Vertical Datum (NGVD).

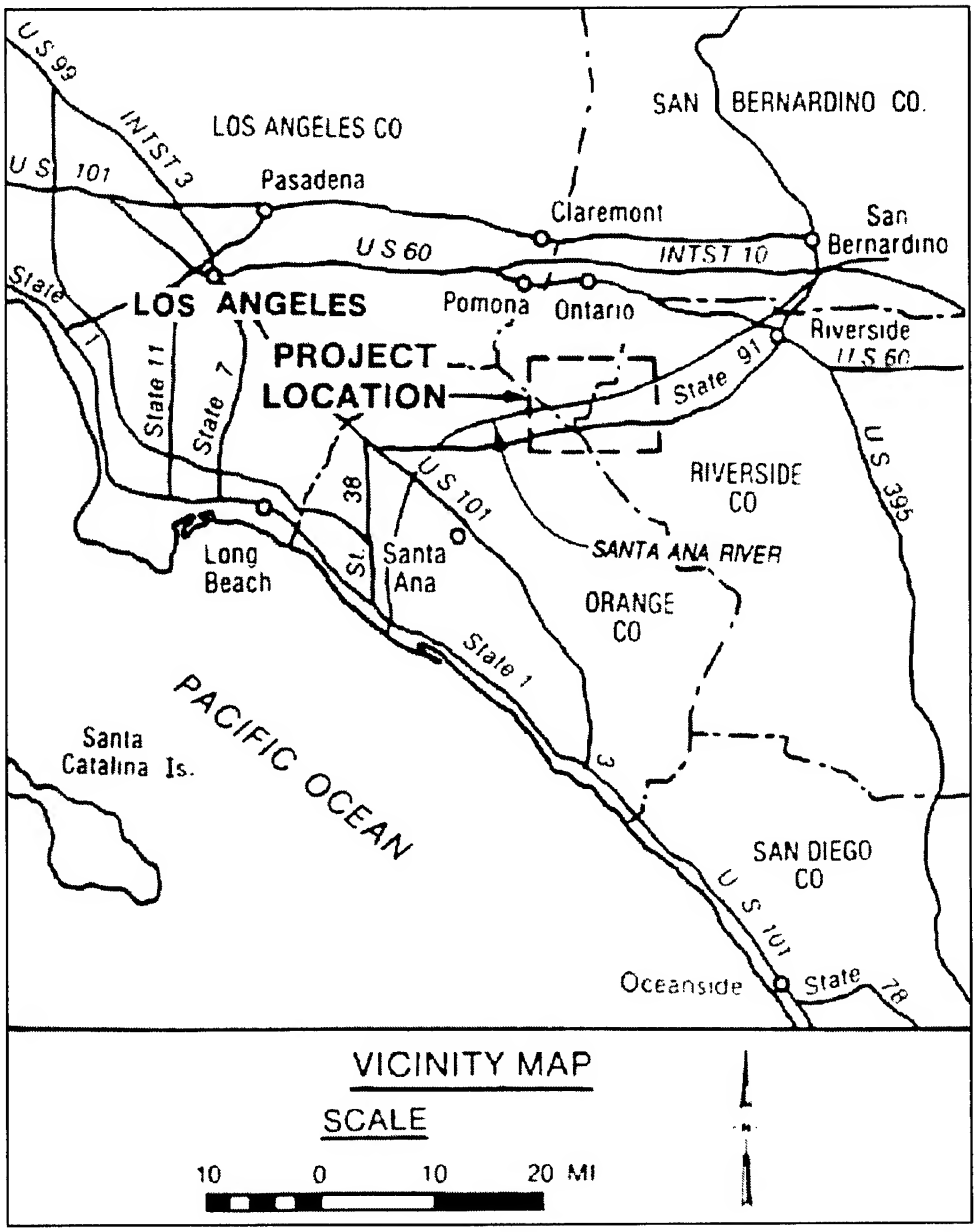

Figure 1. Vicinity map

240 acre-ft per year. In 1941, when the dam was completed, a survey revealed that the capacity was actually 222,840 acre-ft. A 1979 survey indicated that 26,600 acre-ft of sediment had accumulated in the reservoir. This corresponds to a sediment deposition rate of 700 acre-ft per year which is about three times the expected rate.

Project Design Flood

Urbanization in Prado Dam's drainage area and an increase in the PMF design rainfall have resulted in a significant increase in design discharges for the

flood control project. The reservoir currently has capacity to control only a 70-year flood event, and the spillway, which was designed for a discharge of 178,000 cfs, is undersized. Therefore, structural modifications are needed to increase both the dam's storage capacity and the spillway discharge capacity.

To increase the reservoir's storage capacity for the Reservoir Project Flood, it was proposed to raise the spillway crest 20 feet from el 543 to el 563 and to increase the height of the dam from el 566 to el 594.4.

In 1992, at the beginning of this model investigation, the National Weather Service (NWS) had not completed their study to determine the probable maximum precipitation for the Santa Ana River watershed. Therefore the spillway design discharge was unknown, but preliminary estimates suggested that it would be about 847,000 cfs. To increase the spillway capacity without widening the existing spillway, a labyrinth weir was proposed. The labyrinth weir would be constructed just upstream from the existing ogee spillway.

In 1994, the NWS completed their study and it was determined that the spillway design discharge would be only 481,000 cfs. This was still considerably higher than the original discharge of 178,000 cfs, but the need for a labyrinth weir was obviated. Instead, an ogee crest was proposed.

Purpose of the Model Study

The design criteria for the Prado Dam spillway calls for controlling the reservoir pool elevation at 589.9 for the Probable Maximum Flood (PMF). This related to a discharge of 847,000 cfs at the beginning of the study and 481,000 cfs after the NWS completed their PMF rainfall study. Initially, a labyrinth spillway was proposed to increase the capacity of the existing Prado Dam spillway without changing its width. A labyrinth spillway is a spillway with a "zigzag"-shaped wall for a weir crest. When the depth of water flowing over these crests is low, this type of spillway can discharge much more water than a conventional spillway. Since this type of spillway is relatively new and the hydraulics are complex, it was determined that the design of the spillway should not be based on theory alone nor on relationships developed from dissimilar model studies. Therefore a physical model was proposed.

The 1:50-scale model was required because several shortcomings had been identified with an existing 1:80-scale model (George 1989). These were primarily related to scale effects associated with determining weir crest coefficients over the labyrinth weir, and with determining wave effects caused by offset vertical walls in the spillway channel and chute. The restricted forebay length in the 1:80 scale model did not simulate enough of the reservoir pool to adequately account for losses between the pool and the labyrinth spillway crest and also made it difficult to accurately reproduce prototype approach flow conditions.

The 1:50-scale hydraulic model was used to evaluate hydraulic performance of proposed modifications to the Prado Spillway for a range of discharges.

Specifically the model was used to develop or determine the following:

a. Spillway discharge rating curve.

b. Water-surface profiles in the spillway channel and chute.

c. The magnitude and direction of flow velocities in the spillway approach, channel and chute; at the toe of the downstream dam embankment; and in the exit channel.

d. The magnitude of waves and surges at the toe of the dam embankment.

e. Qualitative assessment of the scour and deposition pattern downstream from the flip bucket.

f. Characteristics of nappe aeration.

The model permitted evaluation and development of modifications, if needed, to critical design features such as:

a. Spillway approach channel.

b. Spillway abutments.

c. Weir crest.

d. Spillway chute.

e. Scour protection downstream from the flip bucket.

Hydraulic Theory for Labyrinth Weirs

A labyrinth spillway is characterized by a series of V-shaped weirs that provide a greater crest length compared to a conventional spillway crest occupying the same lateral space. Each of the V-shapes is termed a cycle. The geometry of a labyrinth weir is primarily defined by the cycle width, W, the cycle crest length, L, the apex half-length, A, the sidewall angle, α, the weir height, P, and the number of cycles, n. Discharge over labyrinth weirs has been shown to be primarily a function of the length magnification ratio, L / W, and the total head ratio H / P. The effect of the sidewall angle, α, is implicitly included in the length magnification ratio. Tailwater effects can be important if the weir crest is submerged. The labyrinth weir designed for Prado Dam would not be submerged. Defining parameters for a typical labyrinth weir are shown in Figure 2.

The labyrinth spillway is particularly well suited for rehabilitation of existing spillways, such as Prado spillway, and for providing a large-capacity spillway in a site with restricted width. This is caused by the significant increase in crest length for a given width. This characteristic provides for a large increase in discharge with a relatively small increase in reservoir pool elevation.

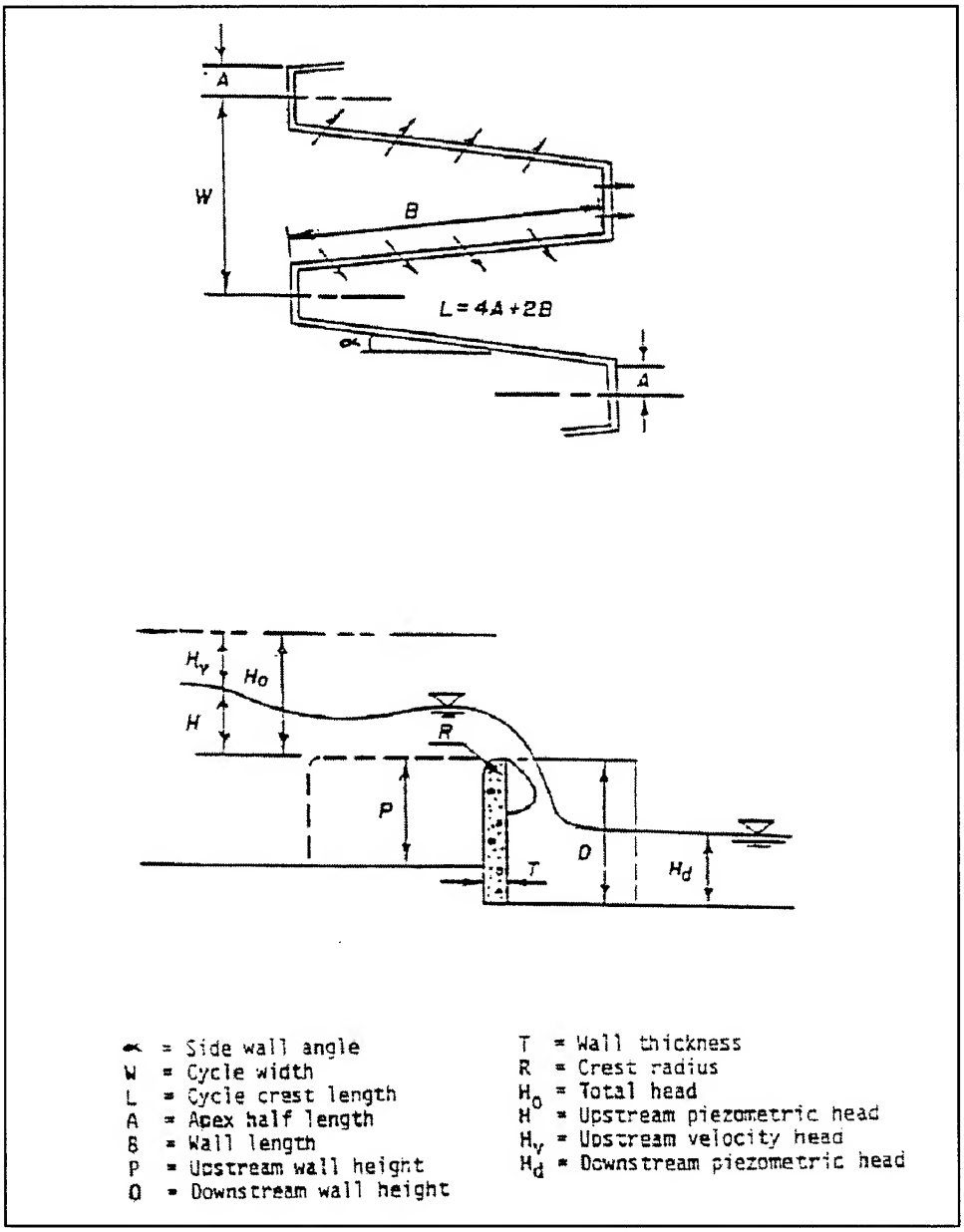

Figure 2. Definition of labyrinth parameters

The labyrinth spillway hydraulic characteristics are extremely sensitive to approach flow conditions. Lux and Hinchliff (1985) determined that the direction of the approach flow and the shape of the spillway abutments are the two major factors affecting labyrinth spillway performance. Houston (1983) found that the approach flow conditions have a large effect on the efficiency of labyrinth weirs. Her experiments with a two-cycle labyrinth weir indicated that the approach flow conditions could change the discharge over the crest by as much as 20 percent for a constant upstream reservoir level. This sensitivity to approach flow conditions makes it beneficial to place the labyrinth weir axis in a position where approach flow can be perpendicular to the axis. Labyrinth

spillway designs require verification by a physical model study if they are to be implemented (HQUSACE 1990).

A spillway-rating curve for a sharp-crested weir oriented perpendicular to the flow can be calculated from the generalized weir equation reported by Rouse (1960):

$$Q=\frac{2}{3}\sqrt{2g}\ C_d\, L\, H_o^{1.5} \qquad (1)$$

where

Q = weir discharge

C_d = discharge coefficient

H_o = difference in elevation between the upstream energy head and the weir crest elevation

L = length of a weir

The discharge coefficient is a function of the total head ratio, H_o / P, where P is the upstream height of the weir.

Rouse (1960) also reports an empirical equation developed by Rehbock for determining the discharge coefficient for a sharp crested weir oriented perpendicular to flow.

$$C_d = 0.605 + 0.08\frac{H_o}{P} + \frac{1}{305H_o(ft)} \qquad (2)$$

The second term embodies the combined geometric effects of vertical contraction and the velocity of approach. The third term reflects the effects of surface tension at low heads.

The discharge coefficient for labyrinth weirs must account for the effects of angled approach flow, nappe interference, and lack of aeration on the downstream side of the nappe.

At low discharges, the flow over a labyrinth weir is normal to the crest. Equation 2 gives the discharge coefficient, and Equation 1 gives the discharge for sharp crested labyrinth weirs. As the head increases, the momentum of the flow causes the flow to pass over the weir at an angle. This effectively reduces the weir length, which must be accounted for with the discharge coefficient. Theoretically, the form of the discharge coefficient equation should be similar to Equation 2; however, the equation should include a negative term that accounts for the flow angle. After accounting for the flow angle, the discharge coefficient equation for a labyrinth weir would apply to all weir orientations from perpendicular to parallel with the flow. Additional references to flow over

angled side weirs can be found in Hager (1987), Hager (1989), Holley (1989), Jain and Fischer (1981), and Ramamurthy (1978).

Flow over labyrinth weirs is further complicated by the interference of jets at the upstream apex of each weir cycle. The length of the interference increases with head on the weir. Hay and Taylor (1970) reported that as the head on a labyrinth weir increases so does the tailwater depth, especially between the nappe and the labyrinth wall. Because of convergence of opposing nappes, the higher tailwater depths and the restricted area at the upstream apexes, aeration under the nappe at these apexes becomes difficult. Up to a point, the lack of aeration creates a reduced pressure under the nappe, increasing the discharge coefficient. The pressure can be low enough to cause the nappe to adhere to the downstream face of the labyrinth wall. This clinging nappe can result in alternating atmospheric and sub-atmospheric pressures under the nappe producing nappe oscillation and noise and may induce structural problems from vibration and resonance. This effect can be prevented using splitter piers on the crest of the weir (Houston 1982, 1983). At higher heads, the downstream depth may increase enough to submerge the crest, thus decreasing the discharge coefficient. Lux and Hinchliff (1985) called the nappe "transitional" when there was reduced pressure under the nappe and "suppressed" when the crest was submerged. The published values of the discharge coefficients for a transitional nappe should be used with caution since surface tension effects are large for the model scales used in determining the correlations.

Considering all of the above effects, the discharge coefficients for a labyrinth weir should be a function of the relative depth of flow over the weir and the sidewall angle.

Based on results from several hydraulic model studies, Lux and Hinchliff (1985) developed the following equation for discharge over a labyrinth weir.

$$Q = C_w \left(\frac{W/P}{W/P + k} \right) n\, W\, H_o \sqrt{g\, H_o} \qquad (3)$$

where

H_o = difference in the height of the upstream energy grade line and the weir crest elevation

g = acceleration of gravity, n is the number of weir cycles

k = empirical constant

The value of k is 0.18 and 0.10 for triangular and trapezoidal shapes respectively. The discharge coefficient, C_w, uses the subscript, w, because it is influenced by cycle width, W. A family of curves have been developed that relate the relative head, H_o/P, and the cycle crest length to width (or magnification) ratio, L/W, to the discharge coefficient.

Design of Labyrinth Weirs

Flume studies conducted by Taylor (Taylor 1968; Hay and Taylor 1970) form the basis for the design of labyrinth weirs. The U.S. Bureau of Reclamation (Houston 1982) performed additional flume and model studies extending the limits of Taylor's work which led to a design procedure described in Houston and DeAngeleis (1982). This procedure was used to design the dimensions of the Prado labyrinth weir. It should be noted that Taylor defined upstream head as the water-surface elevation, and Houston defined the upstream head as the total energy head. With that adjustment, the methods of Taylor and Houston produce consistent results. Discharges calculated using weir coefficients from Houston and DeAngeleis (1982) produced discharges 20 to 25 percent lower than those calculated using weir coefficients from Lux and Hinchliff (1985) when the head on the weir was 10 ft or less. When the head was greater than 15 ft, the predicted discharges using Houston and DeAngeleis (1982) were slightly higher than those calculated using Lux and Hinchliff (1985).

Under normal conditions the cycle width to weir height ratio, W/P, should be 2.5 or greater and the head to weir height ratio, H_o/P, should be less than 0.6. Hinchliff and Houston (1984) report that when H_o/P is above 0.6, the labyrinth behaves more like a straight weir and no benefit is obtained by increasing the cycle length to cycle width ratio, L/W.

Houston (1983) found that quarter round crest shape was the most efficient when used with upstream vertical-faced cantilever walls.

In addition to the studies already mentioned, useful information regarding design of labyrinth weirs can be found in the following reports of hydraulic model investigations: Babb (1976), Magalhaes and Lorena (1989), Mayer (1980), Phelps (1974), CH_2M Hill (1974), Vermeyen (1991), and Walsh and Jones (1980).

Hydraulic Theory for Ogee Weirs

Theory and design of ogee crested weirs are much more advanced than for labyrinth weirs. Spillway geometries for maximum efficiency have been determined for a wide range of hydraulic conditions using physical model studies. High efficiency ogee spillways are designed with a crest shape that closely approximates the shape of a fully ventilated nappe of water flowing over a sharp crested weir. The shape of the nappe is affected by the relative head on the weir, H_o/H_d, (where H_d is the design head or the head at the design discharge), the approach depth and velocity, and the upstream slope of the weir. Equations for designing the crest profile for an ogee spillway are reported in HQUSACE (1990).

Flow over an ogee spillway is governed by the following relationship.

$$Q = C L H_o^{1.5} \tag{4}$$

where

Q = discharge

C = discharge coefficient

L = effective length of the crest

H_o = energy head above the crest

The discharge coefficient is dependent on the relative head, submergence of the crest, the height and slope of the upstream weir face, approach velocities, and the shape of the abutments. Spillway discharge coefficients for free-fall over a wide range of hydraulic conditions are reported in HQUSACE (1990). The effect of site specific factors such as flow angularity resulting from complex approach flow geometry must be investigated by a site-specific model study.

2 Scale Model

Description

The 1:50-scale hydraulic model of the Prado spillway reproduced the topography in an approach area that extended approximately 1,700 ft upstream from the center line of the spillway crest and had a width of 3,200 ft. The model simulated the spillway crest, spillway channel and chute, dam embankment, and approximately 2,500 ft of exit channel. The model had the capability to simulate spillway discharges as high as 850,000 cfs. The model spillway, exit channel, and reservoir are shown in Figures 3-5. The general model layout is shown in Plate 1.

The model was designed to permit installation of moveable bed material downstream from the flip bucket to qualitatively simulate scour potential in the exit channel. The model was incapable of simulating the magnitude of the anticipated scour hole because of the scale effects associated with the bed material. However, it indicated areas where scour and deposition would be expected.

The spillway capacity of a labyrinth weir is sensitive to both the magnitude and direction of approach flows. To insure proper simulation of spillway approach flows in the physical model, a two-dimensional numerical model of the entire reservoir was developed. It was used to determine the magnitude and direction of flows at the physical model boundaries. The inflow to the physical model was adjusted to reproduce the approach flow patterns determined from the numerical model.

The model spillway was constructed of sheet metal and marine plywood. The surface was painted to obtain as smooth a surface as possible. The approach and exit channels and the dam itself were molded in concrete mortar to sheet metal templates.

Model Appurtenances

Water used in the operation of the model was supplied by a circulating system. Water was pumped from a large sump into the model headbay. Discharge was controlled using valves. Discharges were measured with elbow meters

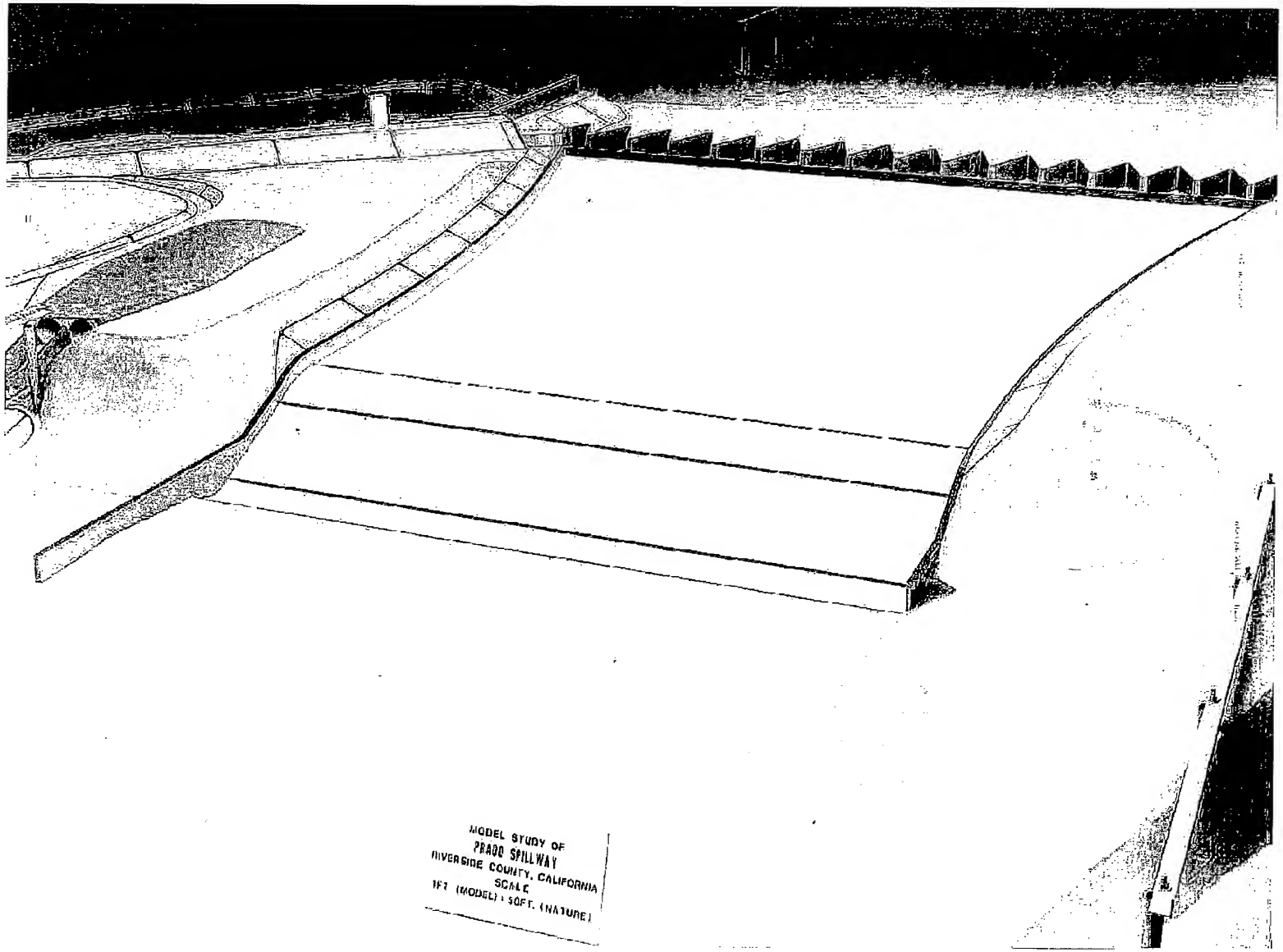

Figure 3. Prado Spillway model looking upstream at the labyrinth weir

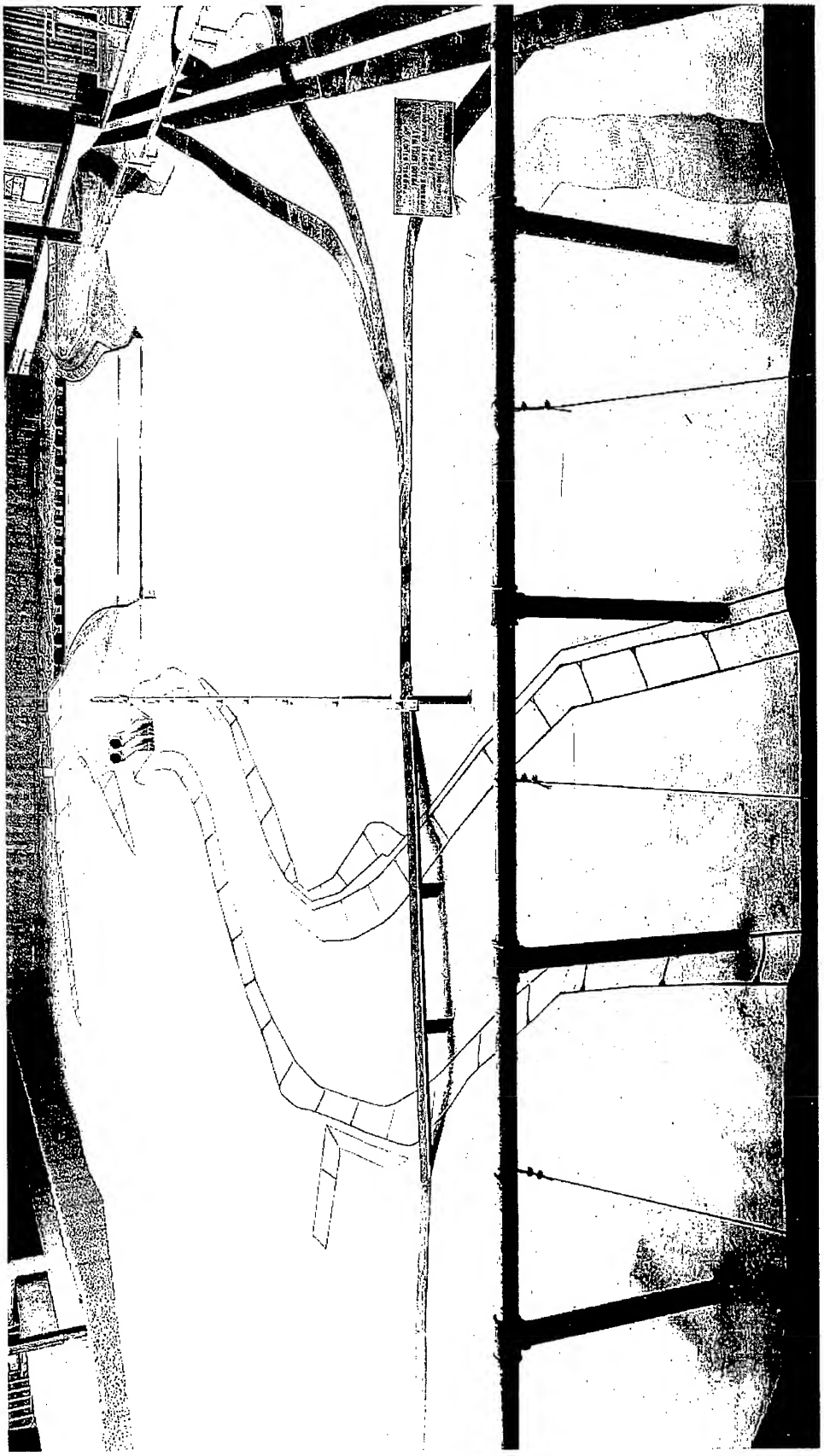

Figure 4. Prado Spillway model downstream conditions

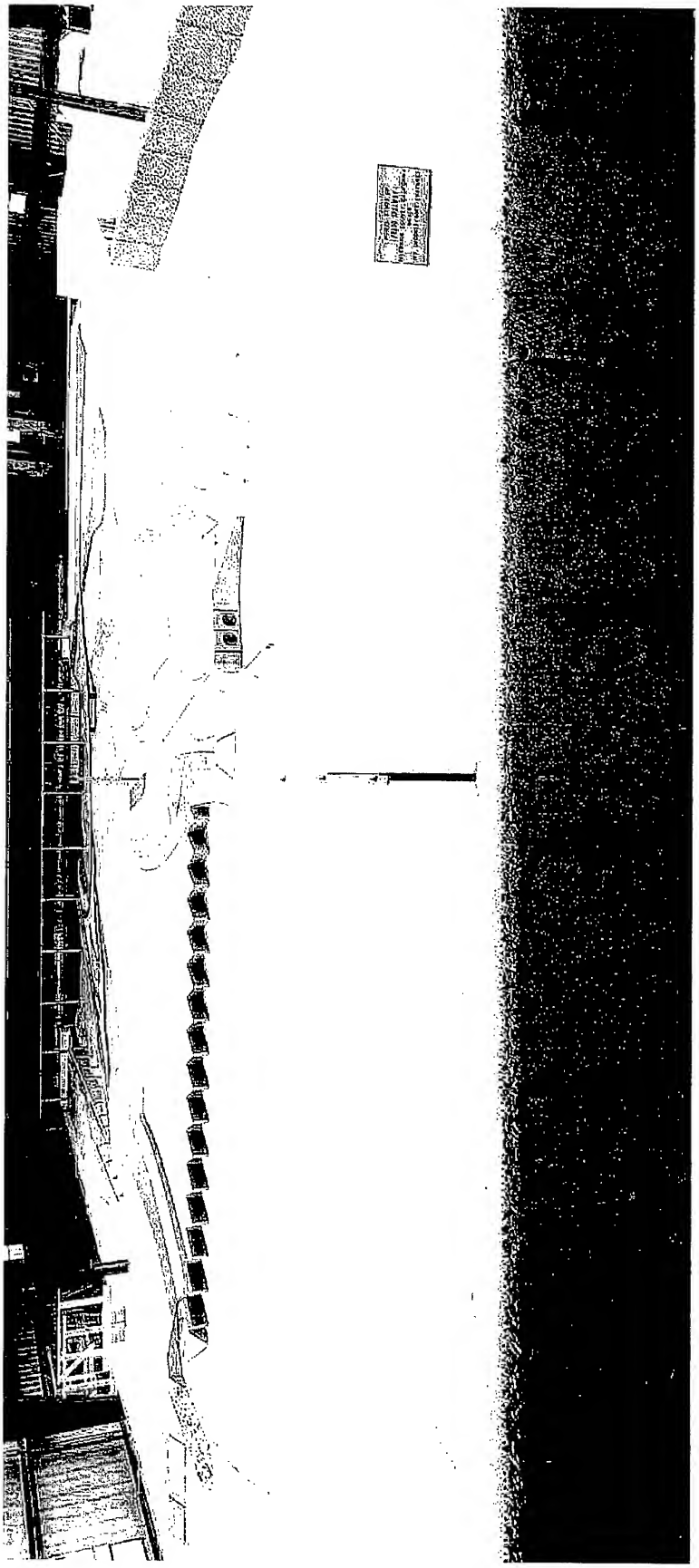

Figure 5. Prado Spillway model reservoir looking downstream

installed in the flow lines and were baffled before entering the model. Elbow meters were calibrated volumetrically using the model headbay. Tailwater in the model was controlled by the downstream geometry of the model. Water leaving the model flowed back into the sump.

Velocities were measured with electronic paddle-wheel velocity meters that were mounted to permit measurement of flow from any direction and at any depth. Water-surface elevations were measured with point gauges. Different designs and various flow conditions were recorded photographically.

Scale Relations

The principle of dynamic similarity, which requires that ratios of forces be the same in model and prototype, is the basis for the design of physical models and the interpretation of results. Models involving a free surface are scaled to the prototype using the Froude criteria because primarily gravitational and inertial forces determine the flow phenomena. General relations for the transference of model data to prototype equivalents are presented as follows:

Characteristic	Dimension[1]	Scale Relations
Length	L_R	1 : 50
Area	$A_R = L_R^2$	1 : 2,500
Velocity	$V_R = L_R^{1/2}$	1 : 7.0711
Time	$T_R = L_R^{1/2}$	1 : 7.0711
Force	$F_R = L_R^3$	1 : 125,000
Discharge	$Q_R = L_R^{5/2}$	1 : 17,678

[1] Dimensions are in terms of length.

Model measurements of discharge, water-surface elevations, and velocities can be transferred quantitatively to prototype by the scale relations. Unless otherwise noted, all results reported herein will be given in prototype units.

Viscous and surface tension forces also affect discharge over weirs in hydraulic models. Scale effects from surface tension occur when the spillway nappe attaches itself to the downstream side of a vertical weir. This is most likely to occur in the model at low heads when there is insufficient aeration under the nappe. Viscous effects are more important with an ogee crest where friction can be significant. Maynord (1985) reviewed the literature relating to scale effects in hydraulic models of weirs. He concluded that surface tension and viscous effects would be negligible when the head over the weir exceeded 0.3 ft. This turned out to be a very conservative estimate in Maynord's experiments. Using data from his own investigation Maynord found less than a 1 percent error in discharge coefficient with a model head of 0.2 ft and less than a 5 percent error in discharge coefficient with a model head of 0.1 ft.

Rehbock (Rouse 1960) developed an equation for determining the discharge coefficient for a sharp-crested weir that considers the effect of surface tension.

$$C_d = 0.605 + 0.08\frac{H_o}{P} + \frac{1}{305 H_o} \qquad (2)$$

where

C_d = discharge coefficient

H_o = total head on the crest of the spillway in feet

P = height of the spillway wall in feet

The last term in the equation represents the effect of surface tension on the discharge coefficient. From this equation it can be determined that when the head on the model spillway is 0.3 ft, the maximum error due to surface tension is less than 2 percent. It can also be determined that when the head on the model spillway is 0.1 ft the maximum error due to surface tension is less than 6 percent.

In the Prado spillway model the 0.3-ft head criterion corresponds to a pool elevation of 578. This pool elevation resulted in a spillway discharge of about 450,000 cfs with the labyrinth and about 250,000 cfs with the ogee weir. Therefore, for the labyrinth and ogee spillways, at the design discharges of 847,000 and 481,000 cfs, respectively, surface tension and viscous effects were negligible.

3 Model Results

Labyrinth Weir Experiments

Calculation of approach flow with numerical model

Labyrinth weir capacity is very sensitive to approach flow conditions. Therefore it was important that the flow approaching the spillway in the physical model simulated natural flow patterns. The 1:50-scale physical model of the Prado spillway simulated only 1,700 ft of the topography upstream from the spillway crest. A numerical model that simulated the entire Prado Reservoir was used to calculate velocity magnitudes and directions in the spillway approach channel. These calculated velocities were then used to adjust boundary conditions in the physical model.

The vertically averaged two-dimensional numerical model, STREMR (Bernard 1992), was used to calculate velocities. STREMR is a rigid lid numerical model that approximates the two-dimensional Navier-Stokes equations for incompressible flow. The equations are solved for depth-averaged velocity. The term "rigid lid" means that the water-surface elevation is specified and held constant throughout the calculations. This limitation was not considered significant for this study because the reservoir pool was assumed to be constant throughout the area of interest. The model would not be appropriate for modeling flow over the spillway itself because assumptions of constant water-surface elevation and hydrostatic pressure distributions would be violated. Therefore, spillway details were not included in the numerical model.

The entire Prado Reservoir, below el 589.0, was simulated with the numerical grid. The maximum pool elevation was 589.9 for a discharge of 850,000 cfs. Areas where ground surface elevations changed rapidly were avoided or excluded from the numerical grid to avoid numerical instability problems in the numerical model. More grid resolution was provided in the vicinity of the reservoir spillway which provided more accuracy in the area of interest. Elevations obtained from recent aerial photographs of the reservoir were used to set the ground surface elevations in most of the numerical model. However, elevations around the spillway were digitized from Plates contained in the Prado Dam General Design Memorandum (GDM) (U.S. Army Engineer District, Los Angeles, 1988).

Inflow and outflow conditions were determined from hydrologic studies conducted by the Los Angeles District. Based on HEC-1 reservoir routing computations, for spillway outflows of 850,000 cfs, 600,000 cfs, and 300,000 cfs, pool elevations were 589.9, 582.5, and 574.5, respectively. Since the STREMR model does not account for reservoir storage, inflows at the reservoir boundaries were assigned based on inflow percentages at the peak reservoir inflow. The reservoir has four inflow points. These are listed with their assigned inflow percentage in parenthesis: Chino Creek (8.3), Cucamonga Creek (7.3), Santa Ana River (74.0), and Temescal Creek (10.4). A sketch of the numerical model boundaries with inflow points designated is shown in Plate 2.

The bottom roughness is accounted for in the numerical model using the Manning equation. The reservoir, which is typically dry, has various land uses including open agriculture land, scrub or low-height brush, and a grove of eucalyptus trees located near the dam. Initially, the entire reservoir was assigned a roughness coefficient of 0.030. This served as a base condition from which changes in the velocity patterns or streamlines could be compared. The effect of raising the roughness coefficient to 0.040 throughout the reservoir was found to have no significant effect on calculated flow distribution in the reservoir.

The objective of the STREMR study was to provide depth-averaged velocity magnitudes and directions that could be used to adjust flows in the physical model. The flow characteristics of interest were located near the boundaries of the physical model. The boundaries of the physical model were identified on the numerical grid to define three inflow boundaries: left, center, and right. These are shown in Plate 2.

The effect of the eucalyptus grove, located about 1,000 ft upstream from the spillway, on flow distribution across the designated boundary of the physical model was calculated using the numerical model. The bed surface in the eucalyptus grove was assigned roughness coefficients of 0.080 and 0.300 in separate computer simulations. In the numerical calculations, the trees were found to have only a slight effect on velocity magnitudes and directions for all three discharges. Differences in flow distribution across the designated physical model boundaries were also small. Calculated distributions are listed in the following tabulation.

Discharge cfs	n Value In Eucalyptus Grove	Percentage Across Left Boundary	Percentage Across Center Boundary	Percentage Across Right Boundary
850,000	0.030	13.6	51.2	35.2
850,000	0.080	13.8	50.8	35.4
850,000	0.300	16.6	46.0	37.4
600,000	0.030	12.8	51.6	35.6
600,000	0.080	13.2	51.0	35.8
600,000	0.300	15.8	46.6	36.7
300,000	0.030	11.8	52.2	36.0
300,000	0.080	12.0	52.0	36.0
300,000	0.300	14.2	48.6	37.2

The results of the STREMR numerical model study showed no significant change in flow distribution across the physical model limits for discharges ranging between 300,000 cfs and 850,000 cfs. The numerical model also showed that the eucalyptus grove did not significantly affect the physical model inflow distributions or velocities.

Adjustment of approach flow

Flow patterns calculated using the two-dimensional numerical model considered the topography of the entire reservoir and were considered to be representative of prototype conditions. The physical model headbay was designed to permit adjustments in flow rate all along the headbay weir and through the rock baffle. Thus, the approach flow at the boundary of the physical model could be adjusted to ensure that the magnitude and direction of the physical model approach flows were similar to those calculated using the numerical model. After minor adjustments to the headbay and rock baffle, the magnitude and direction of approach currents measured in the physical model were similar to approach flows calculated using the two-dimensional numerical model. Physical and numerical model prototype approach velocities for discharges of 300,000 and 600,000 cfs are compared in Plates 3 and 4.

Type 1 spillway design

The type 1 spillway design was a labyrinth weir constructed immediately upstream from the existing ogee spillway. Both the right and left abutments of the existing ogee spillway have crests at el 563.0, and they become overflow berms in the labyrinth weir design (Figure 6). The weir was designed by the Los Angeles District using criteria from the U.S. Bureau of Reclamation (Houston and DeAngelis 1982). The labyrinth weir was designed to pass the spillway design discharge of 847,000 cfs at a pool elevation of 589.9. Flow over the top of the left and right abutments of the existing ogee spillway were ignored in these calculations. The details of the labyrinth weir design are shown in Figure 7. The weir itself was a 33-ft-high zigzag wall, 2-ft-thick, with a crest elevation of 563. The upstream edge of the wall consisted of a one-fourth-rounded crest with a radius of 1 ft. The weir cycle width, *W*, was 66.67 ft, and the magnification ratio, L / W was 2.6. There were 15-½ cycles on the spillway providing a total weir crest length of 2,697 ft and a weir length per cycle, *L*, of 174 ft.

A spillway-rating curve was computed for the type 1 spillway design using an equation developed by Lux and Hinchliff (1985). The U.S. Bureau of Reclamation developed this equation subsequent to the work of Houston and DeAngelis using additional flume data.

$$Q = C_w \left(\frac{W / P}{W / P + k} \right) n W H_o \sqrt{g H_o} \qquad (3)$$

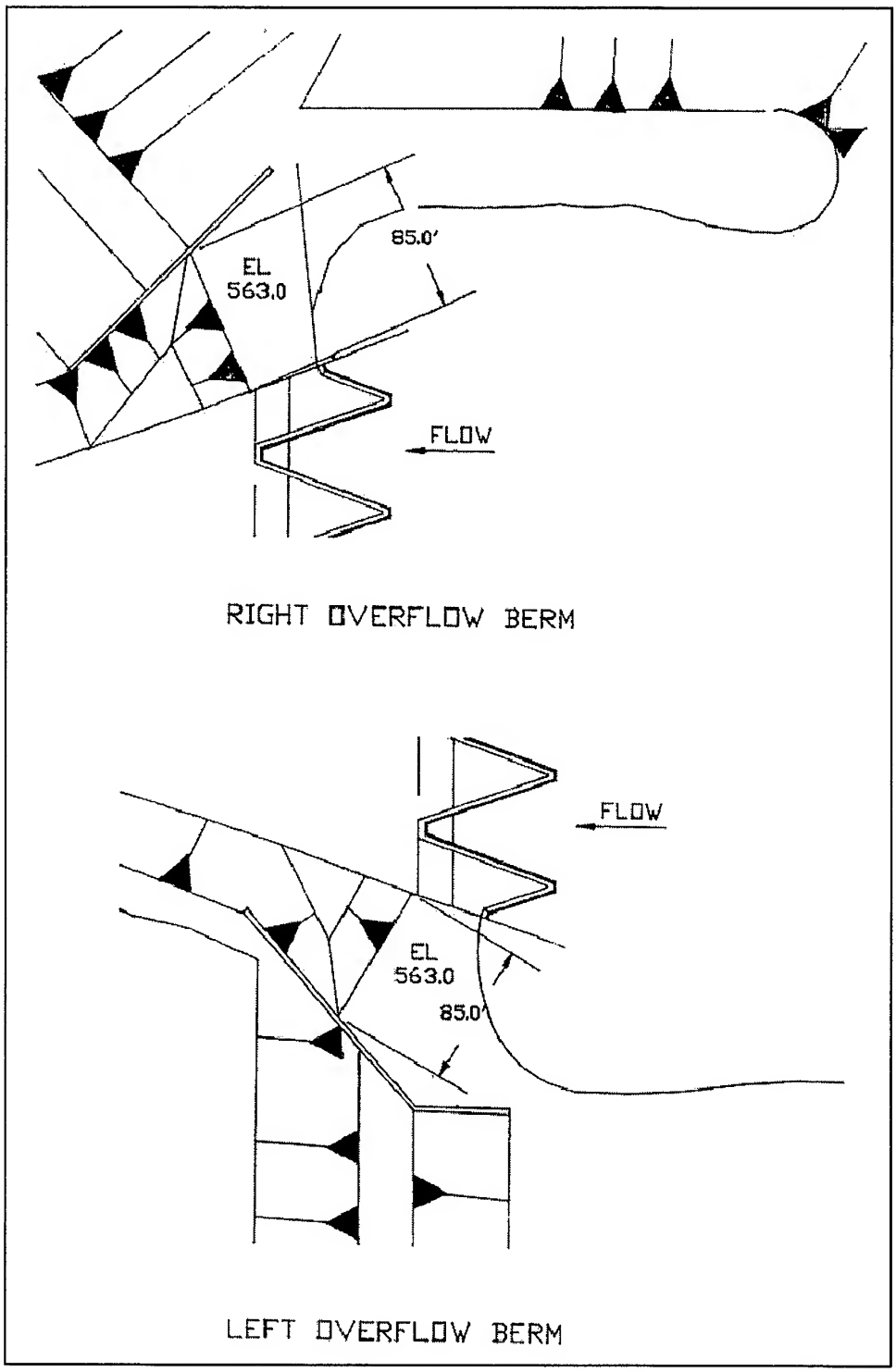

Figure 6. Spillway abutments type 1-4 designs

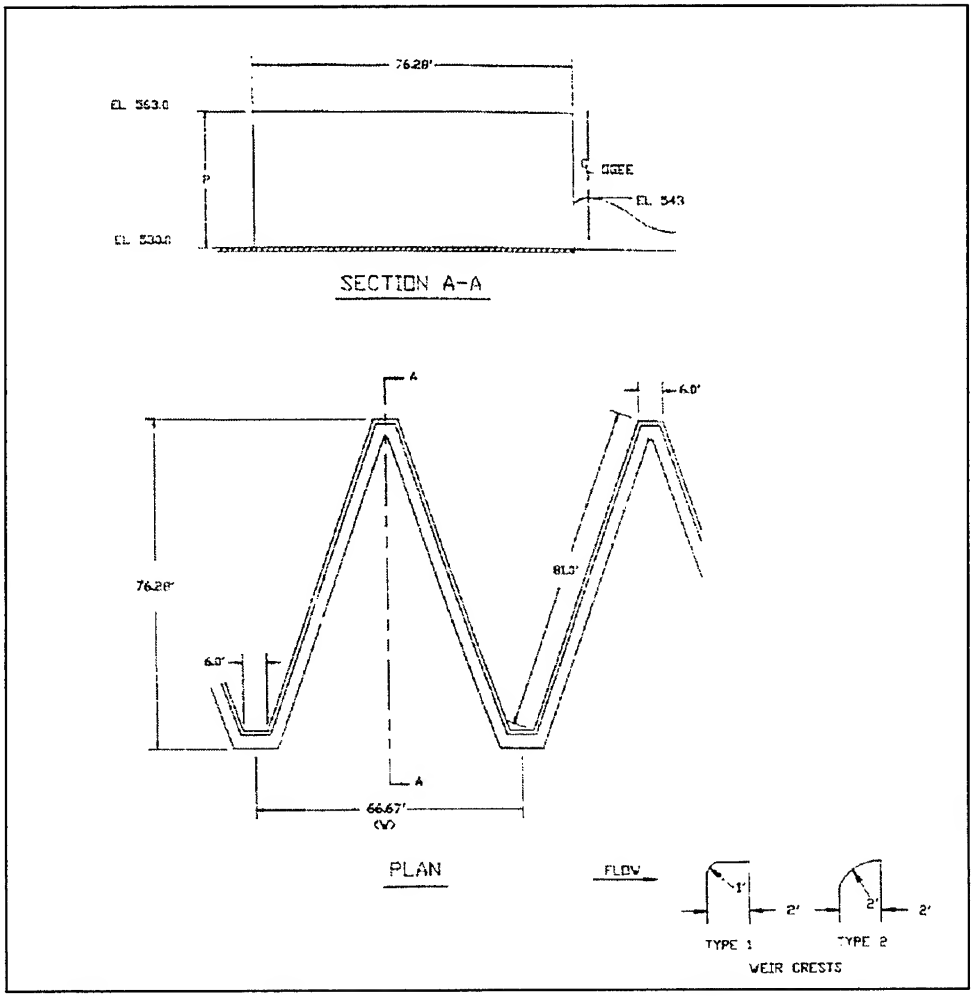

Figure 7. Type 1 and 2 spillway design labyrinth details

where

Q = total discharge over the weir

P = height of the weir (33 ft)

H_o = difference in the height of the upstream energy grade line and the weir crest elevation

n = number of weir cycles

g = acceleration of gravity

k = empirical constant

The value of k is 0.18 and 0.10 for triangular and trapezoidal shapes respectively. The type 1 spillway design was considered to have a trapezoidal shape, so k = 0.10. The magnification ratio, L/W, was 2.6. The weir coefficient, C_w, is a

function of the weir height ratio, H/P, and is based on flume data from Lux and Hinchliff (1985) as shown in Plate 5.

A spillway-rating curve for the type 1 spillway design was also determined from the 1:50-scale physical model by measuring the pool elevations for various discharges. The pool elevation was measured with point gauges at two locations as shown in Plate 1. For any discharge, the water-surface elevation at point gauges 1 and 2 was essentially the same (Figure 8). Thus, only point gauge 1 was used for subsequent experiments. The spillway rating curve determined from the physical model is compared to the spillway rating curve predicted from Equation 3 in Figure 8. The spillway-rating curve determined from the model allows for flow over the left and right spillway abutment berms. Despite this extra capacity in the physical model, a comparison of the measured and predicted discharge rating curves indicate that for discharges above 400,000 cfs, the spillway is less efficient than predicted by Equation 3.

The initial experimentation with the type 1 spillway design revealed several design problems. The major problems were:

a. The labyrinth weir had insufficient capacity – at a spillway design discharge of 847,000 cfs there was less than 1.5 ft of freeboard on the dam embankment and water lapped over the top of the dam because of wave action in the pool.

b. At well below the design discharge, flow overtopped the spillway channel walls and flowed down the abutment toward the dam embankment – there should be at least 2.5 ft of freeboard on these walls.

c. Flow conditions at the flip bucket were unstable – flow depth in the flip bucket should be less than 20 percent of the bucket curve radius.

d. Flow conditions in the exit channel downstream from the spillway-included waves and circulation at the toe of the dam embankment.

Flow conditions with the type 1 spillway design were documented with photographs. Time lapse photography was used to show spillway approach flow patterns in Photos 1-3 for discharges of 300,000; 600,000 and 750,000 cfs, respectively. These photos demonstrate that flow approaches few of the labyrinth cycles perpendicular to the spillway axis. Flow over the labyrinth weir itself for discharges of 100,000; 200,000; 300,000; 600,000 and 750,000 cfs is shown in Photos 4-8, respectively. The labyrinth weir was relatively effective up to 300,000 cfs, but began to lose effectiveness by the time the discharge reached 600,000 cfs. Flow conditions at the right spillway chute wing wall and the flip bucket are shown for discharges of 300,000; 600,000 and 750,000 cfs in Photos 9-11, respectively. These photos show water overtopping the wing wall at all three discharges. Flow conditions in the exit channel for discharges of 300,000; 600,000 and 750,000 cfs are shown in Photos 12-14, respectively. These photos and Photos 9-11 show the ineffectiveness of the flip bucket.

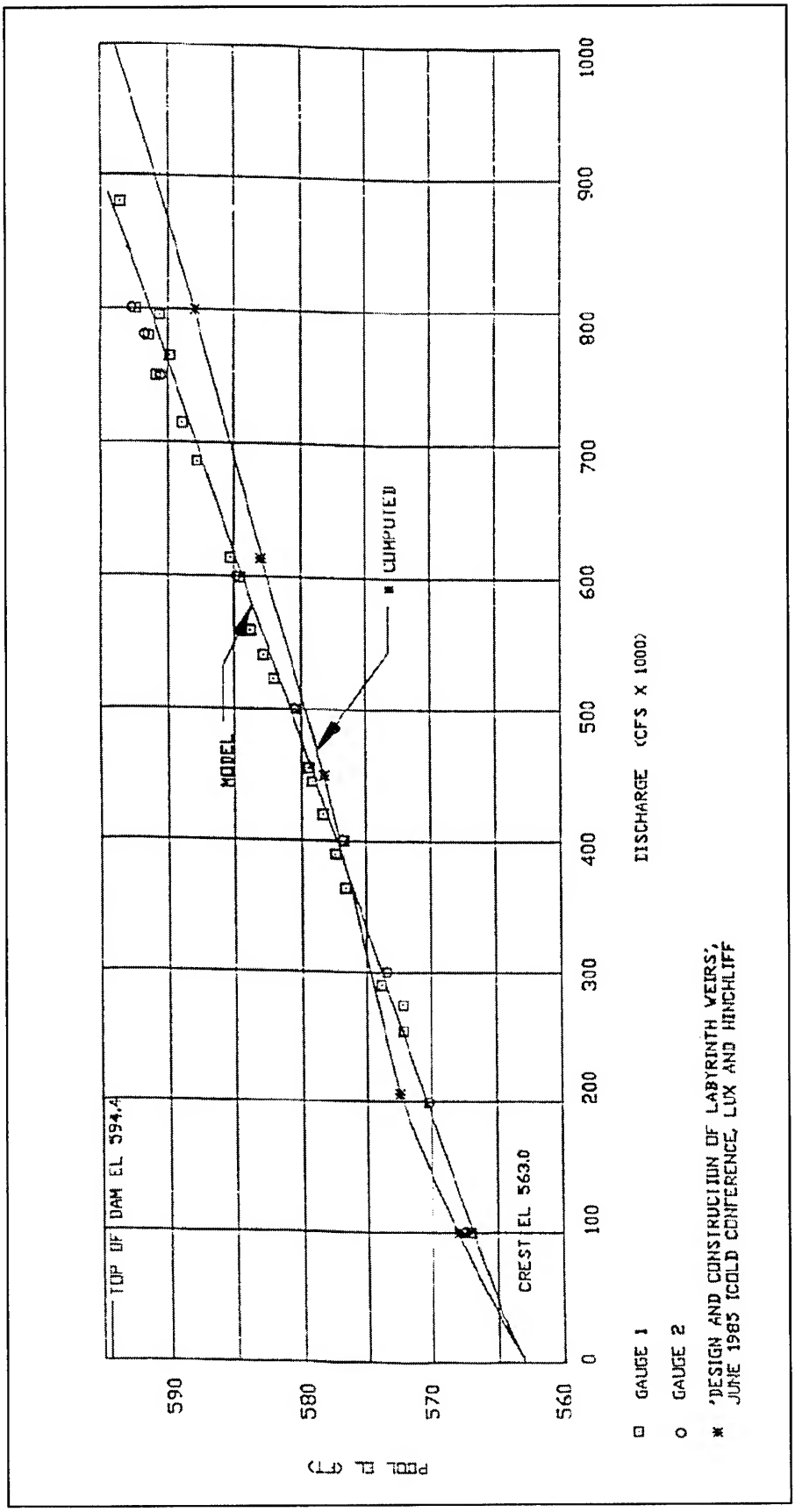

Figure 8. Type 1 spillway design rating curve

Type 2 spillway design

The type 2 spillway design was an attempt to increase weir capacity by streamlining the top of the weir crest. The one-fourth-rounded crest with a 1-ft radius curve on the upstream side of the 2-ft-wide weir was replaced with a fully rounded crest and a 2-ft radius curve. The measured points defining the spillway rating curves for the type 1 and type 2 designs are shown in Plate 6 and indicate no significant difference in efficiency. The basic data for the spillway rating curves measured in the model for the type 1 and type 2 designs are tabulated in Plate 7.

Effect of abutments and lateral flow

To isolate the effects of the abutments and lateral flow on spillway capacity, the general model was modified to simulate a section model with a four-cycle labyrinth weir (Plate 8). The section model was designed to eliminate flow contractions caused by the abutments and lateral flow. Spillway rating curves determined from the section model are shown in Plate 9. The basic data for these curves are tabulated in Plate 8. The rating curve for the section model was computed using Equation 3, and this curve is shown in Plate 9. This comparison indicated that the section model spillway is less efficient than the computed curve. It was concluded that approach flow conditions are not entirely responsible for the difference in computed and measured spillway capacity.

Surge heights

The existing topography downstream from the spillway constricts flow and creates a pool that backs up against the dam. Waves created during spillway flow break on the dam embankment are shown in Photo 15. Maximum surges on the downstream slope of the dam embankment were measured in the physical model for discharges between 100,000 and 750,000 cfs. Surge height is the distance between the trough and crest of the surge, measured along the slope of the dam, as shown in Figure 9. Measurements were made about 1,500 ft from the center line of the spillway using a point gauge. Measured surges and corresponding tailwater elevations 100 ft upstream from the Corona Highway Bridge are tabulated below. The surges were about the same magnitude along the full length of the downstream face of the dam embankment.

Discharge, Cfs	Surge, ft	Tailwater Elevation, ft
100,000	13	491.5
200,000	21	496.5
300,000	42	497.0
400,000	44	498.0
500,000	46	499.0
600,000	50	499.0
700,000	42	499.0
750,000	42	499.0

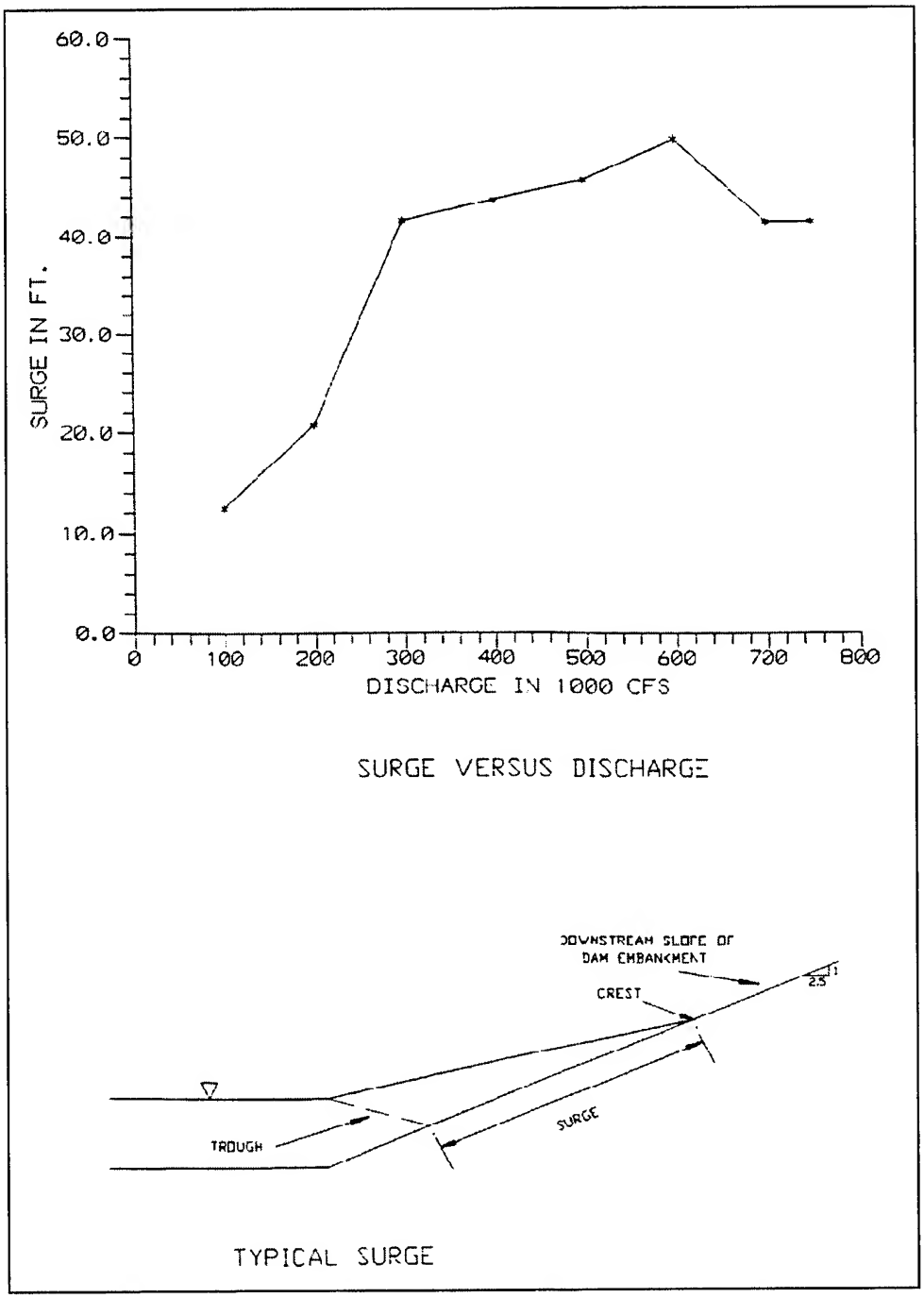

Figure 9. Surge against the downstream dam embankment

Type 3 and type 4 spillway designs

Experiments with the type 3 and type 4 spillway designs were conducted to determine if the geometry downstream from the labyrinth weir was causing submerged flow conditions across the weir. The area between the labyrinth weir and the existing ogee weir was filled to the elevation of the ogee crest for the

type 3 spillway design. The existing ogee weir was removed for the type 4 spillway design. Sketches of the type 3 and type 4 spillway designs are shown in Figure 10. The type 2 labyrinth weir crest was retained for both the type 3 and type 4 spillway designs. A spillway rating curve that includes data from type 1-9 spillway designs is shown in Plate 6. The basic data for the spillway rating curve measured in the model for the type 3 and type 4 spillway designs are tabulated in Plate 7. The data indicate that the type 3 and type 4 spillway designs do not improve or affect the efficiency of the labyrinth weir. It was concluded that retaining the existing ogee spillway would not adversely affect the efficiency of the labyrinth weir. The existing ogee spillway was not replaced in the model for subsequent experiments.

Type 5 through 8 spillway designs

The right and left spillway abutments are diagramed in Figure 6. Flow directions approaching the right and left spillway abutments at a discharge of

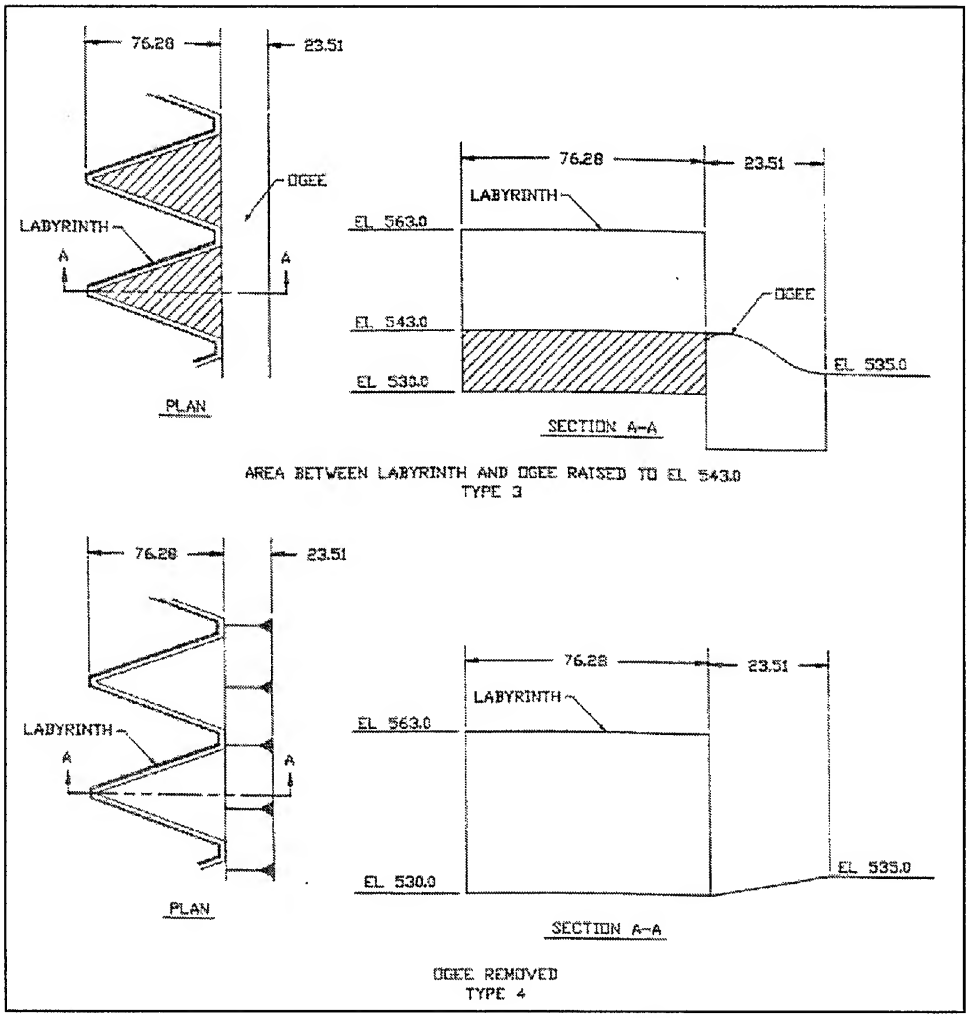

Figure 10. Types 3 and 4 spillway designs

750,000 cfs are shown in Photos 16 and 17. Photo 16 demonstrates that the right spillway abutment was subjected to considerable lateral flow that inundated the first two labyrinth weir cycles. Bottom velocities around the right abutment were excessive. Hydraulic performance at the left abutment was considered satisfactory. Measured flow patterns and bottom velocities at both abutments for a discharge of 700,000 cfs are shown in Plate 10.

The effect of eliminating flow over the spillway abutments and streamlining the approach flow was evaluated with the type 5 spillway design. Wing walls were added to the spillway abutments and flow was prevented from passing over the spillway abutment berms by the addition of non-overflow walls. The right abutment wing wall in the type 5 spillway design was effective in redirecting the lateral flow, as shown by the current vectors in Plate 11. The first two labyrinth cycles were not inundated by lateral flow. A spillway rating curve that includes data from the type 5 spillway design is shown in Plate 6. The basic data for the spillway rating curve measured in the model for the type 5 spillway design are tabulated in Plate 7. The type 5 spillway design improved approach flow conditions, but slightly decreased the spillway capacity by eliminating flow over the berms. With the type 5 spillway design, hydraulic conditions were still considered unsatisfactory at the right abutment, but hydraulic performance at the left abutment was considered satisfactory.

The effect of removing the non-overflow walls on the abutments was evaluated with the type 6 spillway design. Current directions with the type 6 spillway design are shown in Plate 12. The basic data for the spillway rating curve measured in the model are shown on Plate 6 and tabulated in Plate 7. The spillway efficiency of the type 6 spillway design was greater than for previous designs. A comparison of the type 2 and type 6 spillway designs can be used to assess the influence of approach flows on spillway efficiency. Both designs allowed for flow over the berms. The only difference between these two designs is an improvement in the approach flow with the type 6 spillway design. The type 6 spillway design data show greater discharges for a given head than the type 2 spillway design. This may be attributed to increased flow over the berms brought about by the approach flow improvements, to improved efficiency over the weir caused by improved approach flow conditions, or to both.

Experiments were conducted to document hydraulic performance with a right abutment design similar to the existing (prototype) right abutment design. This was the type 7 spillway design. Current directions and bottom velocities with the type 7 spillway design are shown in Plate 13. Bottom velocities were similar to those measured with the type 4 spillway design. Also, the first two labyrinth weir cycles were inundated by lateral flow. Thus, the type 7 spillway design was considered unsatisfactory.

A curved training wall was constructed on the right abutment and the invert of the approach channel was excavated with the type 8 spillway design. Bottom velocities measured with a discharge of 700,000 cfs are shown in Plate 14. Current velocities near the right abutment in the type 8 spillway design were about 50 percent less that those measured in previous designs. Flow passed over the labyrinth weir normal to the spillway axis. The first two weir cycles were not

inundated by lateral flow as observed in previous designs. Data points to define a spillway rating curve are plotted in Plate 6 and tabulated in Plate 7. The type 8 spillway design was more efficient for discharges above 300,000 cfs than previous designs evaluated. The data and flow observations indicate that the excavated approach and training wall reduced lateral flow, thus increasing the flow efficiency of the berm and spillway.

Effect of obstructions in the approach channel

The type 9 spillway design was similar to the type 8 spillway design except for the simulation of trees (porous blocks) in the approach to the spillway. The simulated trees located as shown in Plate 15, blocked 55 percent of the flow area and extended in height from the bottom to the water surface. Results from the type 9 spillway design are similar to the type 8 spillway design. Therefore, these experiments demonstrate that the trees simulated in the model had no significant effect on spillway efficiency. The type 9 spillway rating curve data are plotted in Plate 6 and tabulated in Plate 7.

Hydrostatic pressures on labyrinth spillway

Piezometers were installed in the labyrinth weir wall with the type 9 spillway design, as shown in Plate 16. The maximum and minimum pressures were documented for a range of discharges over the spillway and are tabulated in Plates 17 and 18. Results from these experiments indicate negative pressures on the downstream face of the labyrinth weir for discharges in the range between 250,000 and 650,000 cfs. These pressures should be considered in the structural design of the weir wall. The negative pressures will increase the efficiency of the weir.

Ogee Spillway Experiments

At this chronological point in the physical model study, the design discharge was reduced from 847,000 cfs to 586,000 cfs. With the reduced discharge, a labyrinth spillway was no longer required to pass the design discharge and still meet the pool elevation requirements. An ogee spillway with a crest elevation of 563.0 was adopted for further study and evaluated using the physical model.

Type 10 spillway design

The type 10 spillway design is the design proposed in the Phase II GDM (USAED, Los Angeles, 1988). It is an ogee-crested spillway constructed on the axis of the existing ogee spillway. The abutments and wing walls used in the type 6 design were also used for the type 10 design. A general plan for the type 10 design is shown in Figure 11. Flow and standing wave patterns for a discharge of 590,000 cfs are also shown in Figure 11. Detail sketches of the left and

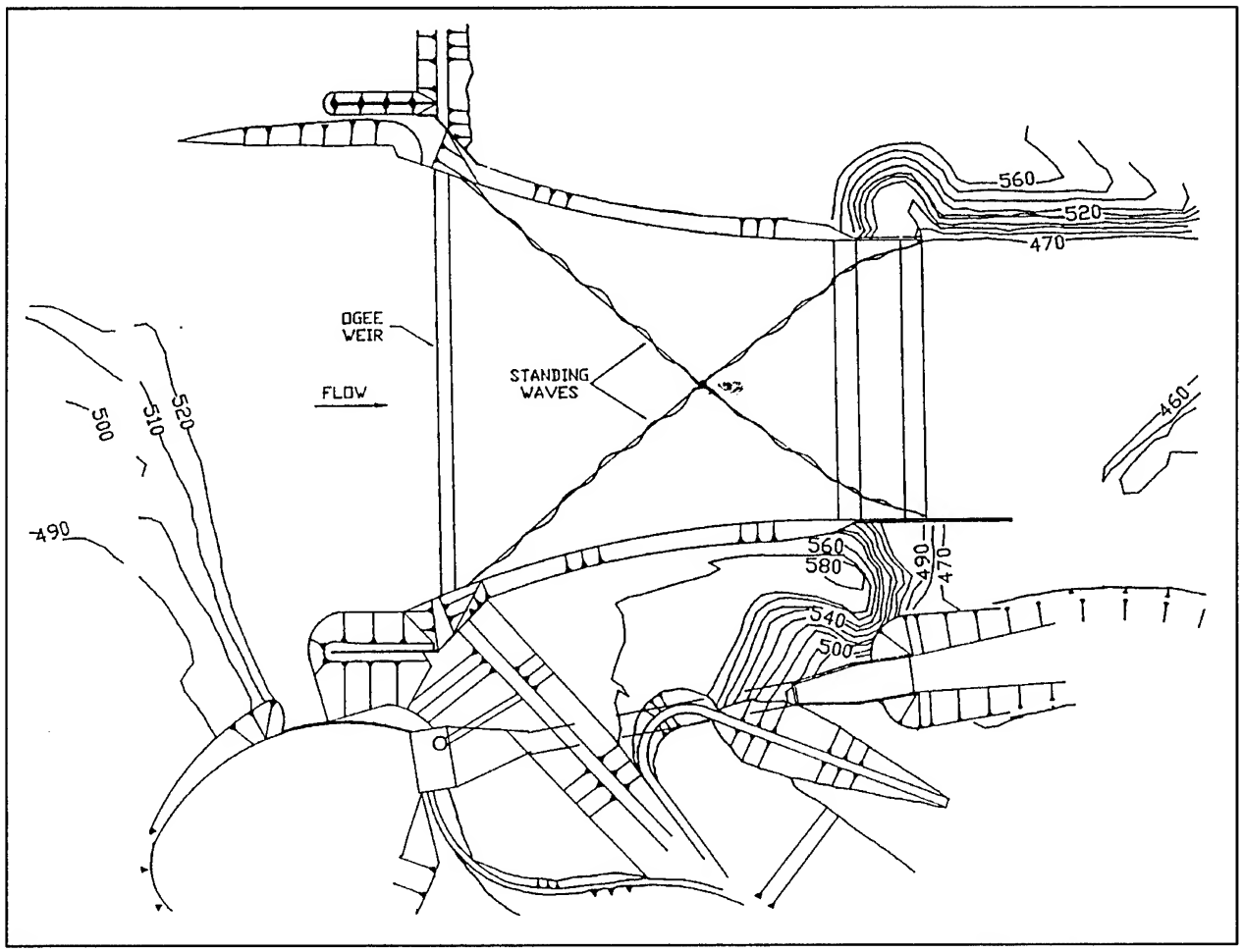

Figure 11. Type 10 spillway design general plan

right abutments and a section through the spillway are shown in Figure 12. The spillway rating curve and the basic data collected from the model for the type 10 spillway design are shown in Plate 19. The spillway-rating curve indicates that the spillway will pass the new design discharge of 586,000 at a pool elevation of about 589.0.

Type 11 though type 16 spillway designs

Model experiments were conducted to see if streamlining the spillway abutments could reduce standing waves in the spillway chute. Designs were compared by measuring the wave height at the intersection of the standing waves on the spillway chute for a discharge of 590,000 cfs. The wave height at this location for the type 10 spillway design was 18.0 ft as shown in Plate 20. The wave height is the difference between the elevation of the top of the wave and the base of the wave. In these experiments the depth of water at the base of the wave was about 19 ft.

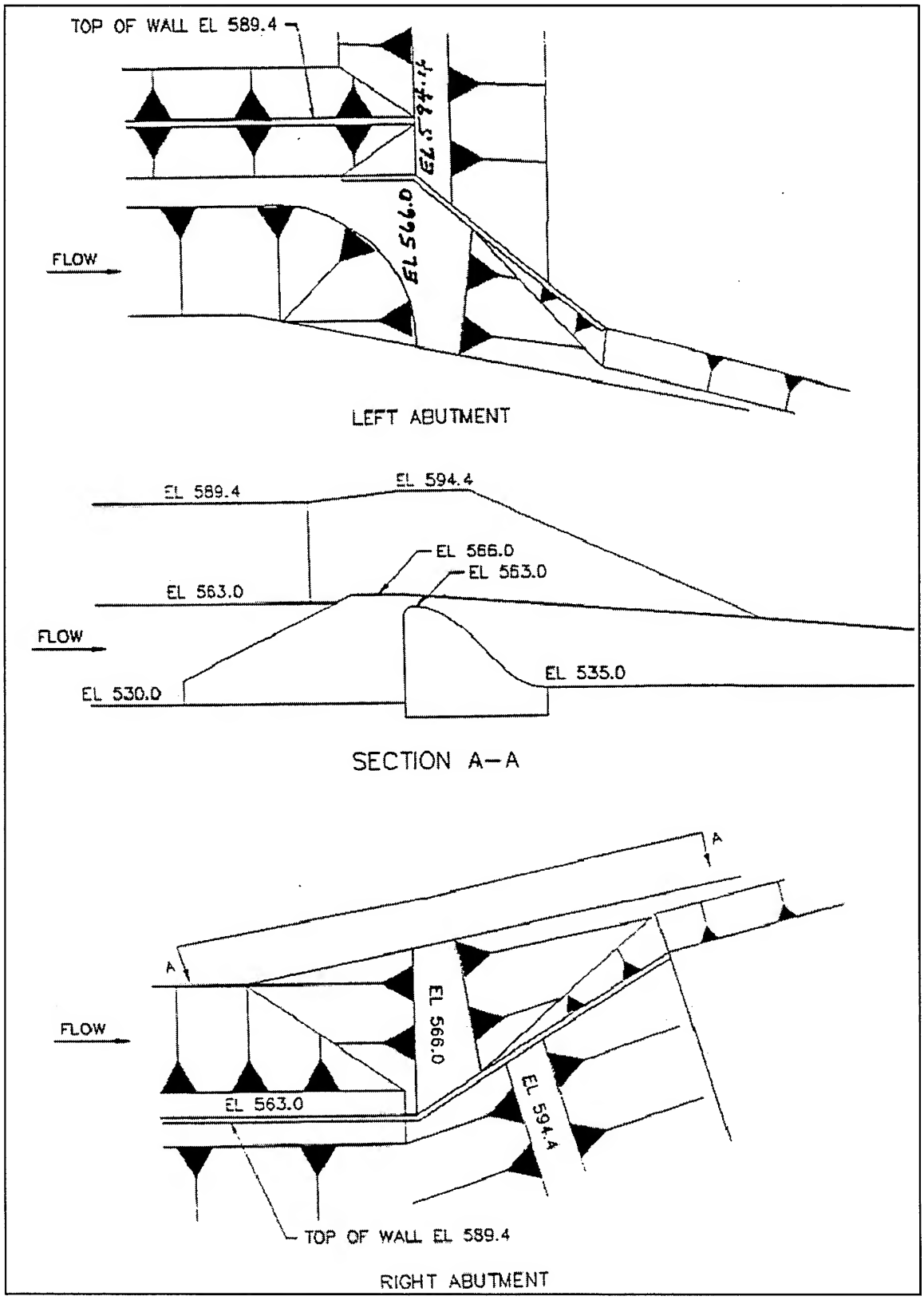

Figure 12. Type 10 spillway design details

Non-overtopping walls were placed on the right and left spillway abutments in the type 11 spillway design (Plate 21). This reduced the wave height at the intersection of the standing waves to about 17.0 ft.

The type 12 spillway design was set up as a base condition to evaluate approach flow modifications (Plate 22). The non-overtopping walls from the type 11 spillway design were removed. Both the right and left approach walls upstream from the spillway were also removed. Without these streamlining features the wave height at the intersection of the standing waves increased to 19.3 ft.

The walls blocking flow over the spillway abutments were returned in the type 13 spillway design (Plate 23). With this change the wave height at the intersection of the standing waves increased to 20.0 ft.

In the type 14 spillway design a vertical training wall extending upstream from the spillway crest was added to the right abutment (Plate 24). With this change the wave height at the intersection of the standing waves increased to 23.0 ft.

Training walls extending upstream from the spillway crest were included on both the right and left abutments in the type 15 spillway design (Plate 25). With this change the wave height at the intersection of the standing waves was 21.3 ft.

A streamlined training wall that extended both upstream and downstream from the spillway crest was placed on the right abutment in the type 16 spillway design (Plate 26). The training wall and non-overtopping abutment wall were removed from the left abutment for this design. With this change the wave height at the intersection of the standing waves was 22.0 ft.

None of the features evaluated in the type 11 through 16 spillway designs significantly reduced the magnitude of standing waves in the spillway chute. In fact, most of the modifications increased the magnitude of standing waves. The presence of standing waves on the chute raised concerns related to structural integrity of the existing concrete slabs that comprise the invert of the spillway chute.

Concrete monoliths

The physical model was used to investigate the stability of the existing concrete monoliths composing the invert of the spillway channel because of concerns related to the oscillating hydrostatic pressures associated with the standing waves. These evaluations were conducted using the type 12 spillway design. The model simulated existing monoliths by reproducing the unit weight of 155 lbf/ ft^3 and the geometric dimensions of the 60- by 60- by 1-ft concrete monoliths. Each model monolith was supported in a watertight tray that held the surface of the monolith flush with the surface of the spillway channel. The monoliths simulated in the model are numbered 1-5, and their locations are shown in Plate 27. The prototype monoliths are keyed together. However, the

model monoliths were not keyed together to produce conservative experimental results. All of the model monoliths except monolith 3 were located in an area where standing waves occurred.

Displacement of monoliths 1, 2, 3, and 4 was observed with a discharge of 100,000 cfs. Displacement of a monolith was defined as complete removal from its initial position. Usually, monolith displacement was preceded by a slight rise in the upstream end of the monolith, followed by uplift and displacement of the entire monolith.

The prototype monoliths are anchored to the underlying sedimentary rock. There are 36 anchors per monolith that provide an estimated resisting force equivalent to the weight of an additional 1 ft thickness of concrete. The Los Angeles District suggested that the thickness of the monoliths be increased to 2 ft in the model to account for this additional resistance to uplift. With this modification, monolith 1 was displaced by a discharge of 200,000 cfs. Monolith 5 was displaced by a discharge of 400,000 cfs. Monoliths 2, 3, and 4 were not displaced with discharges up to 600,000 cfs.

Since the model tray supporting each monolith was watertight, initial displacement of a monolith was caused by hydrostatic pressure acting between the bottom surface of the monolith and the surface of the tray. The joint around the perimeter of each monolith permitted water pressure above the monolith joints to migrate to the bottom surface of the monolith. Water depth above the monolith joints was uneven because of the presence of the standing wave or waves occurring over a portion of the monolith. The migration of pressure through the joints resulted in a differential hydrostatic pressure acting upward on a portion of the monolith causing its subsequent displacement.

Since the prototype spillway includes a subdrain system under the spillway invert and the monolith joints will be resealed, the prototype monoliths would not be subject to uplift pressures because of surface pressure migrating through the joints of the monolith. The joints in the model monoliths could not be sealed without inducing an artificial impediment to monolith displacement. Thus, numerous holes were drilled in the bottom of the trays to ensure that the monoliths in the model would be affected only by pressure action on the top surface of the monoliths.

Experiments conducted with the pressure relief holes beneath the 1-ft-thick monoliths revealed no displacement of the monoliths for spillway discharges up to 600,000 cfs.

Type 17 spillway design

The right and left spillway abutments were revised by adding streamlined training walls that extended both upstream and downstream from the spillway crest for the type 17 design (Plate 28). This design prevented flow over the abutment berms, and the abutment training walls were increased in height to prevent overtopping for discharges up to 600,000 cfs. The flow conditions

through the spillway chute significantly improved with this design in comparison to the type 10 spillway design. The spillway rating curve for the type 17 spillway design was measured using the model. The resulting spillway rating curve and basic data are shown in Plate 19. Eliminating flow over the spillway abutments resulted in a slight increase in the spillway-rating curve (about 1.2 ft at 600,000 cfs).

Type 18 spillway design

At this point in the model study, the design discharge was reduced for the final time down to 481,000 cfs. The final spillway design was the type 18 design in which the spillway abutments were streamlined by placing riprap behind the training walls as shown in Figure 13. Experiments were conducted with flows up to the probable maximum flood (481,000 cfs). The experiments consisted of calibrating the spillway, measurement of current velocities and water-surface profiles in the spillway channel and chute, and measurement of velocities and surges on the downstream dam embankment.

The spillway-rating curve and basic data obtained from the model are shown in Plate 29. Water-surface profiles along the left and right side of the spillway channel and chute are shown in Plates 30 and 31, respectively. The basic water-surface profile data are tabulated in Plate 32. Standing waves originating at the spillway abutments intersected in the spillway channel at sta 18+70. The cross-section water-surface profile with an isovel at this station are shown in Plate 33. Velocities in the fixed bed exit area and surges along the dam embankment are shown in Plate 34.

Downstream Scour Experiments

The physical model was used to make a qualitative assessment of the scour potential downstream from the spillway and to design features that would reduce the potential for undermining the spillway. To make these assessments, a portion of the concrete bed in the physical model was replaced with a sand bed. The depth of the sand bed extended 80 ft (prototype) below the existing bed of the exit channel. Thus, maximum scour in the model was to el 380. The tests were necessarily qualitative because the composition of the bed material in the exit channel was unknown, and the bed material in the physical model did not simulate sedimentation properties of the prototype bed.

It was determined that scour potential would be evaluated by simulating the PMF hydrograph up to the peak of 481,000 cfs. The experiments were terminated after the peak discharge was simulated for 5 hr (prototype) in the model. The PMF outflow hydrograph is shown in Plate 35.

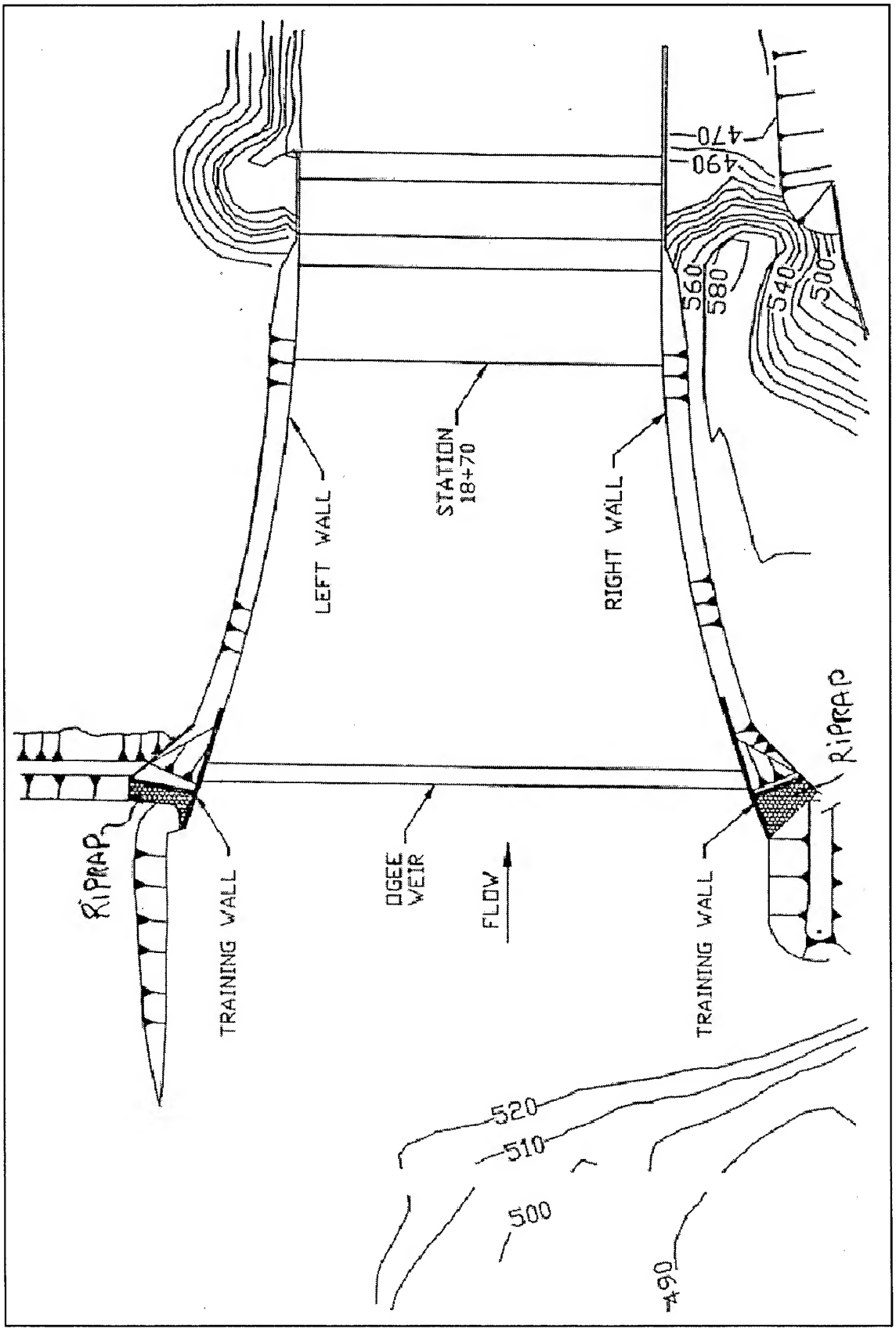

Figure 13. Type 18 spillway design general plan

Type 1 exit channel design

The initial topography in the type 1 exit channel was identical to that used in the type 18 spillway design. The top of the right descending training wall at the end of the spillway was el 490.0. The model prior to commencement of the first experiment is shown in Photo 18. During the experiments, the design spillway hydrograph was simulated up to the peak flow. Model boundary conditions are tabulated in the following table. Tailwater elevations were controlled by the downstream topography, which was subject to change depending on the deposition of sand from the scour hole.

Discharge, Cfs	Time, hr	Tailwater, el[1]
25,000	20	484.5
100,000	15	487.9
200,000	8	492.4
350,000	2	496.6
450,000	3	499.7
481,000	5	499.7

[1] Tailwater measured in exit channel at Corona Bridge.

Flip bucket performance with the type 1 exit channel design, at the peak discharge of 481,000 cfs, is shown in Photo 19. Photo 20 and the contour plot shown in Plate 36 document the resulting scour patterns. As previously discussed, the model bed material downstream from the spillway was not scaled to the prototype, so scour depths are to be considered only for qualitative evaluations.

With the type 1 exit channel design the scour pattern downstream from the spillway was relatively symmetric. Slightly more scour occurred on the right side of the channel, and there was a rightward tendency for the scour hole and sediment deposit. Scour occurred against the flip bucket cutoff wall on both the right and left corners of the spillway, adjacent to the left natural bank, and adjacent to the right training wall. The scour hole extended to the backside of the training wall as the model bed maintained the sand's angle of repose. The structural integrity of the training wall was questioned because of the excessive scour on both sides of the wall. Scour depths in the model were limited by the model's concrete floor.

Type 2 exit channel design

To assess the consequence of failure of the right training wall, it was removed for the type 2 exit channel design. The model was remolded back to the same initial conditions shown in Photo 18 prior to initiating the experiment. The design spillway hydrograph was simulated up to the peak flow. Model boundary conditions were the same as those for the type 1 exit channel design.

Flip bucket performance for the type 2 exit channel design, at a discharge of 481,000 cfs, is shown in Photo 21. The resulting scour patterns are shown in

Photo 22 and in a contour plot in Plate 37. The concrete floor of the model limited scour depths in the model.

Without the training wall, the scour pattern downstream from the spillway was not symmetric. An eddy developed on the right side of the spillway exit channel which resulted in less flip on the right side of the spillway flip bucket, and consequently a deep scour hole developed against the spillway cutoff wall on the right side of the exit channel. The lateral extent of the scour hole toward the proposed outlet works was limited in the model by artificial constraints left over from the original model construction (cinder blocks and plywood forms). With more flow and higher velocities concentrated on the left side of the exit channel, the flip was more efficient on the left side of the spillway and scour against the cutoff wall on the left side of the exit channel did not develop as it did with the type 1 exit channel.

It is recommended that the right training wall be retained in the final design and toe protection provided to prevent failure because of the lateral extent of the scour hole and the strength of the return eddy.

With both the type 1 and type 2 exit channel designs, portions of the spillway cutoff wall were protected by sediment deposited by a back roller created by the flip bucket. The effectiveness of the flip bucket is influenced by the tailwater elevation and the elevation of the model bed, both of which have a high degree of uncertainty. With the type 2 design, scour gauges indicated that the protective deposit against the cutoff wall had been at a lower elevation at some point during the hydrograph simulation than at the end of the hydrograph. On the left side of the exit channel, at the gauge closest to the cutoff wall, the bed had been 20 ft lower than the final bed elevation. Previous experiments conducted with a concrete bed in the model indicated that the flip may not occur and thus the protective sediment deposit may not develop. Model results should not be interpreted to indicate that portions of the spillway cutoff wall would be protected from scour. As stated earlier, drawing conclusions relative to scour depth in the model should be done cautiously. The model provided a relative indication of scour patterns.

Type 3 exit channel design

The right training wall with a top elevation of 490 was reinstalled with the type 3 exit channel design. A sloping apron, which would be constructed of roller-compacted concrete, was provided for toe protection. The apron had a 1V on 1H slope and protected both sides of the training wall, the downstream edge of the spillway and 605 ft of the left descending bank (Plate 38). The apron extended down 80 ft to el 380.

The model bed was remolded back to conditions shown in Photo 18. During the experiments, the design spillway hydrograph was simulated up to the peak discharge of 481,000 cfs. Model boundary conditions were the same as for the type 1 exit channel design.

The hydraulic performance of the flip bucket at the design discharge of 481,000 cfs for the type 3 exit channel is shown in Photo 23. The simulated scour patterns are shown in Photo 24 and a contour plot in Plate 38.

The scour had a more symmetrical pattern than with previous experiments. Scour extended all the way to the bottom of the physical model along the toe of the left descending apron and was close to the model bottom adjacent to the toe of the right training wall apron. There was less scour in the center of the exit channel than in previous experiments.

The right training wall was overtopped from the backside at the design discharge with type 3 exit channel design. This resulted in a zone of potentially erosive velocities in the area between the outlet works and the right training wall. These velocities were measured in the physical model at 0.8 and 0.2 depths and are shown in Plate 39. It was recommended that the training wall be raised to el 505 to prevent the eddy and the high velocities behind the wing wall.

Type 4 exit channel design and type 19 spillway design

The next experiment was conducted to assess the influence of tailwater on scour patterns. To achieve a lower tailwater in the physical model it was necessary to remove the raised roadbed of the Corona Freeway that previously had been molded with concrete. In addition, the right training wall was raised to el 505. Model boundary conditions for the type 4 exit channel design are tabulated in the following table. Tailwater elevations were controlled by the downstream topography, which was subject to change depending on the deposition of sand from the scour hole. Compared to the type 1 design exit channel, tailwater elevations with the type 4 design exit channel were about 17 ft lower at 25,000 cfs and 9 ft lower at 481,000 cfs.

Discharge, Cfs	Time, hr	Tailwater, el[1]
25,000	20	467.6
100,000	15	475.6
200,000	8	481.0
350,000	2	487.6
450,000	3	489.4
481,000	5	490.4

[1] Tailwater measured in exit channel at Corona bridge.

A design change was made to the right guide berm of the spillway approach channel upstream from the ogee crest, to reflect the modified plans associated with the outlet works design (type 19 spillway design). Velocities across the guide berm were measured at the design discharge of 481,000 cfs and are shown in Plate 40. A maximum velocity of 12.14 fps was measured across the crest of the berm indicating that this area needs some type of revetment. There were no observable changes in flow patterns across the ogee spillway crest that would be expected to influence downstream scour patterns.

Hydraulic performance of the flip bucket with the type 4 exit channel design is shown in Photo 25. Scour patterns are shown in the contour plot in Plate 41.

As expected, the extent of scour was greater with the lower tailwater. The model bottom was exposed across the entire width of the exit channel. However, the maximum scour depth was located further downstream from the spillway than in previous experiments. This was attributed to a more effective flip due to less submergence by the tailwater. Scour was more extensive along the toe of the left descending apron than along the toe of the right training wall apron.

Type 5 exit channel design

In the type 5 design exit channel, a 605-ft-long training wall was added to the left side of the exit channel. This wall had the same dimensions as the right training wall. In addition, the roller-compacted concrete apron was extended an additional 150 ft downstream on the left descending bank. This extension was deemed appropriate because the scour hole and resultant bank erosion had moved further downstream with the lower tailwater tested in the previous experiment.

Hydraulic performance of the flip bucket with the type 5 design is shown in Photo 27. Scour patterns developed during the experiment are shown in Photo 28 and the contour plot in Plate 42.

With the addition of the left training wall there was about a 50-ft increase in the length of the deposition zone downstream from the end of the spillway. This provided additional protection to the spillway. The benefit of this additional protection would need to be weighed against the cost of the training wall.

Water surface elevations on both sides of the right and left training walls were measured at the design discharge of 481,000 cfs with the type 5 exit channel design. These measurements were taken to aid in the structural design of the training wall. On the spillway side of the training wall there was considerable water surface fluctuation. Measurements reflect both the elevation of the relatively slow moving water directly adjacent to the training wall and the elevation of the aerated plume emerging from the flip bucket. Measured water surface elevations are given in Table 1 and are represented graphically in Plates 43 and 44. The graphs show that the plume reached an elevation higher than that of the training walls on both sides of the channel.

Type 6 exit channel design

A soils investigation conducted downstream from the spillway revealed that a sandstone bench existed downstream from the spillway. The top elevation of the sandstone bench was near the surface of the existing bed at el 460. The sandstone bench extended about 560 ft downstream from the spillway on the left side, about 120 ft downstream at the center line of the spillway, but did not exist on the right side next to the training wall. This approximate bench geometry was incorporated into the physical model and molded with concrete.

Table 1
Measured Water Surface Elevations Prado Exit Channel – Type 5

Station[1]	To Right of Wall	To Left of Wall (non-aerated water)	To Left of Wall (aerated water)
Right Wing Wall			
2085			
2110	489.4	473.025	
2140	488.85	457.45	
2170	487.15	456.75	
2200	487.3	500.4	
2230			507.85
2260	487.25		509.9
2290		488.4	505.3
2315		489.65	495.75
2345	486.9	481.75	499.9
2375	487.65	482.3	487.5
2405	489.2	490.6	491.4
Left Wing Wall			
2085			
2110	489.825	470.3	
2140	491.3	458.525	
2170	487.75	460.5	
2200	489.25	473.1	
2230			502.3
2260	486.5		507.1
2290		484.05	507.8
2315		478.4	505.95
2345	486.9	476.35	507.4
2375	485.3	489.85	492
2405		487.5	492

[1] Station 11+00 is the center line of the crest of the weir.

In addition to the natural sandstone, the type 6 exit channel design consisted of a roller-compacted concrete apron with a 55-ft-wide bench on the right side of the spillway. The new apron design tied into the sandstone bench about 170 ft from the right training wall. The remainder of the bed in the exit channel was molded in sand and returned to the existing bed elevations as shown in Photo 18 and Plate 45. The Los Angeles District determined that the left training wall was not cost effective and it was removed from the model in the type 6 exit channel design.

Hydraulic performance of the flip bucket for the type 6 design exit channel is shown in Photo 29. Scour patterns are shown in photos 30 and 31 and with the contour plot in Plate 45. Hydraulic performance of the type 19 spillway and type 6 exit channel design is shown in Figures 14 and 15. The asymmetric configuration of the sandstone bench did not have an adverse effect on the operation of the flip bucket or on scour potential downstream.

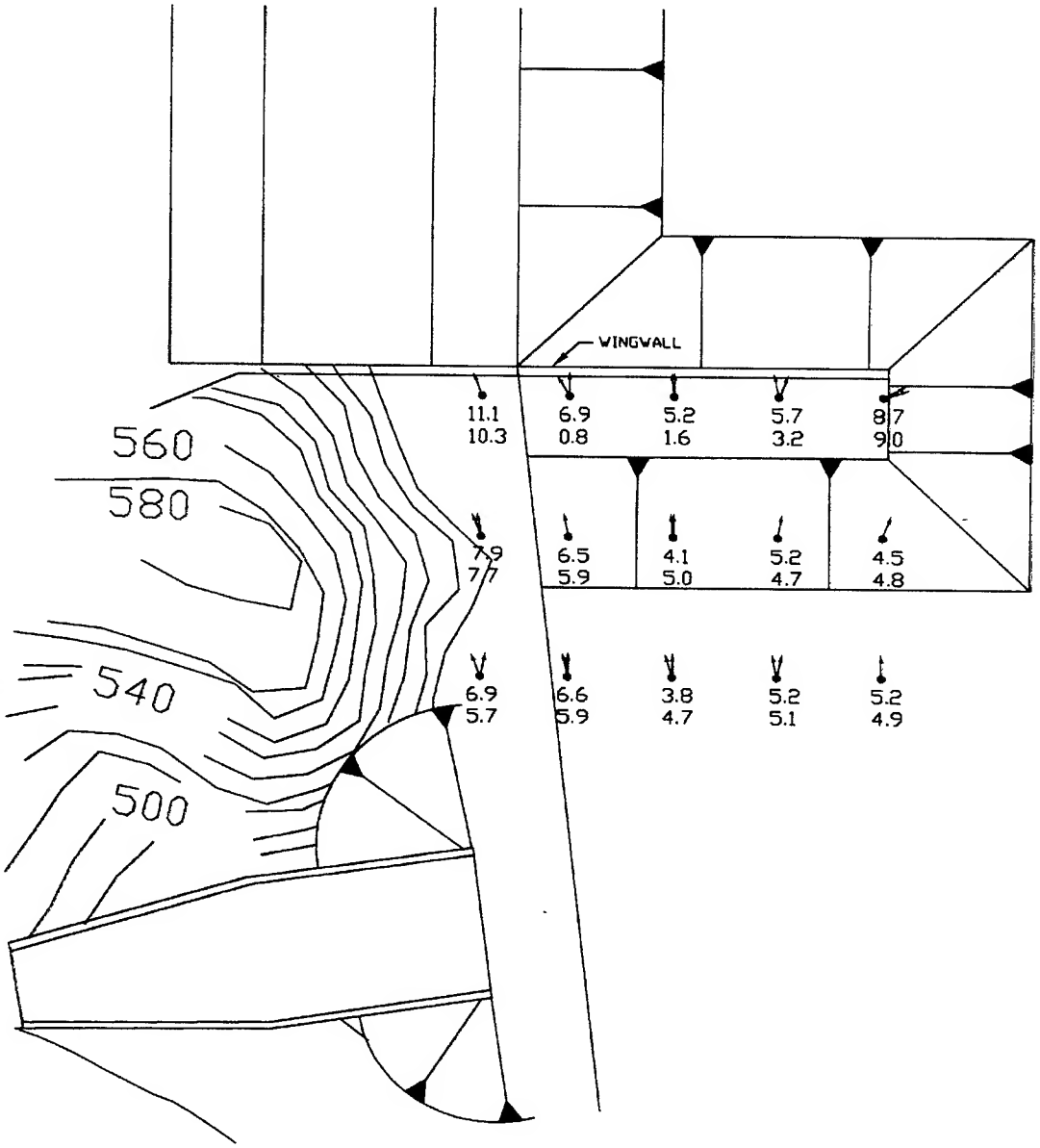

NOTE: VELOCITIES ARE IN PROTOTYPE FT PER SEC AND WERE MEASURED AT 20 AND 80 PERCENT ABOVE THE BOTTOM

3.8 80 PERCENT
4.7 20 PERCENT

EXIT CHANNEL
TYPE 3
VELOCITIES AND CURRENT DIRECTIONS ALONG RIGHT WINGWALL

DISCHARGE: 481,000 CFS

Plate 39

Plate 40

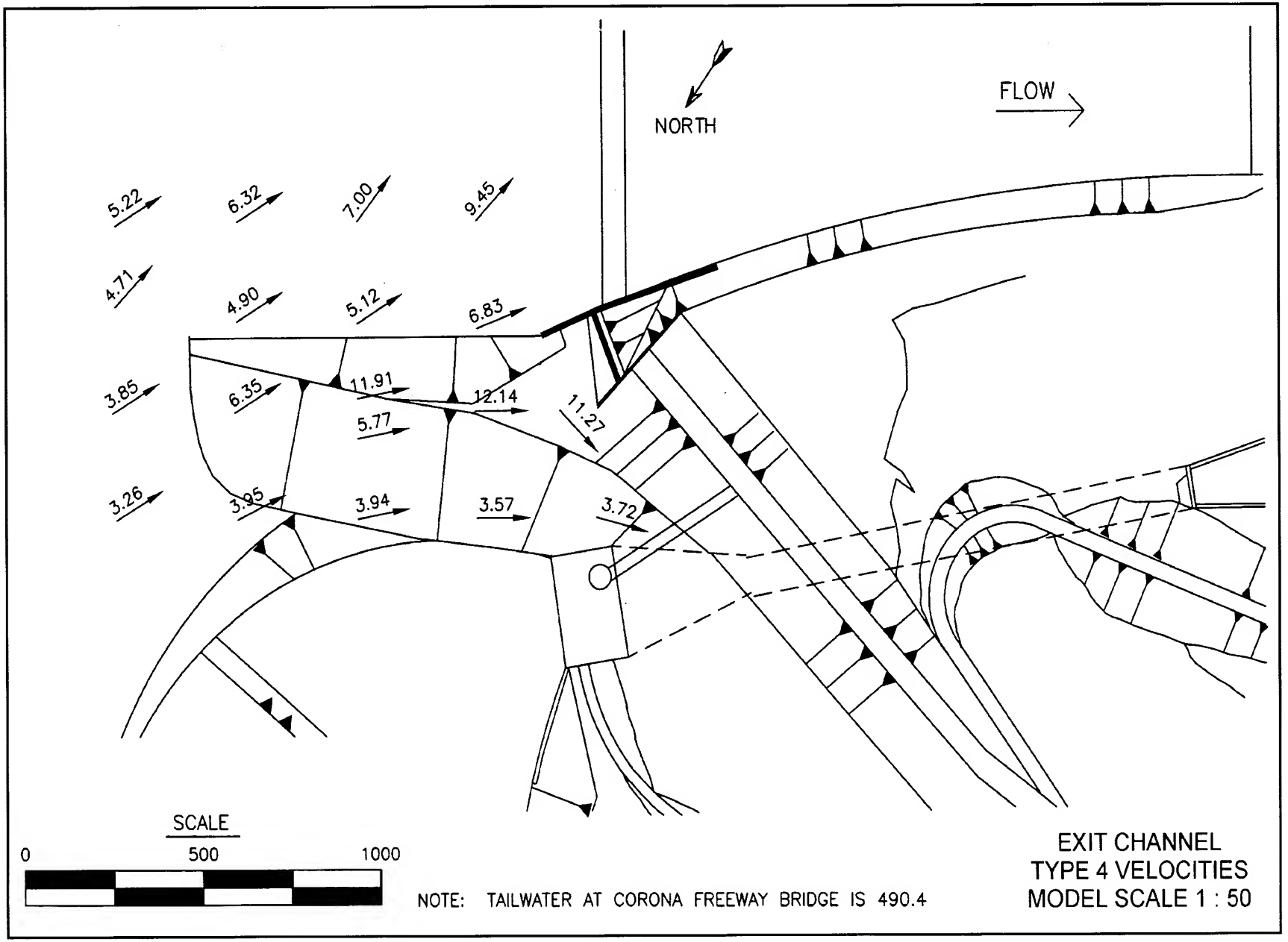
NORTH
FLOW
5.22
6.32
7.00
9.45
4.71
4.90
5.12
6.83
3.85
6.35
11.91
12.14
11.27
5.77
3.26
3.95
3.94
3.57
3.72
SCALE
0
500
1000
NOTE: TAILWATER AT CORONA FREEWAY BRIDGE IS 490.4
EXIT CHANNEL
TYPE 4 VELOCITIES
MODEL SCALE 1 : 50

4 Conclusions

A 1:50-scale hydraulic model was used to determine hydraulic performance characteristics of the Prado Dam spillway. Spillway rating curves were determined for labyrinth and ogee-crested weirs. Velocities were measured in the spillway approach channel and across approach channel abutments and berms. The model was used to evaluate water-surface elevations in the spillway channel and chute, velocities and surges against the downstream dam embankment, scour potential against the downstream spillway training wall and cutoff wall, and to design toe protection for these downstream features.

The model scale was sufficiently large so reliable rating curves could be determined for the labyrinth and ogee weirs. Scale effects associated with viscosity and surface tension were negligible for the discharges investigated in the model.

Both physical and numerical model simulations predicted that the eucalyptus grove, located about 1,000 ft upstream from the spillway crest, would not significantly affect spillway capacity or approach flow. Calculated and measured velocity magnitudes and directions showed only slight differences with trees simulated in the models.

The spillway rating curve developed from physical model measurements for the labyrinth weir indicated a less efficient spillway than calculated from the Lux and Hinchliff (1985) empirical equation. This result emphasizes the need for a physical model for labyrinth weirs.

Labyrinth spillway efficiency was improved only slightly by several modifications evaluated in the physical model. These included streamlining the crest, removing the existing downstream ogee crest, and streamlining the abutments with wing walls and training structures.

The recommended ogee spillway configuration (type 18 design) would be able to pass the design discharge of 481,000 cfs with a pool elevation of 587.5.

Standing waves as high as 22 ft can be expected in the center of the spillway channel at the design discharge of 481,000 cfs. Measured water-surface elevations adjacent to the existing spillway channel walls indicated that the wall would be overtopped during the design discharge.

The weight of the spillway concrete monoliths is sufficient to withstand differential hydraulic surface pressures during all anticipated discharges. Model results indicated, however, that if hydrostatic pressure is allowed to build up beneath the monoliths due to joint leakage and malfunctioning of the subdrain, monolith displacement can be expected.

The model indicated that there is a potential for severe scour against the spillway cutoff wall and the right training wall during the PMF. Failure of the right training wall would result in severe erosion potential in the vicinity of the outlet works and would increase the magnitude of circulation against the dam embankment. A protective apron around the training wall and against the cutoff wall was evaluated in the model and is recommended. It is also recommended that the training wall top elevation be raised to el 505 to prevent overtopping.

References

Babb, A. F. (1976). "Hydraulic model studies of the Boardman Reservoir Spillway," R. L. Albrook Hydraulic Laboratory, Washington State University, Pullman, WA

Bernard, R. S. (1993). "STREMR: Numerical model for depth-averaged incompressible flow," Technical Report TR-REMR-HY-11, U.S. Army Engineer Waterways Experiment Station, Vicksburg, MS.

CH_2M Hill. (1974). "City of Dallas, Oregon, Mercer Dam Spillway Model Study."

George, J. F. (1989). "Model study of Prado Flood-Control Dam, hydraulic model investigation," Technical Report HL-89-19, U.S. Army Engineer Waterways Experiment Station, Vicksburg, MS.

Hager, W. H. (1987). "Lateral outflow over side weirs," *Journal of Hydraulic Engineering*, ASCE, 113(4), 491-504.

Hager, W. H. (1989). "Lateral outflow over side weirs – closure," *Journal of Hydraulic Engineering,* ASCE, 115(5), 684-688.

Hay, N., and Taylor, G. (1970). "Performance and design of labyrinth weirs," *Journal of the Hydraulics Division*, ASCE, 96(HY11), 2337-2357.

Headquarters, U.S. Army Corps of Engineers. (1990). "Hydraulic design of spillways," Engineering Manual 1110-2-1603, Washington, DC.

Hinchliff, D. L., and Houston, K. L. (1984). "Hydraulic design and application of labyrinth spillways," USBR Concrete Dams and Hydraulics Branch Design Memorandum.

Holley, E. R. (1989). "Lateral outflow over side weirs – discussion," *Journal of Hydraulic Engineering,* ASCE, 115(5), 682-684.

Houston, K. L. (1982). "Hydraulic model study of Ute Dam Labyrinth Spillway," Report GR-82-7, Bureau of Reclamation, Denver, CO.

Houston, K. L., and DeAngelis, C. S. (1982). "A site specific study of a labyrinth spillway," *Proceedings of the Conference Applying Research to Hydraulic Structures*, ASCE, 86-95.

Houston, K. L. (1983). "Hydraulic model study of Hyrum Auxiliary Labyrinth Spillway," Report GR-82-13, Bureau of Reclamation, Denver, CO.

Jain, S. C., and Fischer, E. E. (1981). "Uniform flow over skew side-weir," *Journal of Irrigation and Drainage*, ASCE, 108(2), 163-166.

Lux, F., and Hinchliff, D. L. (1985). *Proceedings of the 15th Congress of Large Dams*, Lausanne, Switzerland, 249-274.

Magalhaes, A. P., and Lorena, M. (1989). "Hydraulic design of labyrinth weirs," National Laboratory of Civil Engineering, No. 736, Lisbon, Portugal.

Mayer, P. G. (1980). "Bartletts Ferry Project labyrinth weir model studies," Project No. E-20-619, Georgia Institute of Technology, Atlanta, GA.

Maynord, S. T. (1985). "General spillway investigation – hydraulic model investigation," Technical Report HL-85-1, U.S. Army Engineer Waterways Experiment Station, Vicksburg, MS.

Phelps, H. O. (1974). "Model study of labyrinth weir – Navet Pumped Storage Project," University of the West Indies, Department of Civil Engineering, St. Augustine, Trinidad, West Indies.

Ramamurthy, A. S. et al. (1978). "Lateral weir flow model," *Journal of Irrigation and Drainage*, ASCE, 104(4), 399-412.

Rouse, H. (1960). *Elementary mechanics of fluids.* Wiley & Sons, New York.

Taylor, G. (1968). "The performance of labyrinth weirs," Ph.D. diss., University of Nottingham, Nottingham, England.

U.S. Army Engineer District, Los Angeles. (1988). "Phase II GDM on the Santa Ana River Mainstem, Vol. 2, Prado Dam," Los Angeles CA.

Vermeyen, T. (1991). "Hydraulic model study of Ritschard Dam spillways," Report R-91-08, Bureau of Reclamation, Denver, CO.

Walsh, J. M., and Jones, D. G. (1980). "Upper Waitaki Power Development hydraulic model study of Ohan C Canal labyrinth side-weir," Report No. 3-80/2, Ministry of Works and Development, Central Laboratories, New Zealand.

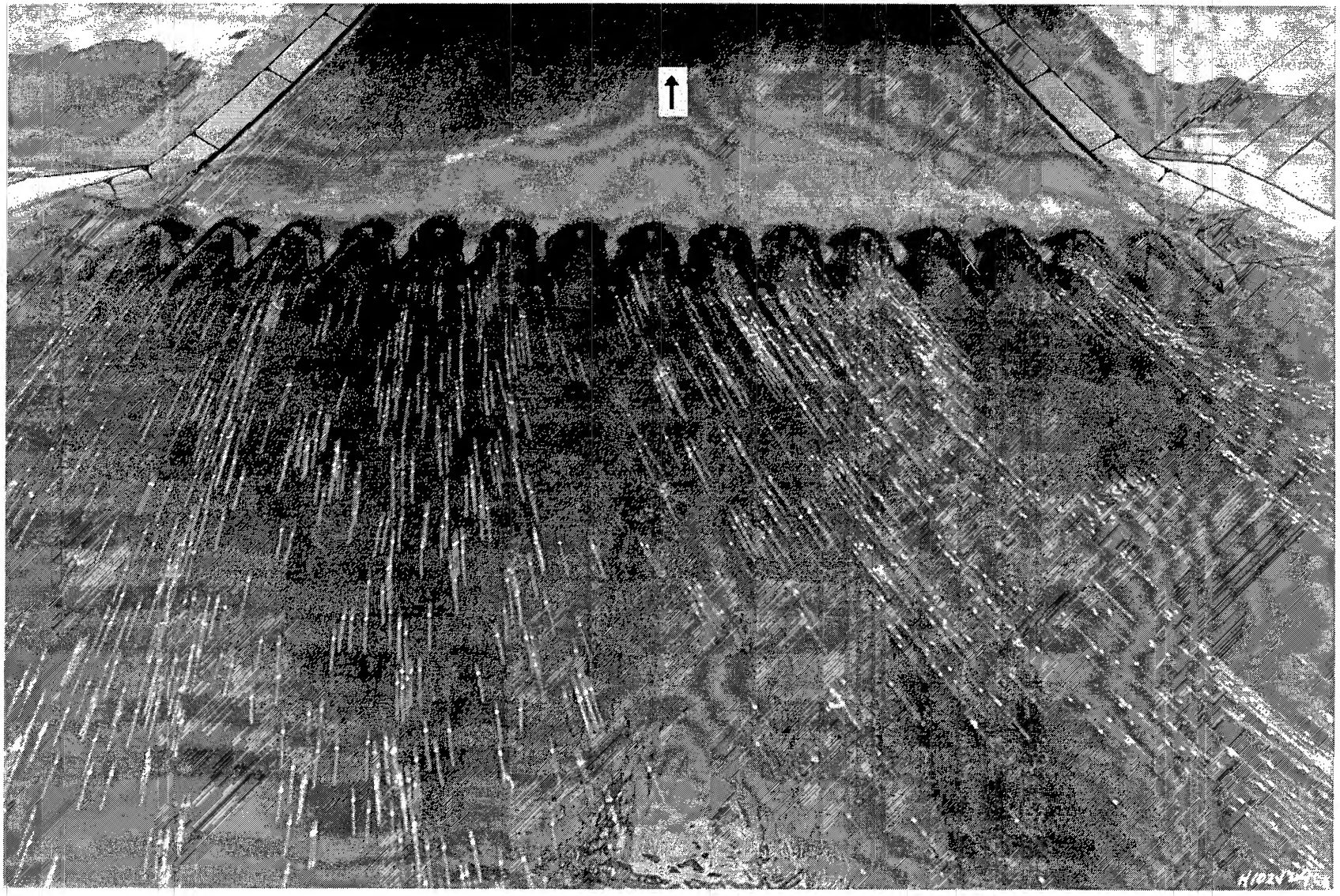

Photo 1. Type 1 spillway design, approach flow to labyrinth spillway, discharge 300,000 cfs, pool el 574.5, exposure time - 7 sec

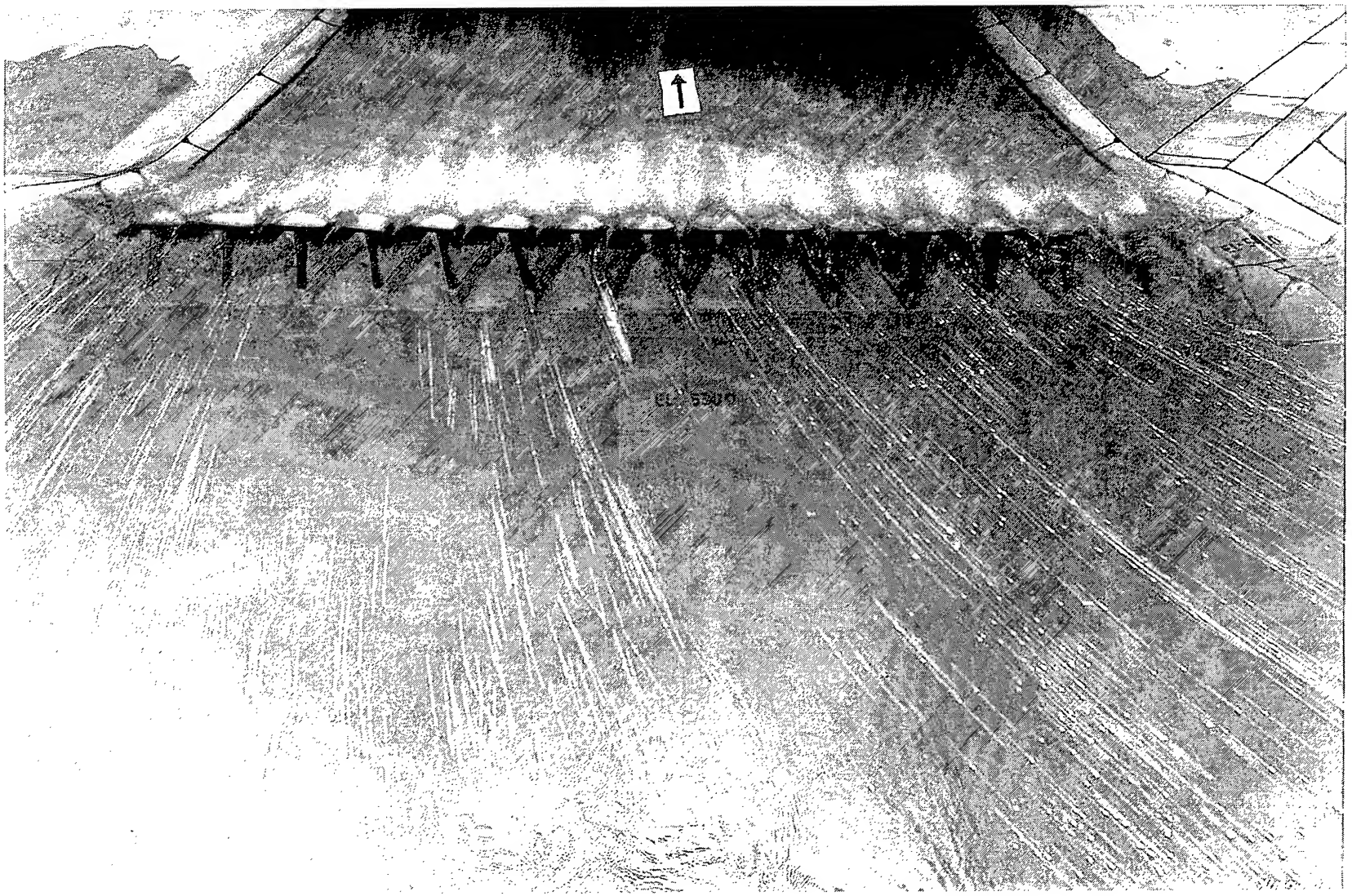

Photo 2. Type 1 spillway design, approach flow to labyrinth spillway, discharge 600,000 cfs, pool el 585.0, exposure time - 7 sec

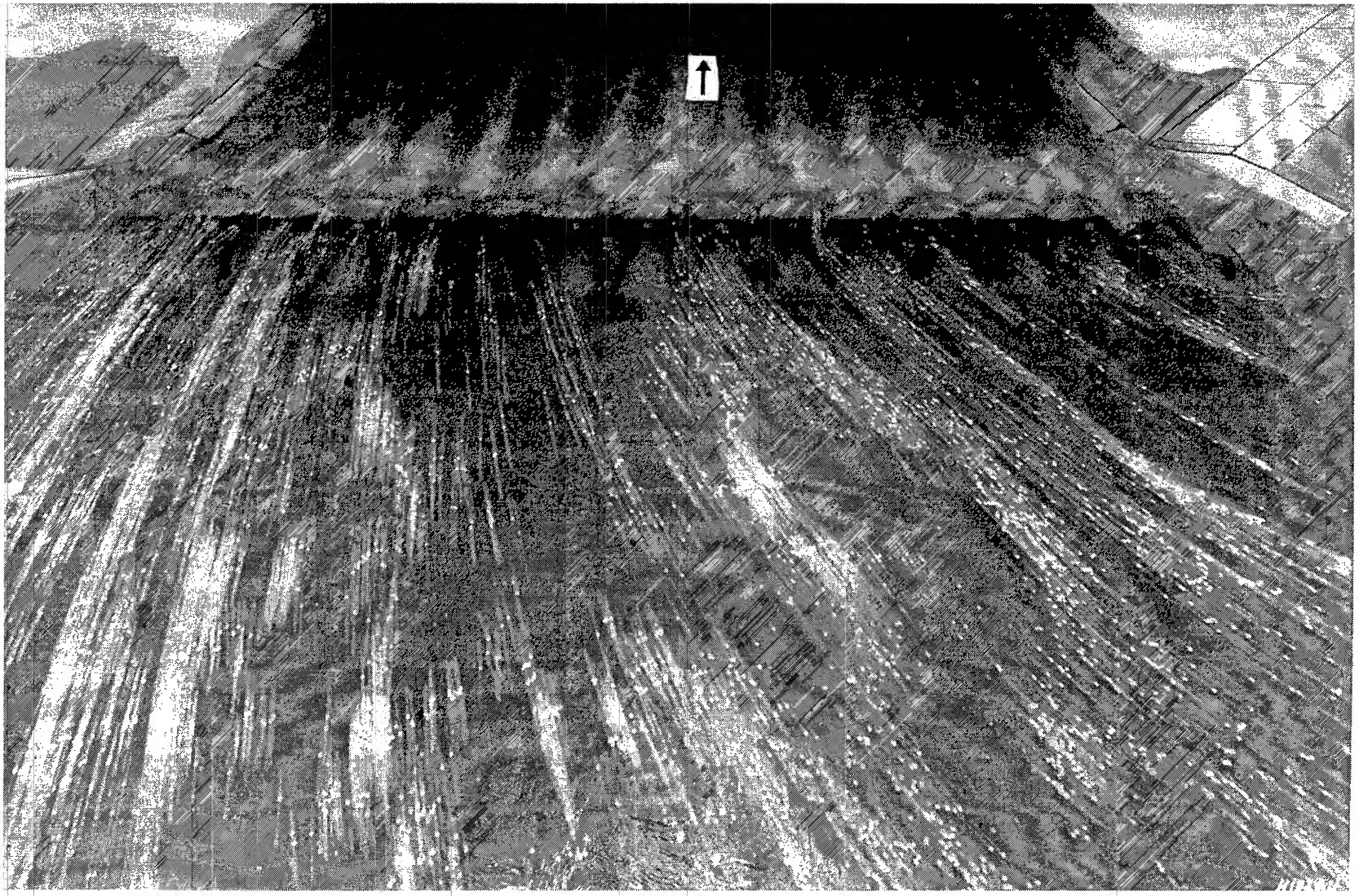

Photo 3. Type 1 spillway design, approach flow to labyrinth spillway, discharge 750,000 cfs, pool el 590.1, exposure - 7 sec

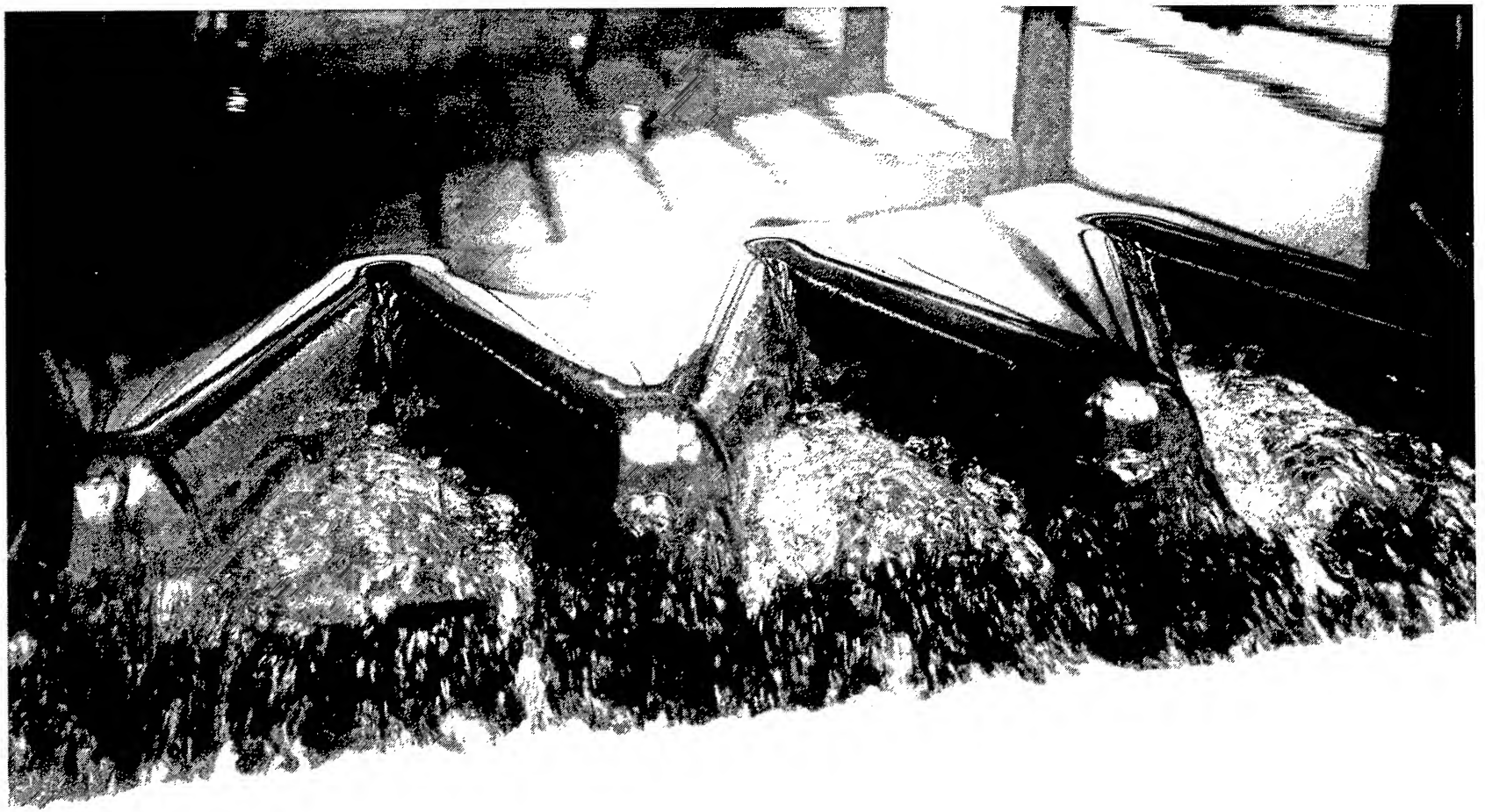

Photo 4. Type 1 spillway design, labyrinth spillway, discharge 100,000 cfs, pool el 568.0

Photo 5. Type 1 spillway design, labyrinth spillway, discharge 200,000 cfs, pool el 570.8

Photo 6. Type 1 spillway design, labyrinth spillway, discharge 300,000 cfs, pool el 574.5

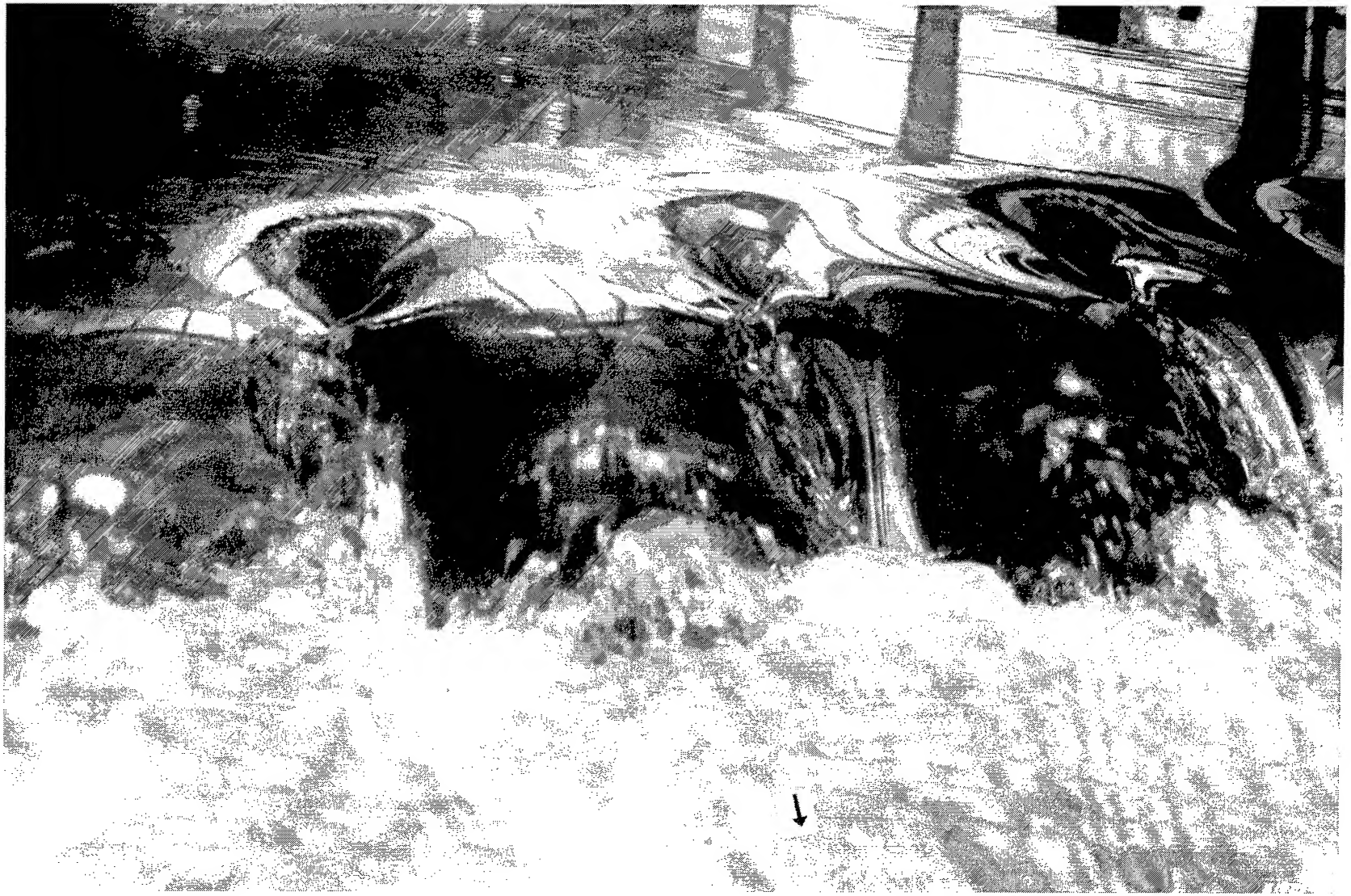

Photo 7. Type 1 spillway design, labyrinth spillway, discharge 600,000 cfs, pool el 585.0

Photo 8. Type 1 spillway design, labyrinth spillway, discharge 750,000 cfs, pool el 590.1

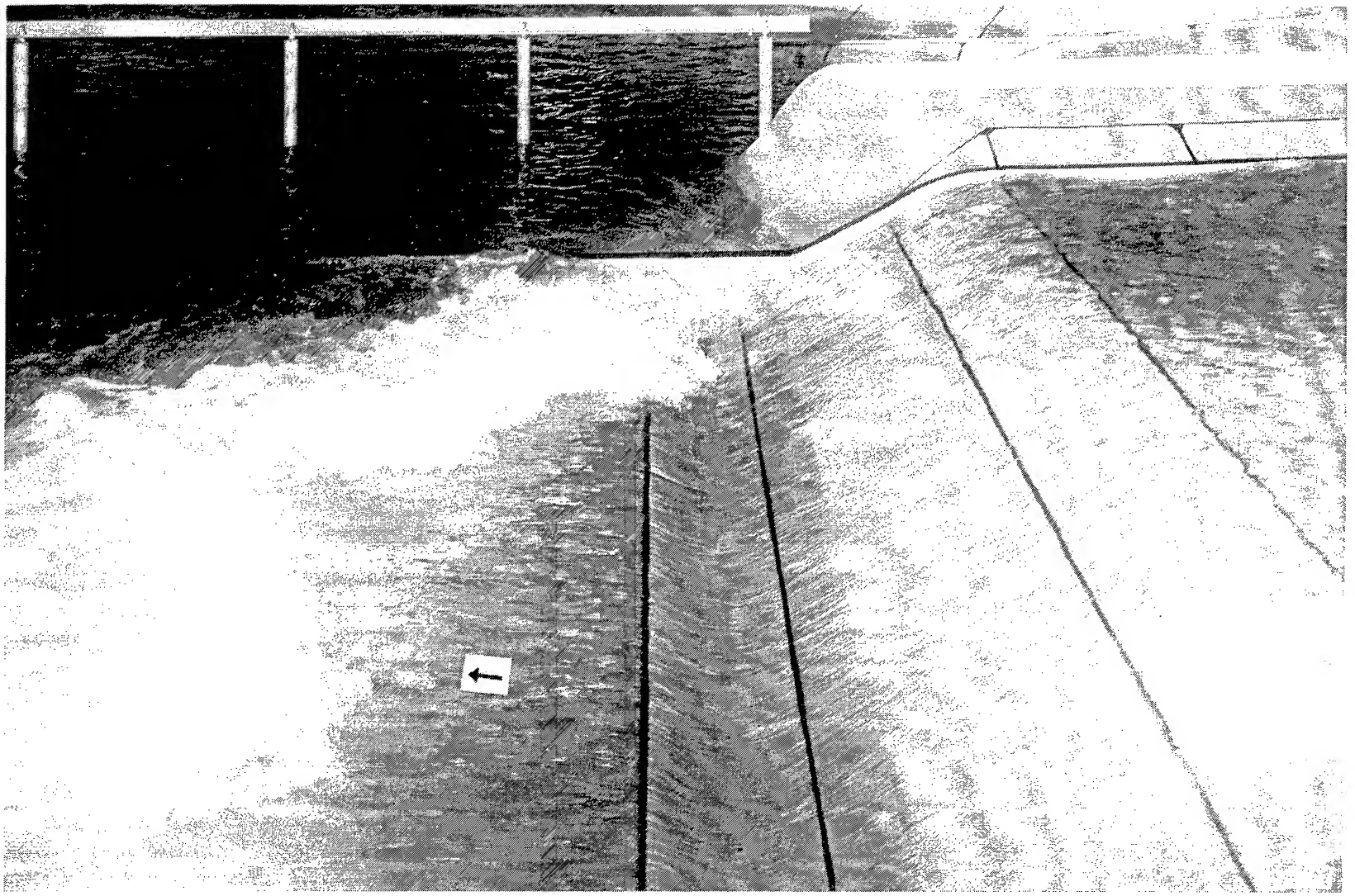

Photo 9. Type 1 spillway design, right side of spillway chute, discharge 300,000 cfs, tailwater el 497.0

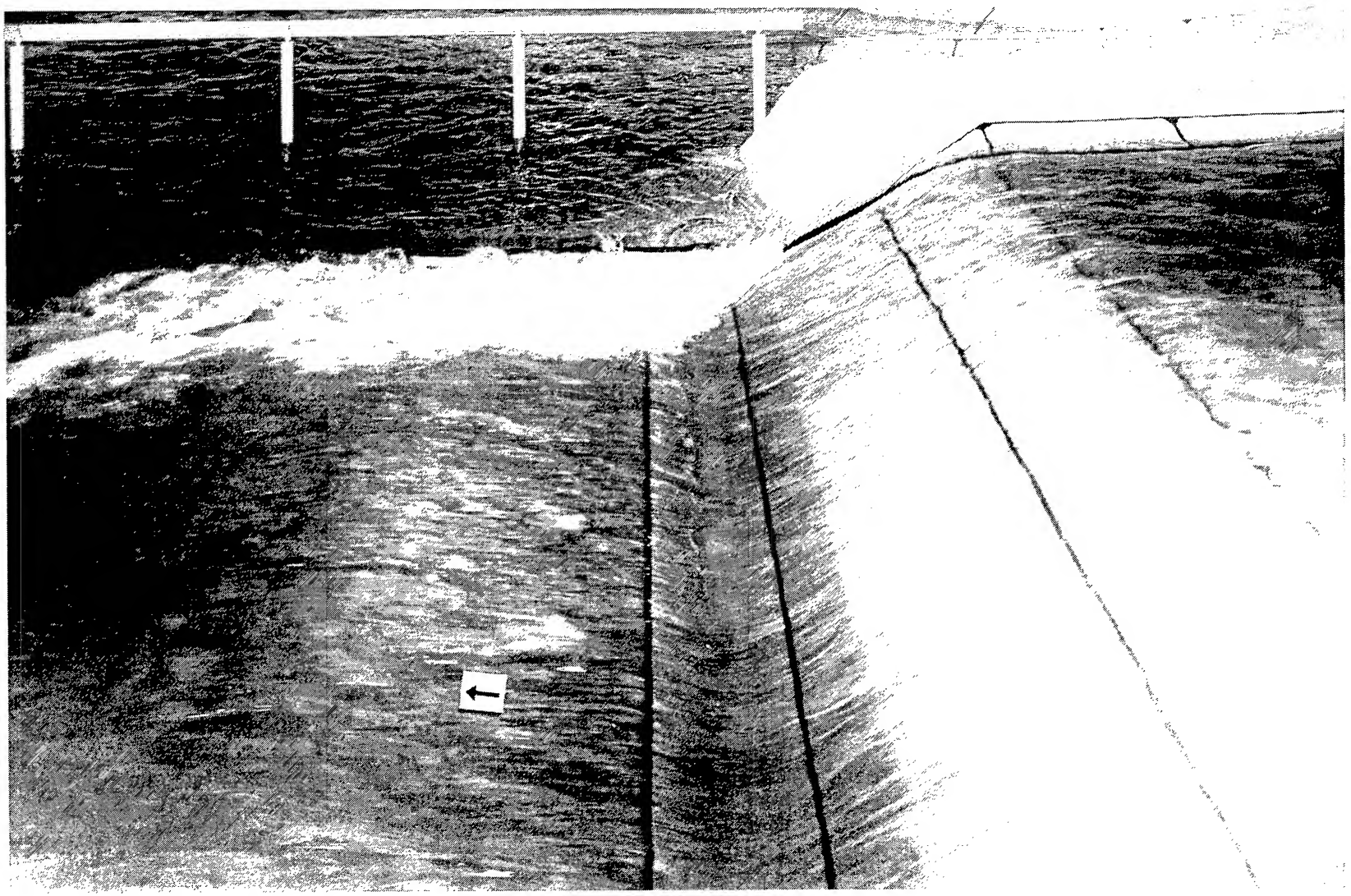

Photo 10. Type 1 spillway design, right side of spillway chute, discharge 600,000 cfs, tailwater el 499.0

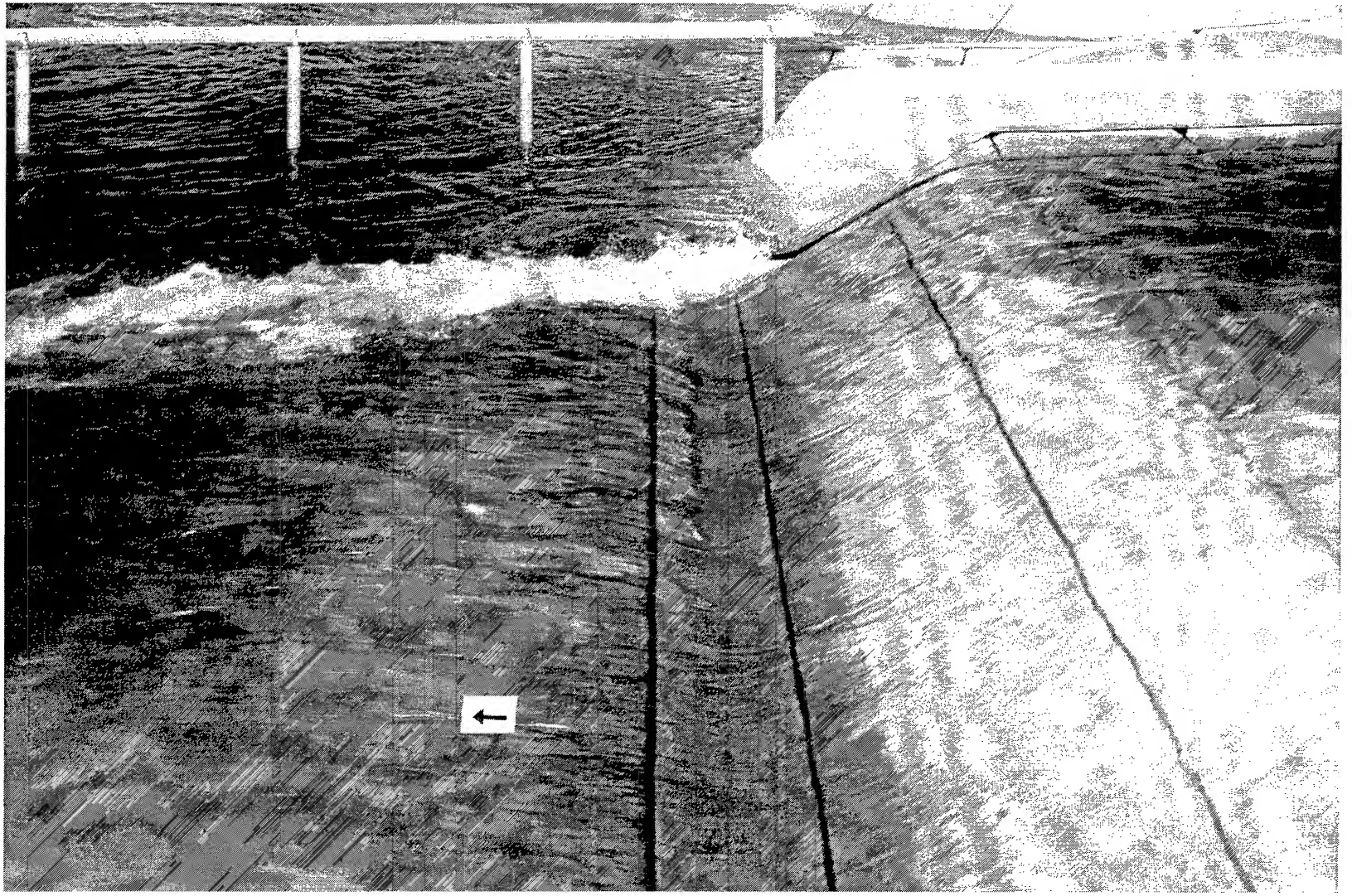

Photo 11. Type 1 spillway design, right side of spillway chute, discharge 750,000 cfs, tailwater el 499.0

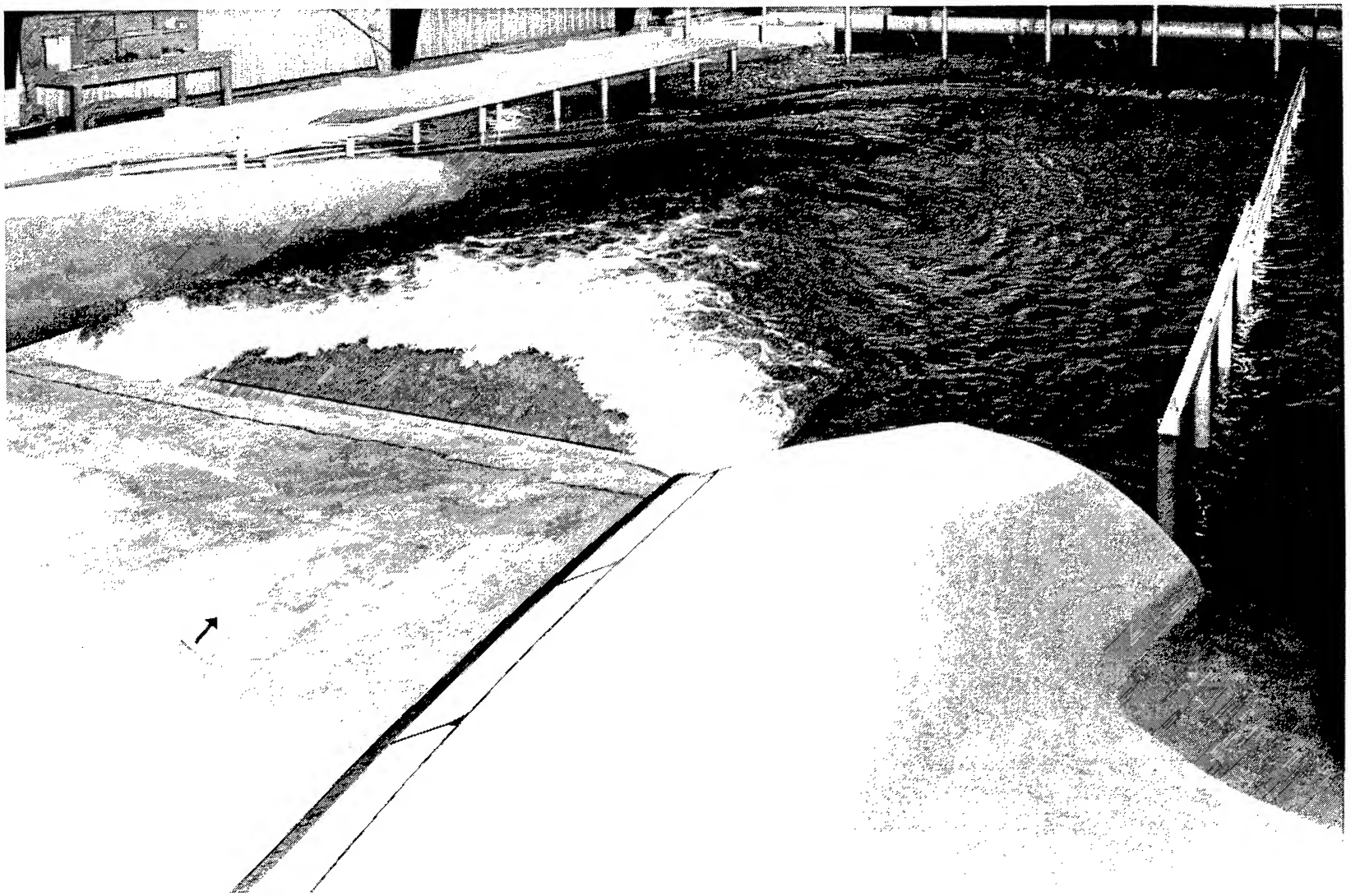

Photo 12. Type 1 spillway design, spillway chute and exit area, discharge 300,000 cfs, tailwater el 497.0

Photo 13. Type 1 spillway design, spillway chute and exit area, discharge 600,000 cfs, tailwater el 499.0

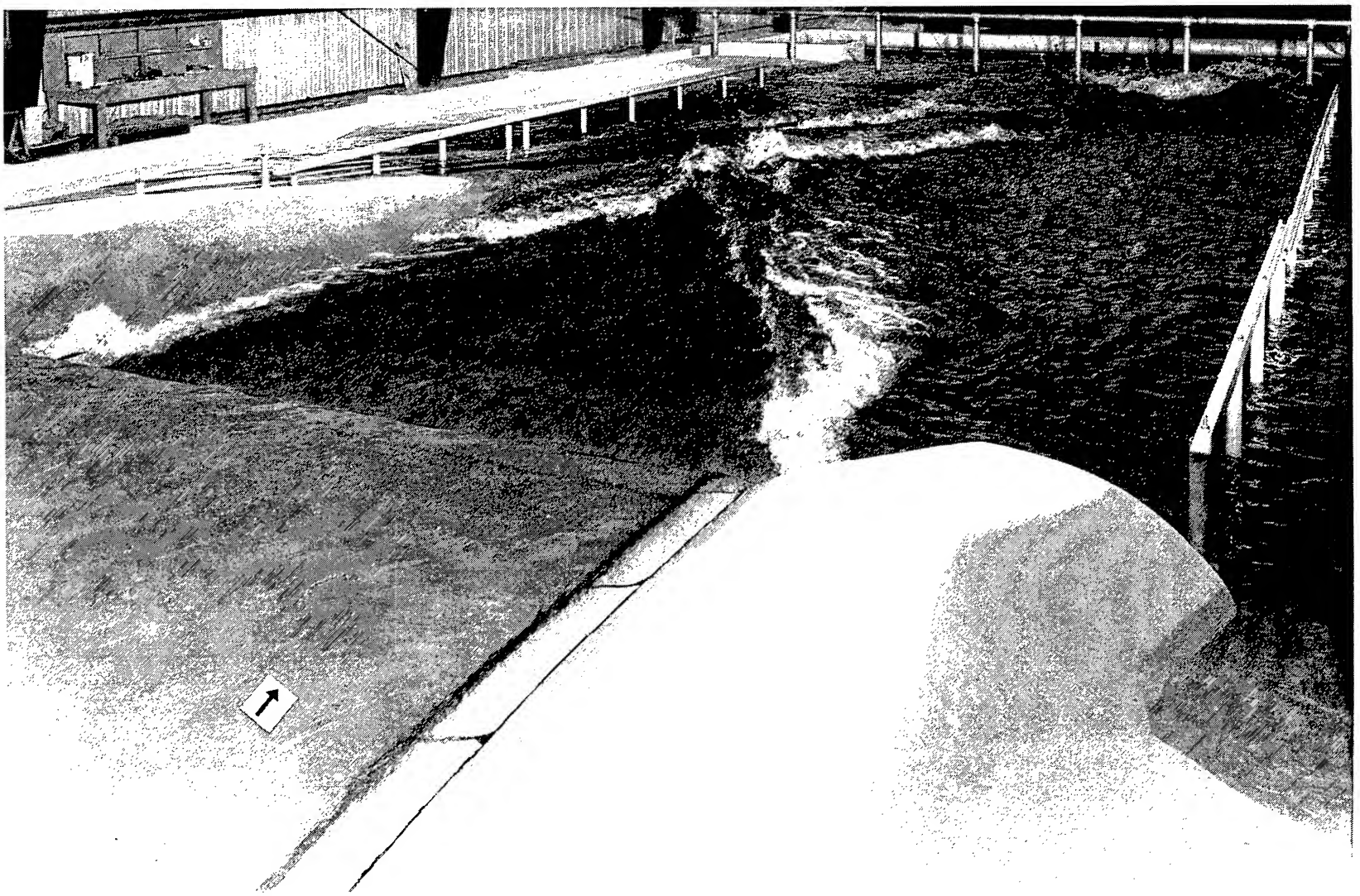

Photo 14. Type 1 spillway design, spillway chute and exit area, discharge 750,000 cfs, tailwater el 499.0

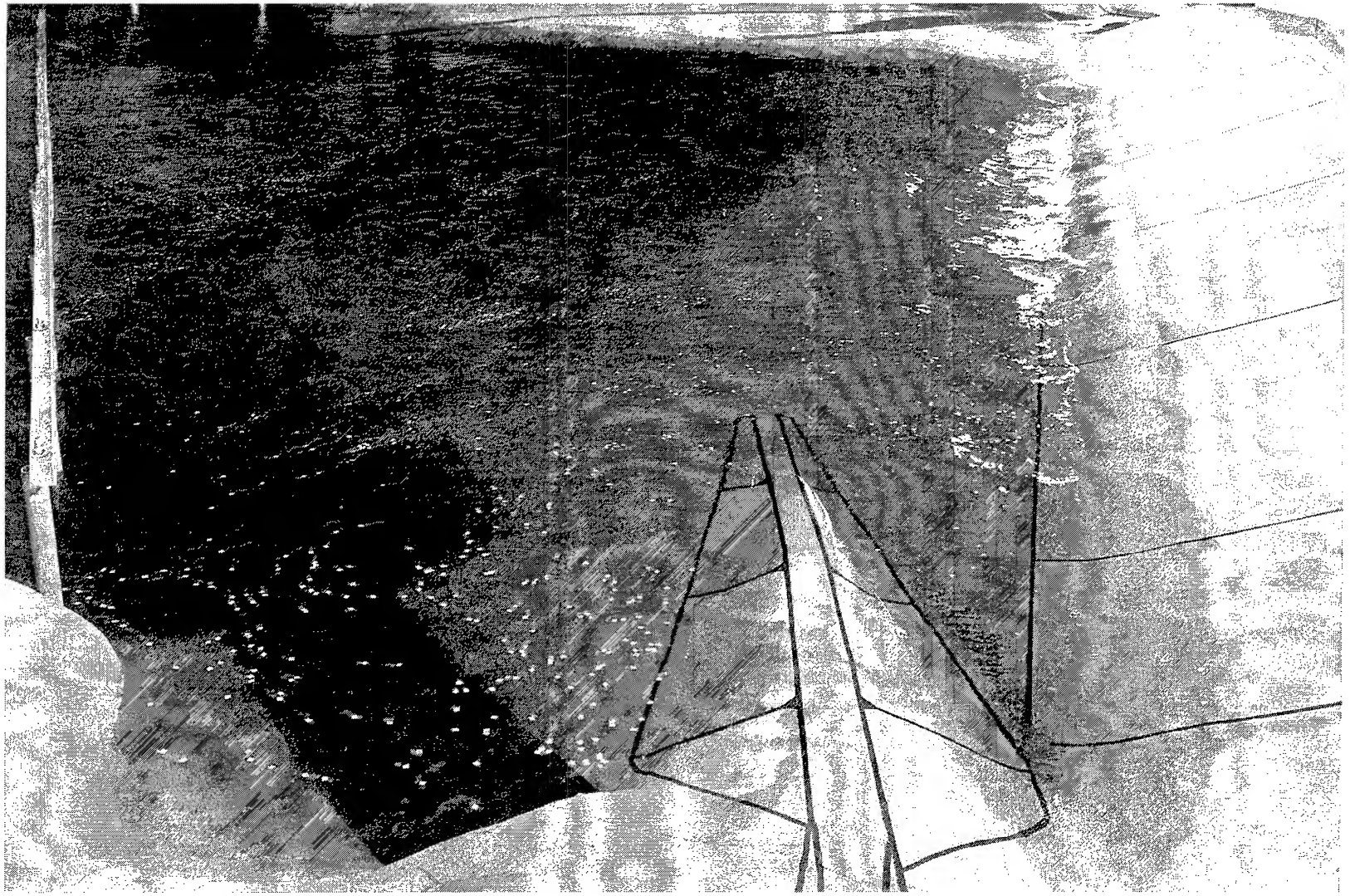

Photo 15. Type 1 spillway design, downstream side of dam embankment, discharge 750,000 cfs, tailwater el 499.0

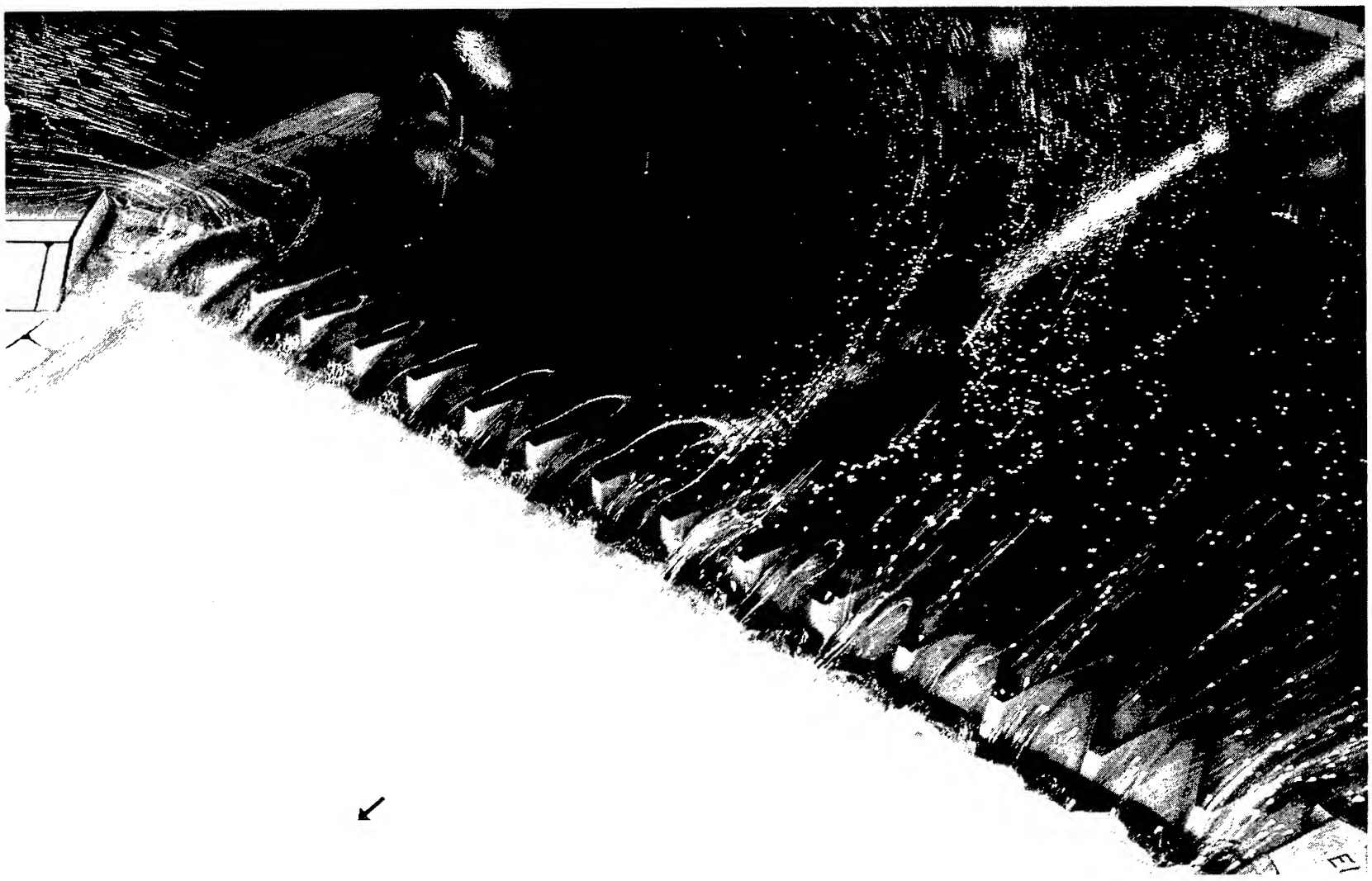

Photo 16. Type 1 spillway design, approach flow to labyrinth spillway, discharge 750,000 cfs, pool el 590.1, exposure 7 sec

Photo 17. Type 1 spillway design, approach flow to left abutment, discharge 750,000 cfs, pool el 590.1, exposure 7 sec

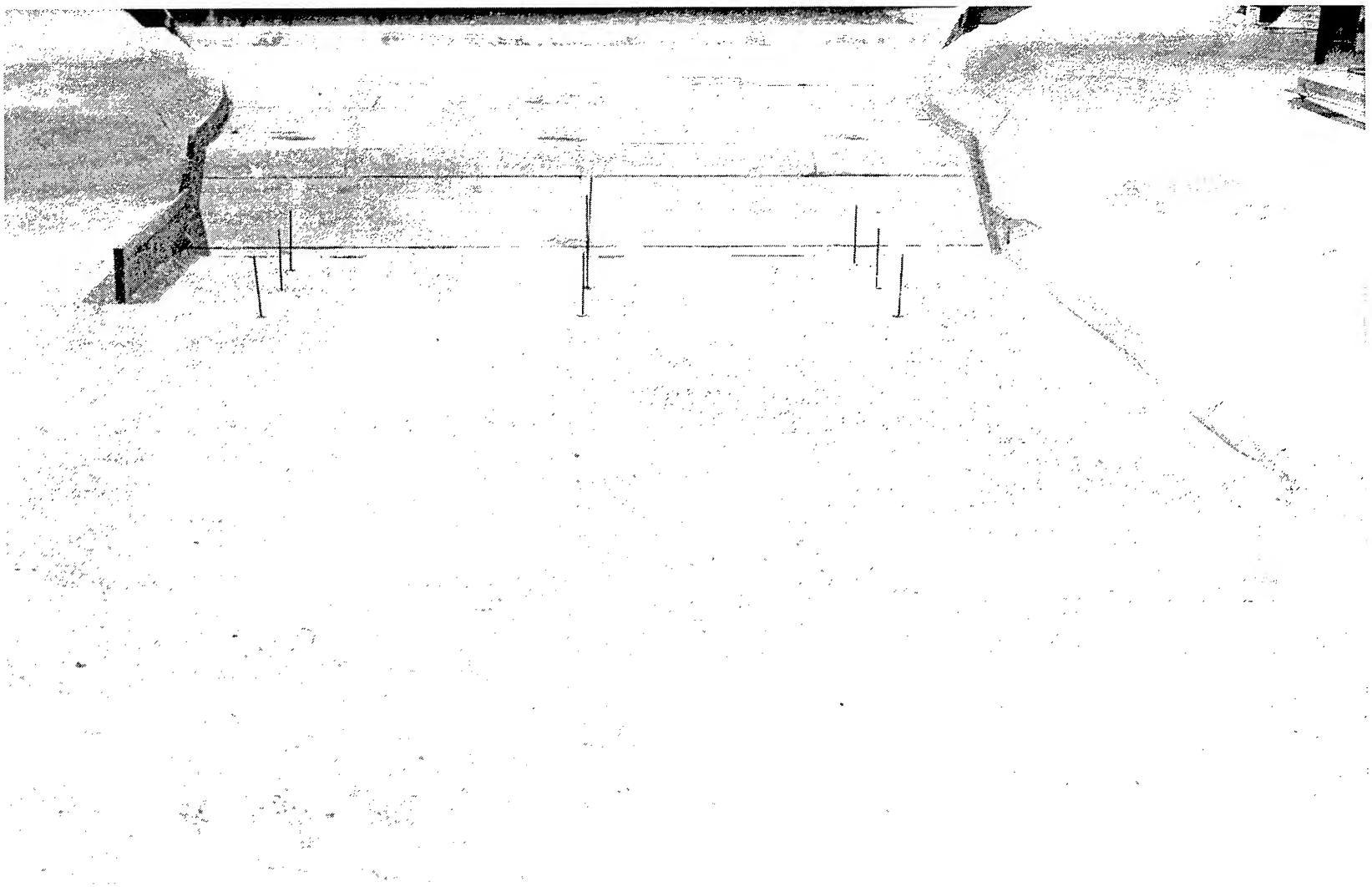

Photo 18. Type 1 exit channel design - dry bed before commencement of experiment

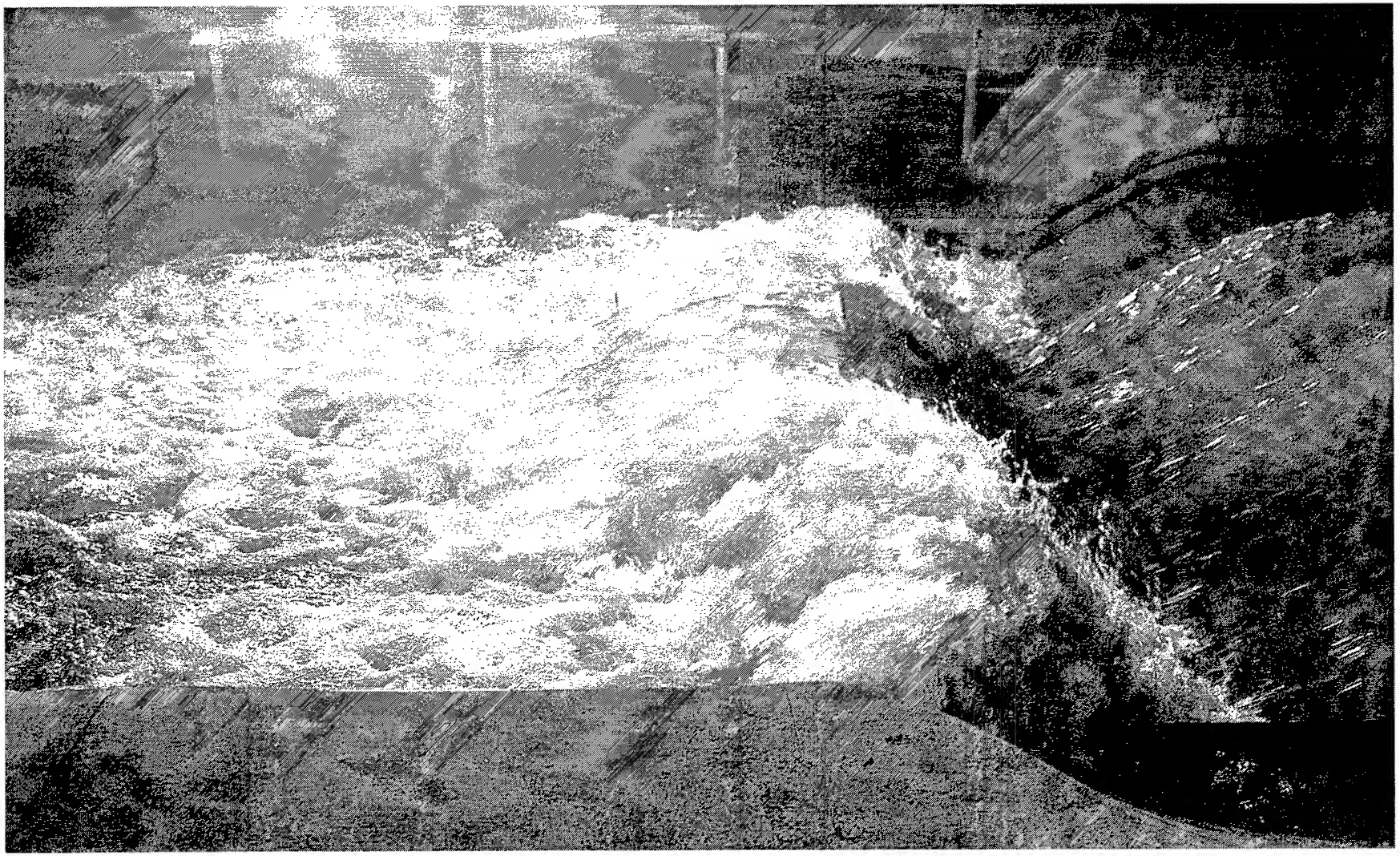

Photo 19. Type 1 exit channel design - flip bucket action at 481,000 cfs, tailwater el 499.7

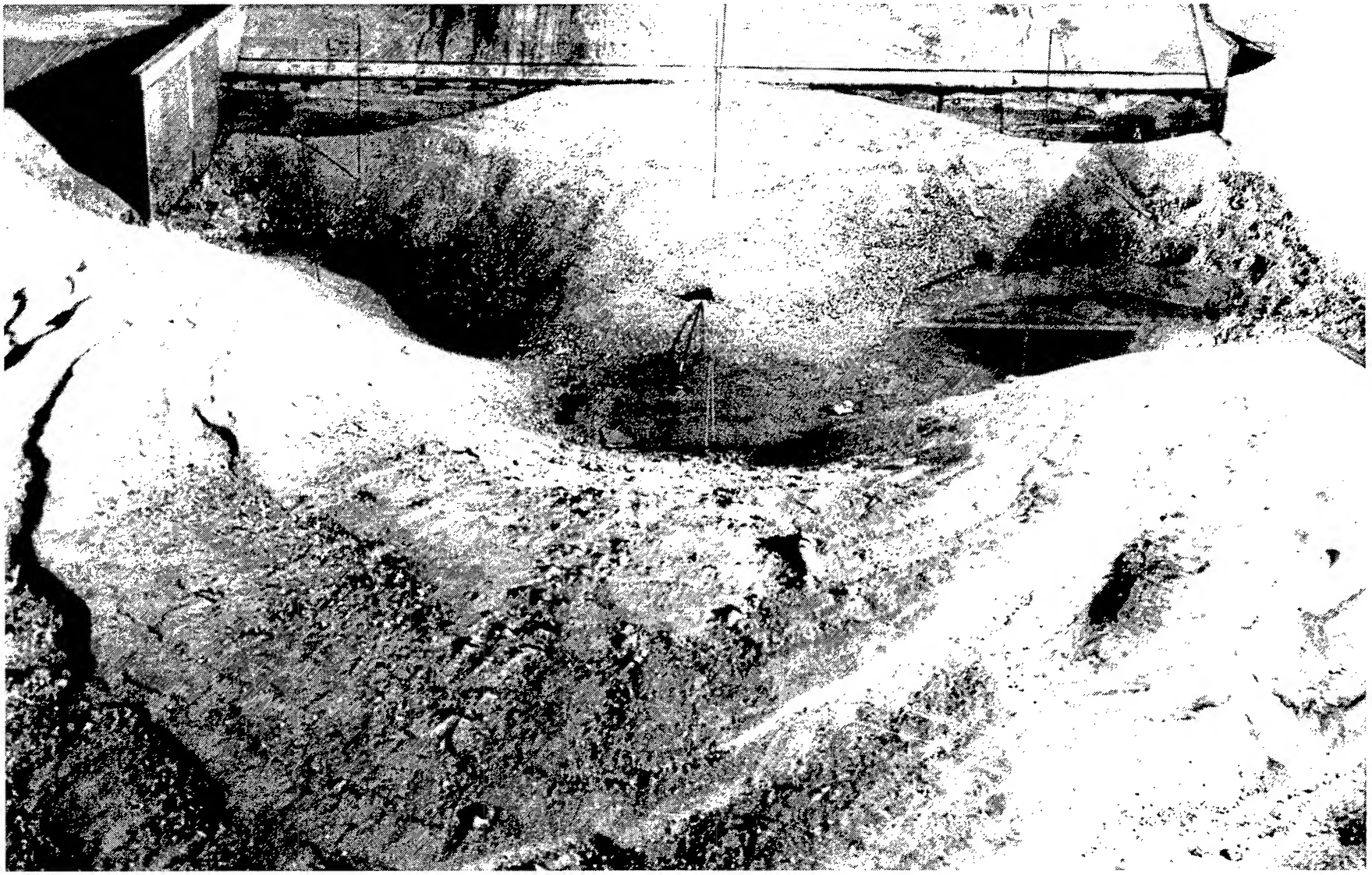

Photo 20. Type 1 exit channel design - scour downstream from spillway at end of experiment

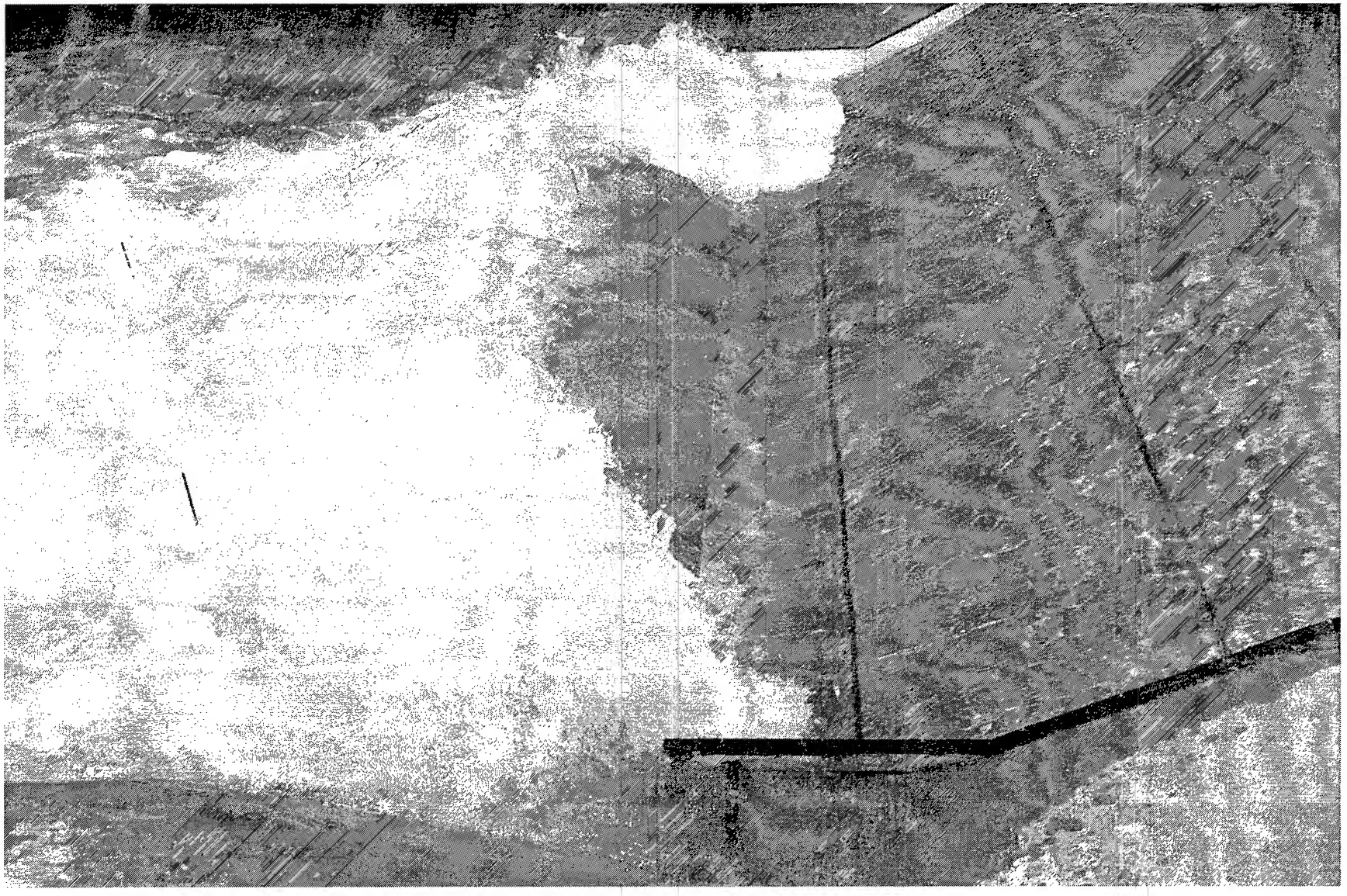

Photo 21. Type 2 exit channel design - flip bucket action at 481,000 cfs, tailwater el 499.7

Photo 22. Type 2 exit channel design - scour downstream from spillway at end of experiment

Photo 23. Type 3 exit channel design - flip bucket action at 481,000 cfs, tailwater el 499.7

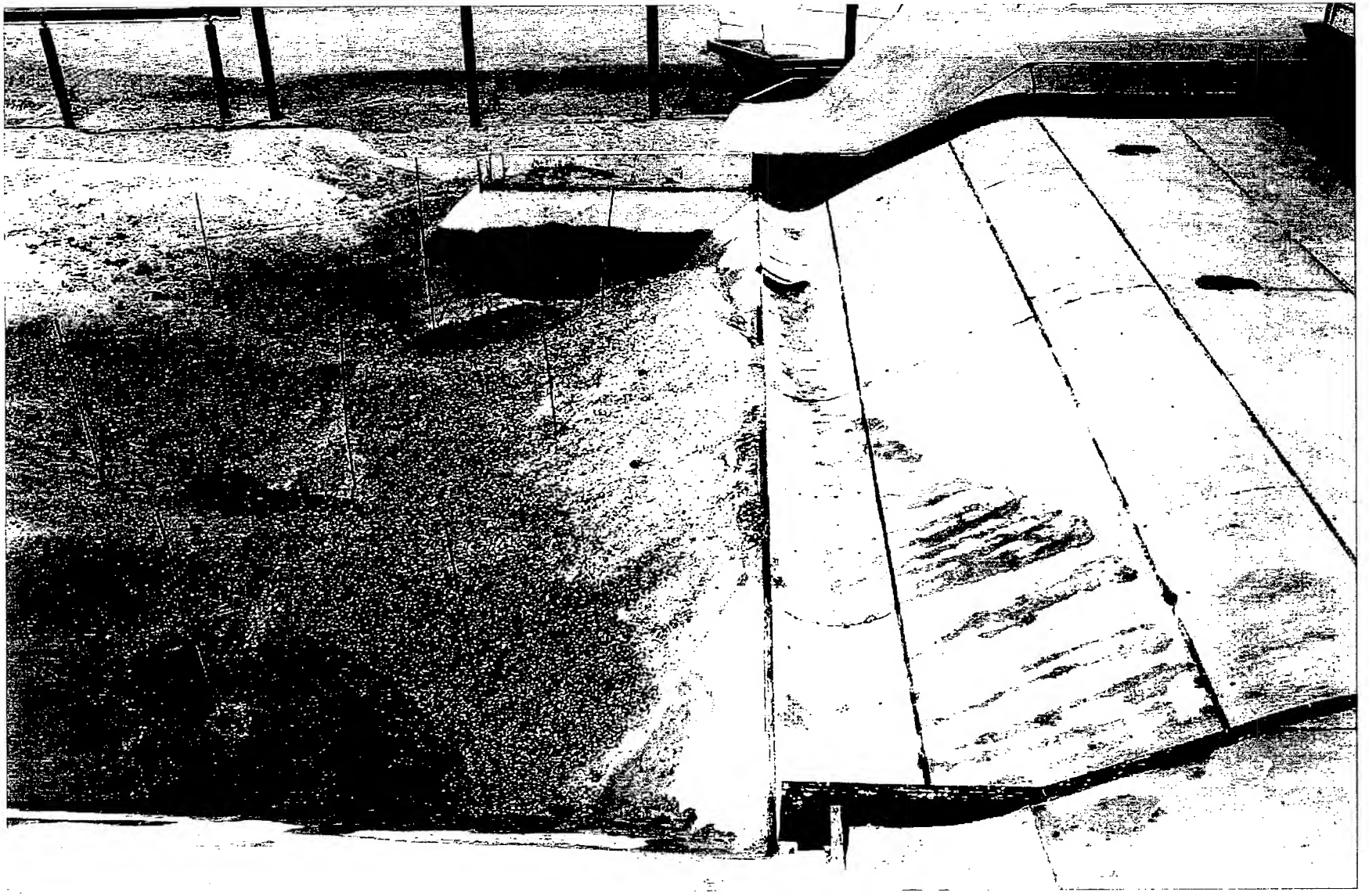

Photo 24. Type 3 exit channel design - scour downstream from spillway at end of experiment

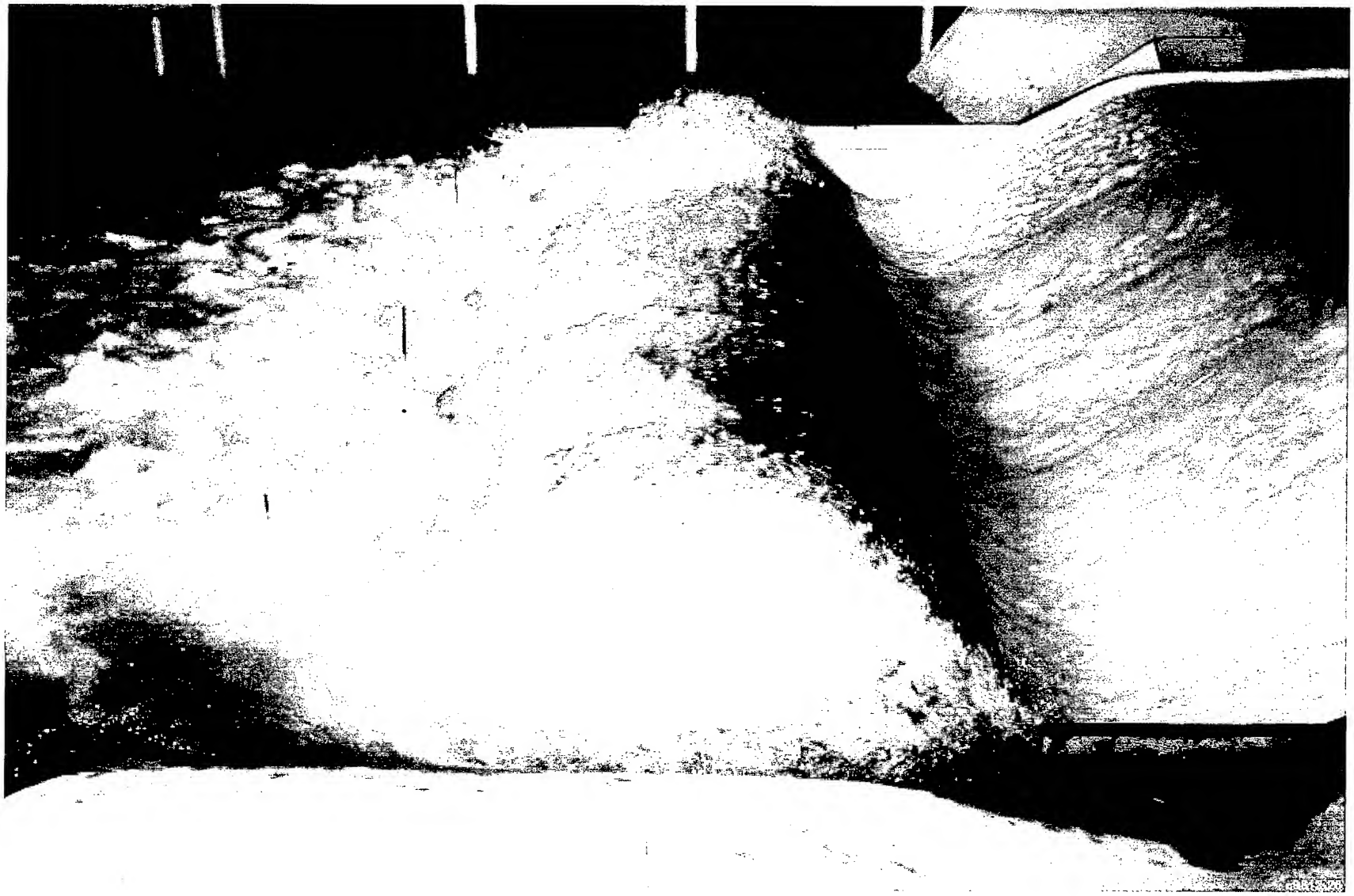

Photo 25. Type 4 exit channel – flip bucket action at 481,000 cfs, tailwater el 490.4

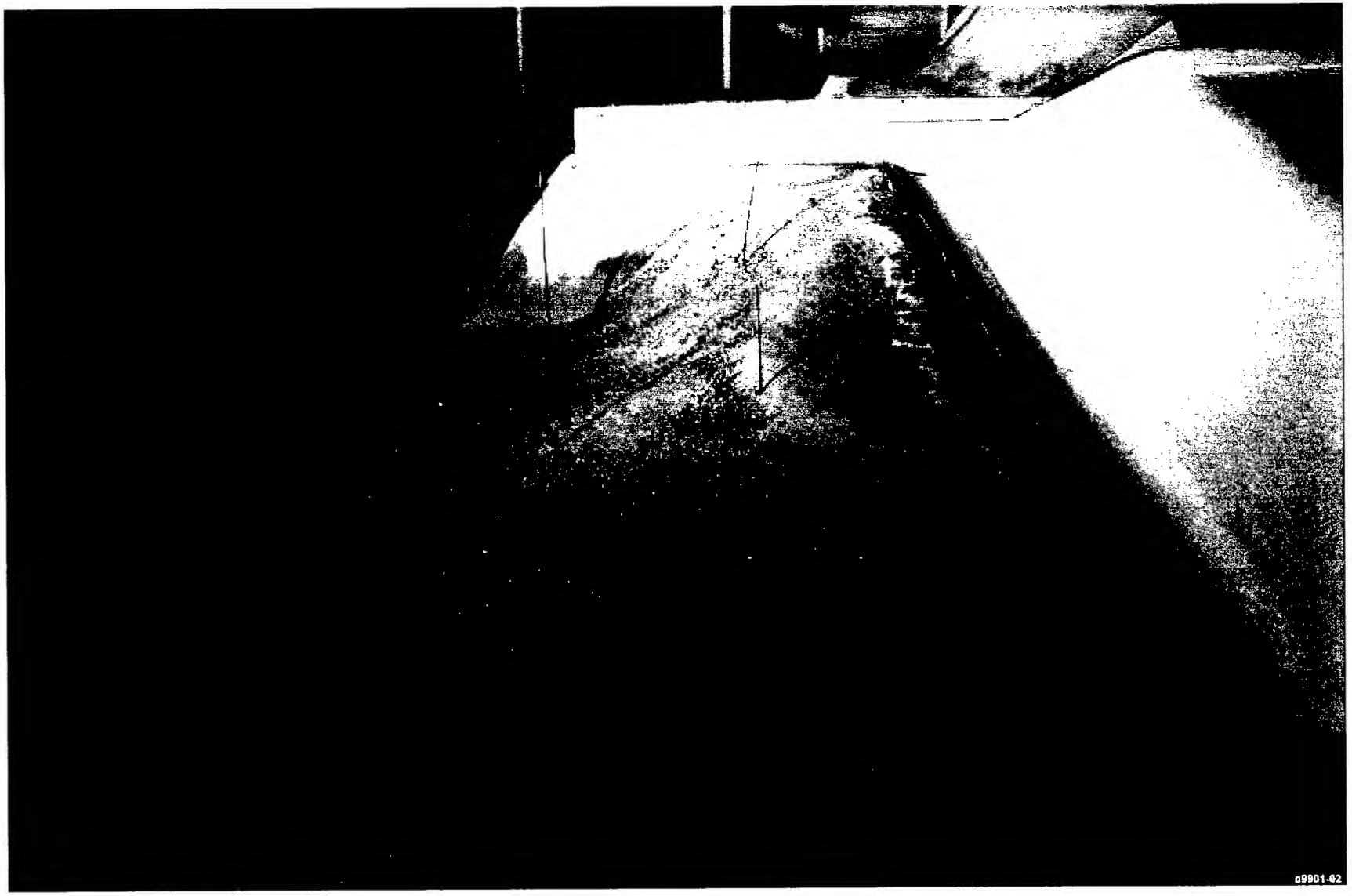

Photo 26. Type 4 exit channel design - scour downstream from spillway at end of experiment

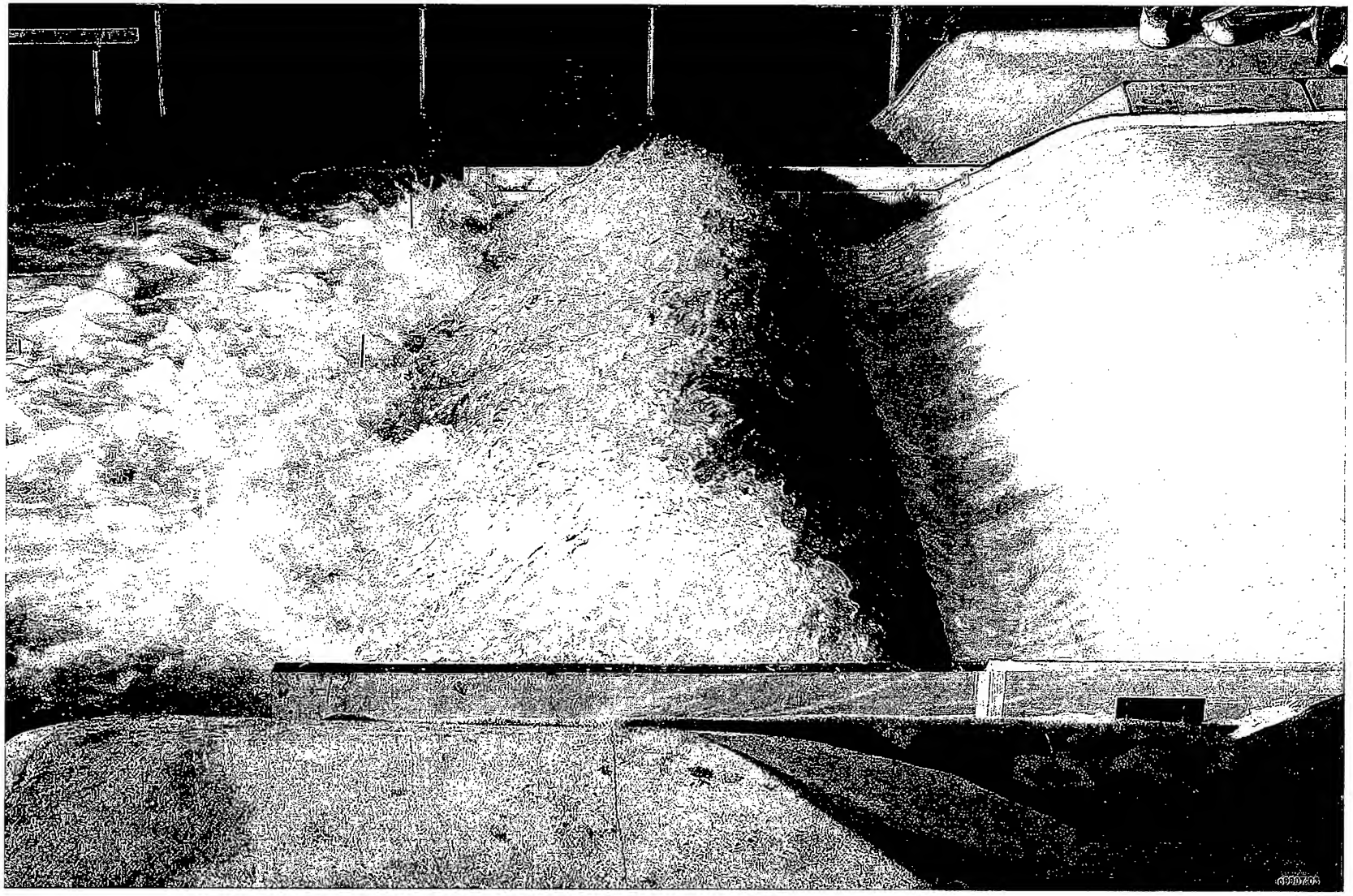

Photo 27. Type 5 exit channel design - flip bucket action at 481,000 cfs, tailwater el 490.4

Photo 28. Type 5 exit channel design- scour downstream from spillway at end of experiment

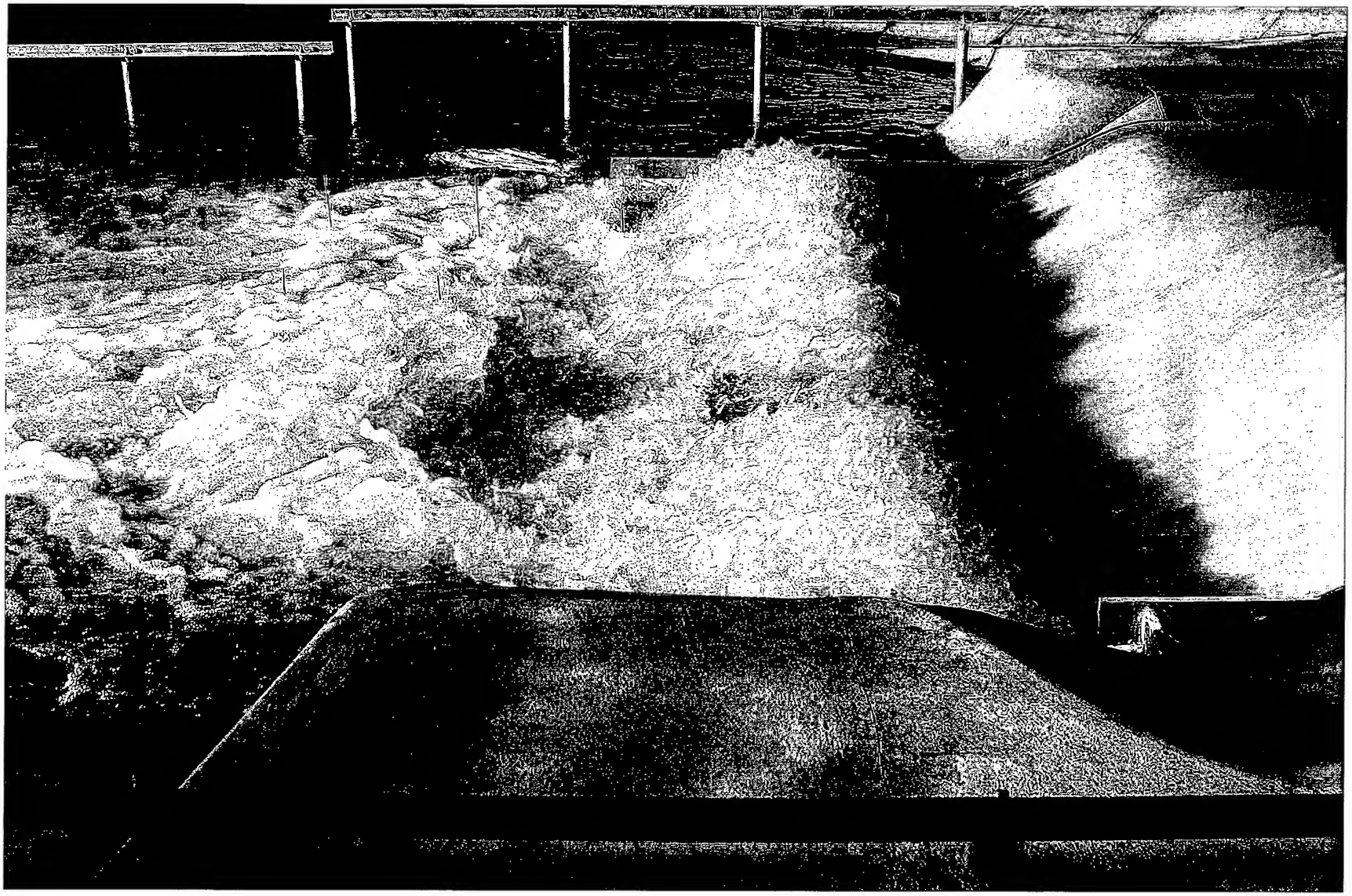

Photo 29. Type 6 exit channel design - flip bucket action at 481,000 cfs, tailwater el 490.4

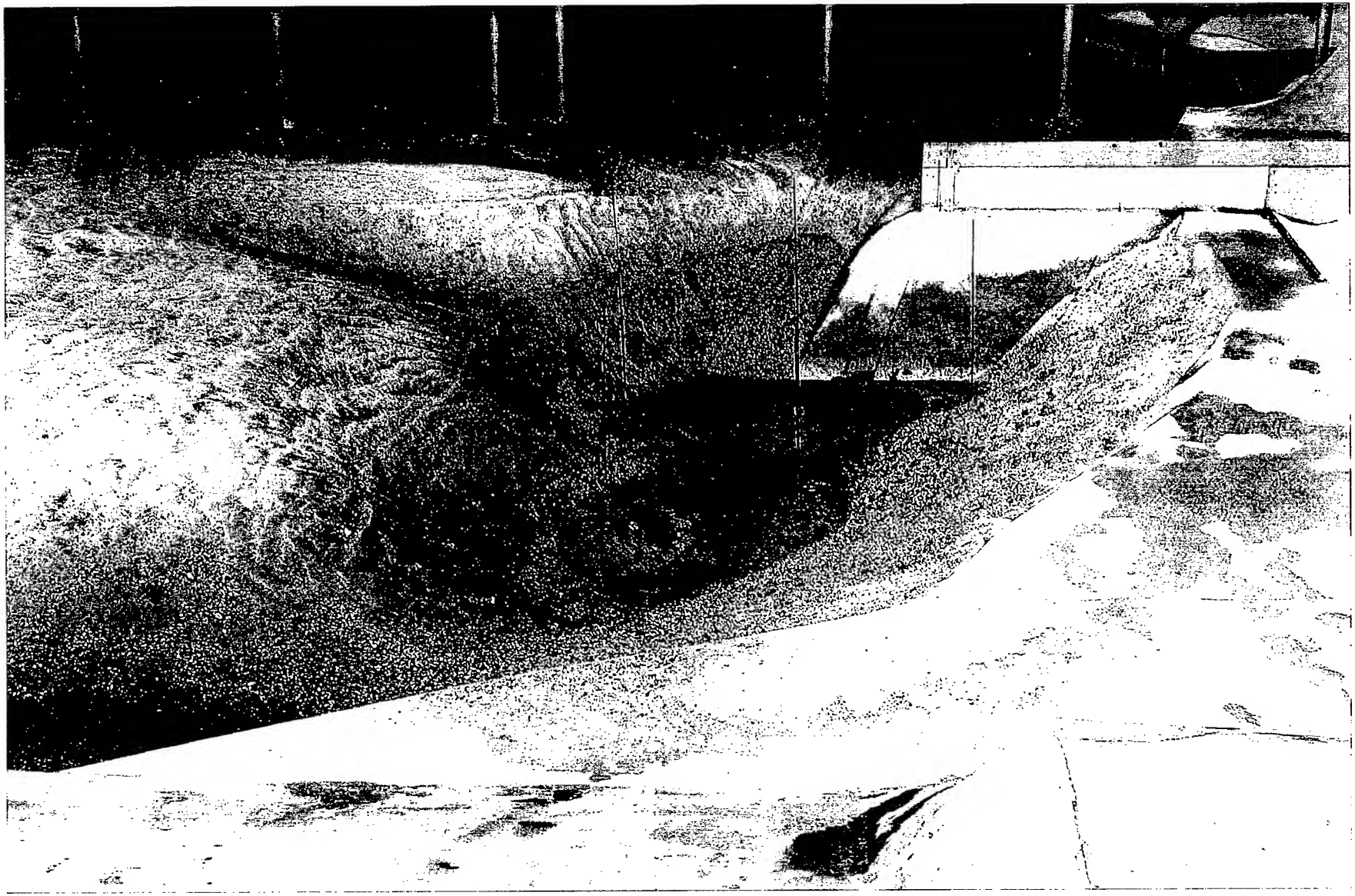

Photo 30. Type 6 exit channel design - scour downstream from spillway at end of experiment looking at right training wall

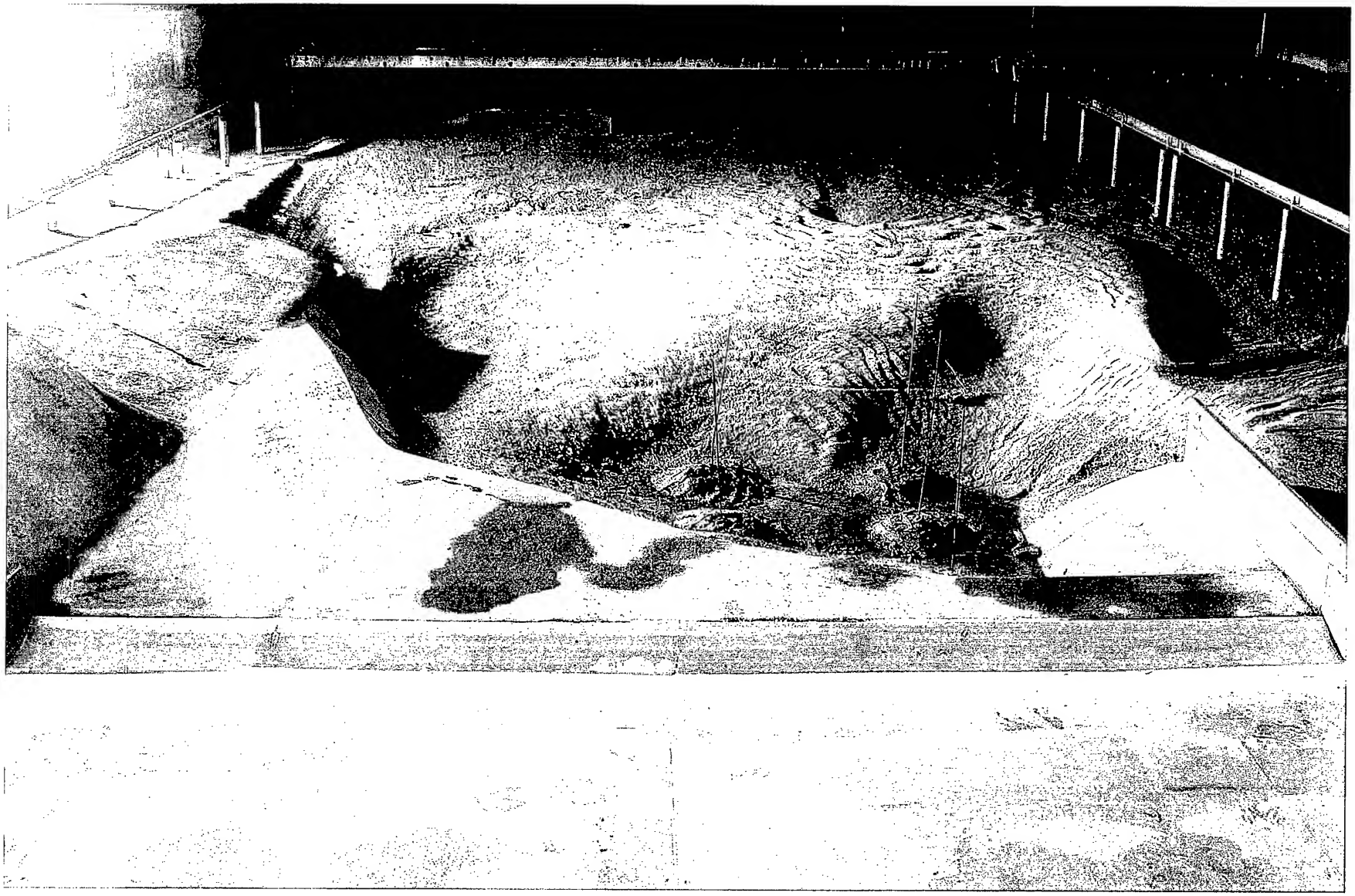

Photo 31. Type 6 exit channel design - scour downstream from spillway at end of experiment looking downstream

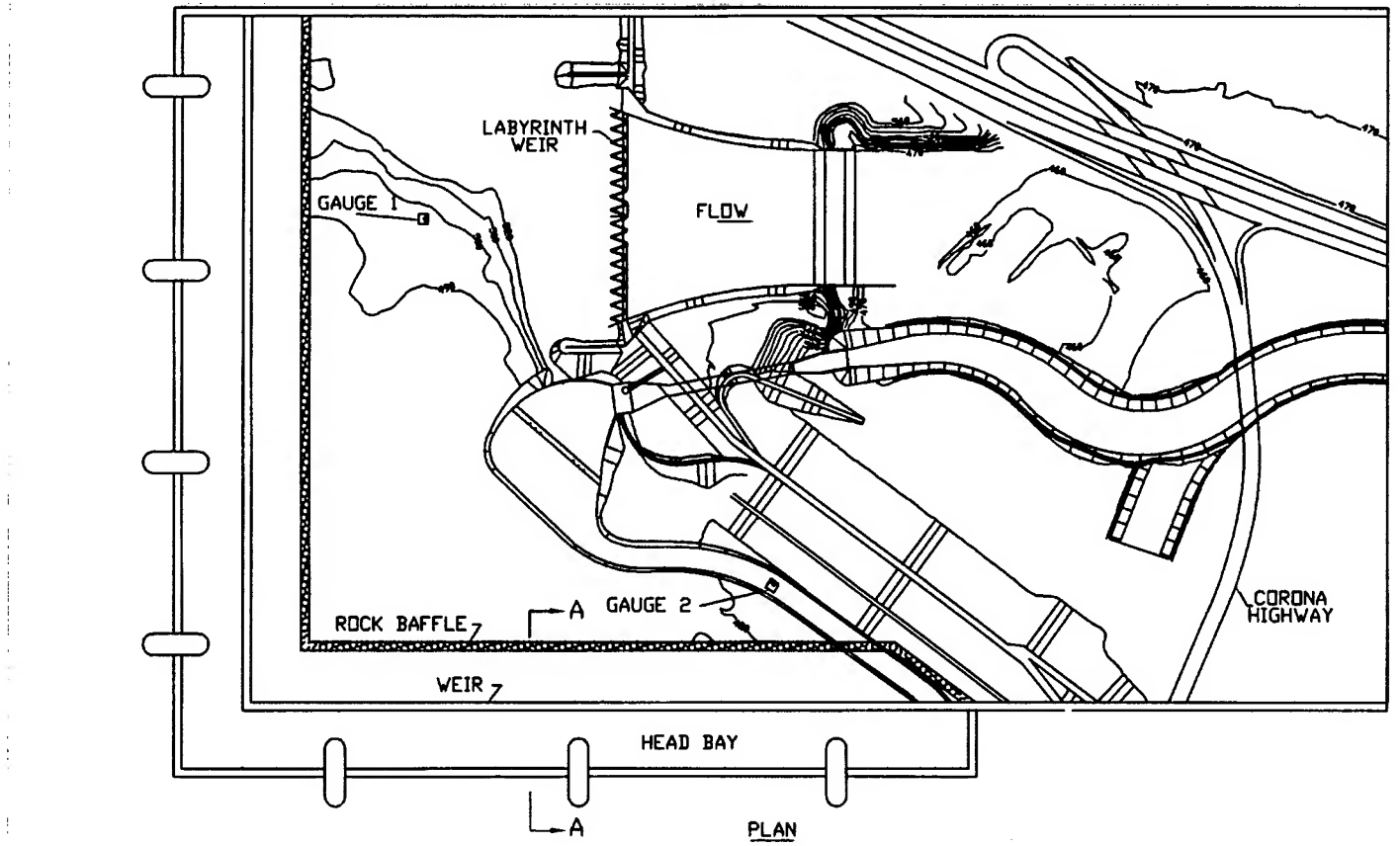

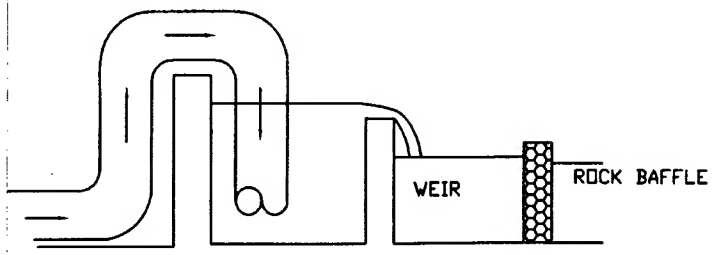

SECTION A-A

MODEL OF PRADO SPILLWAY

SCALE 1 : 50

Plate 1

Plate 2

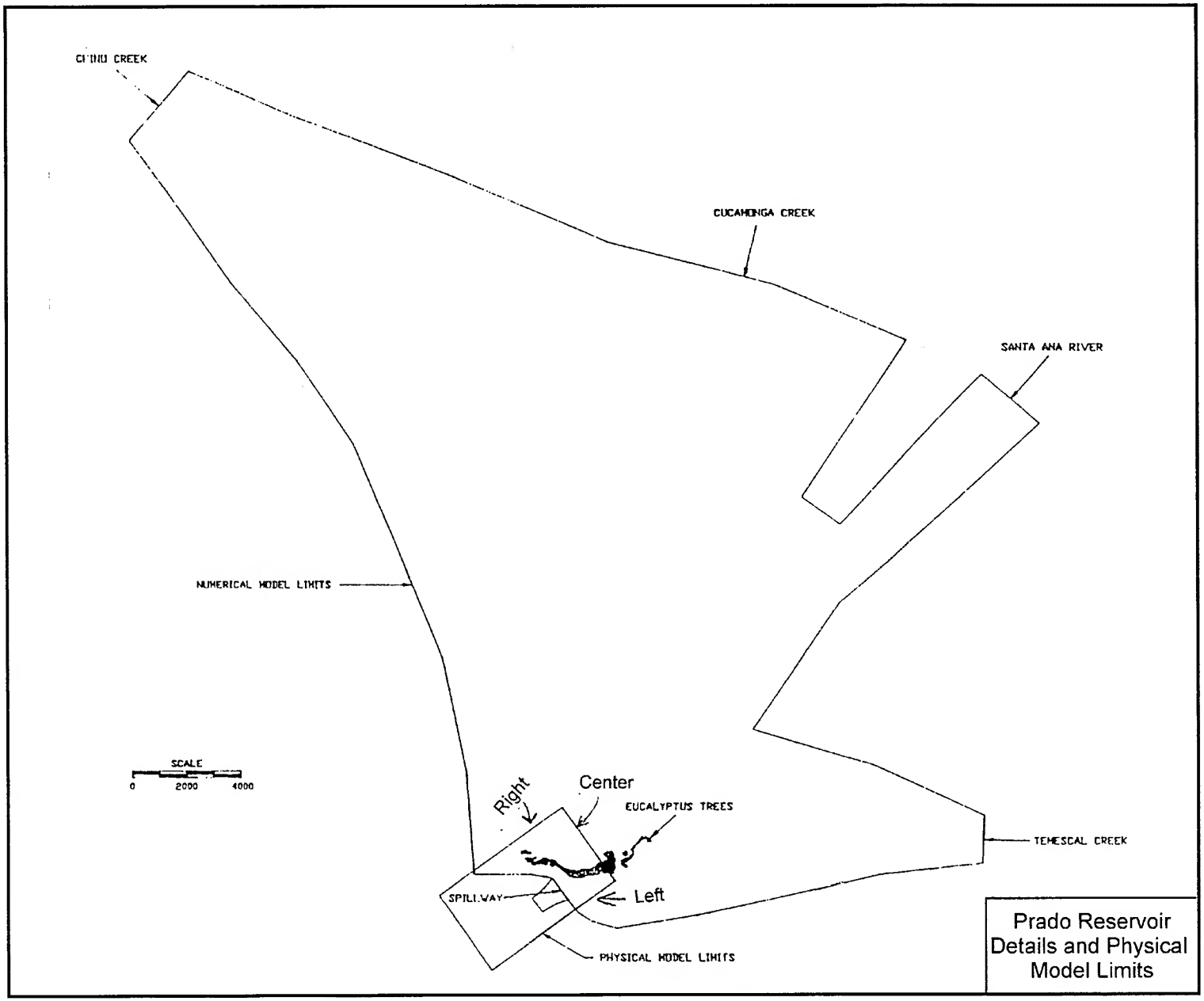
CHINO CREEK
CUCAMONGA CREEK
SANTA ANA RIVER
NUMERICAL MODEL LIMITS
SCALE
0
2000
4000
Right
Center
EUCALYPTUS TREES
TEMESCAL CREEK
SPILLWAY
Left
PHYSICAL MODEL LIMITS
Prado Reservoir
Details and Physical
Model Limits

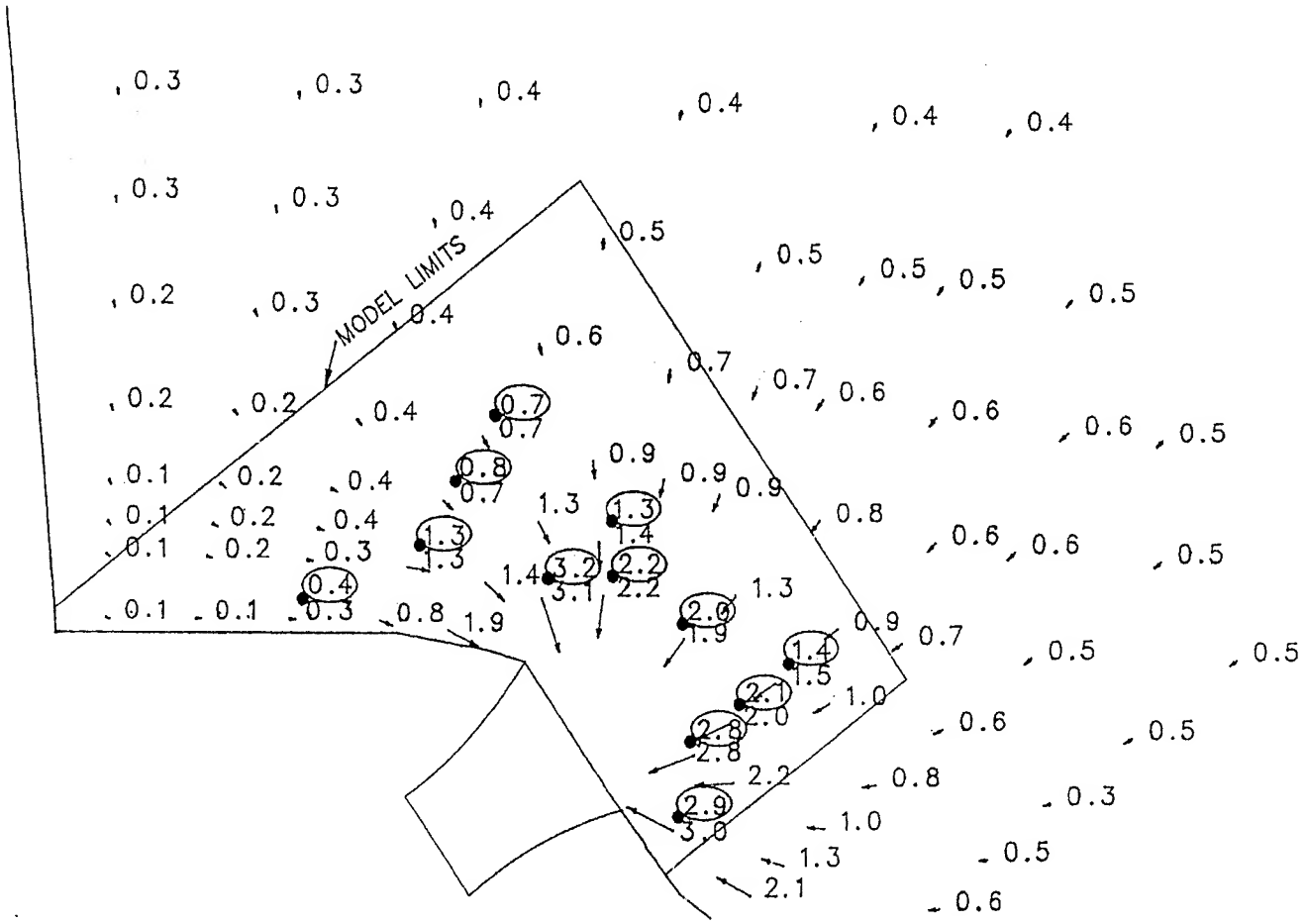

NOTE: VELOCITIES ARE IN FEET PER SECOND
MEASURED OR COMPUTED AT MID-DEPTH.
(1.2) MEASURED IN PHYSICAL MODEL
● POINT WHERE VELOCITY WAS MEASURED AND COMPUTED
1.2 COMPUTED BY MATH MODEL

APPROACH VELOCITIES (PROTOTYPE)
DISCHARGE - 300,000 CFS

Plate 3

Plate 4

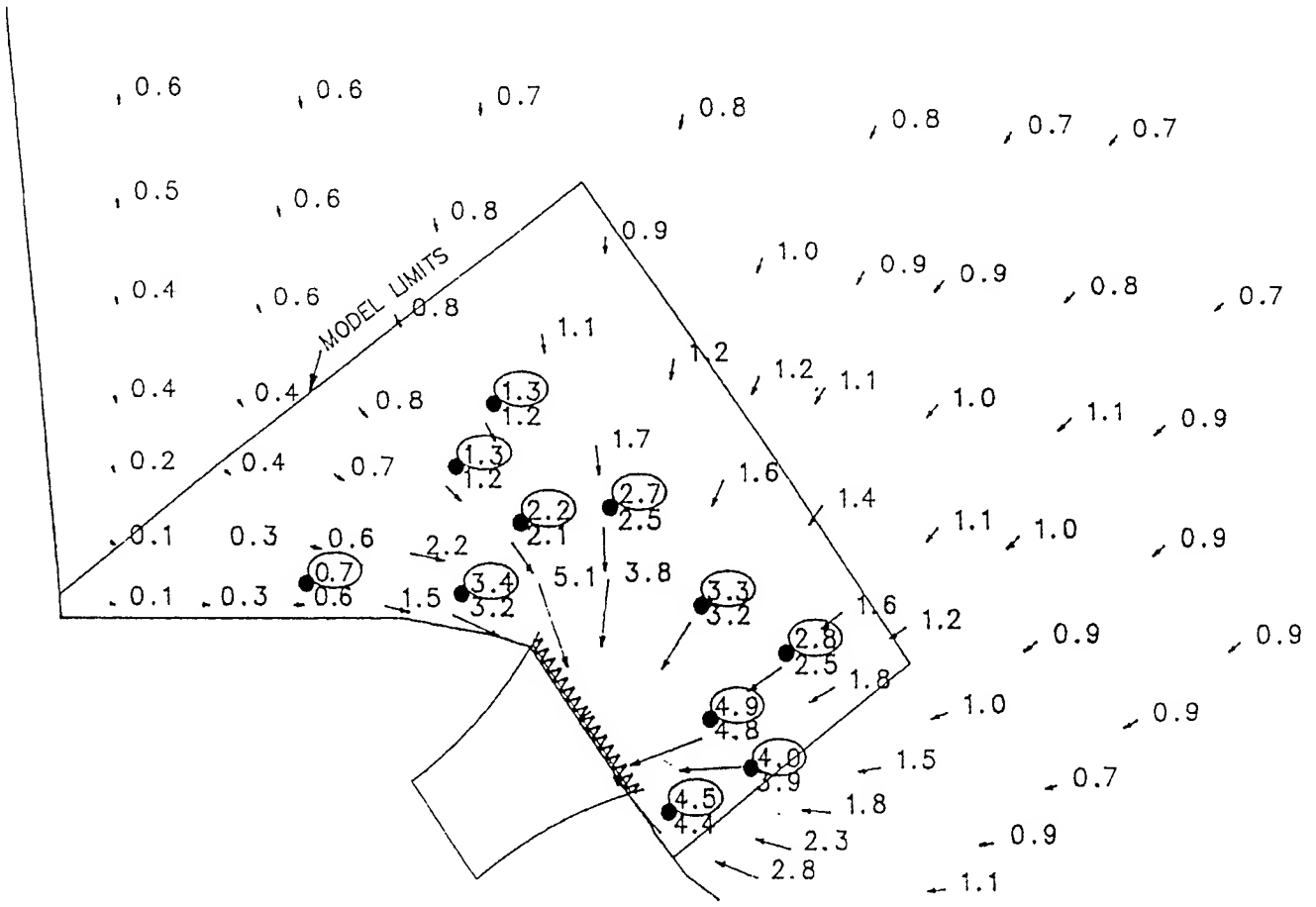

NOTE: VELOCITIES ARE IN FEET PER SECOND
MEASURED OR COMPUTED AT MID DEPTH.
(1.2) MEASURED IN PHYSICAL MODEL
● POINT WHERE VELOCITY WAS MEASURED AND COMPUTED
1.2 COMPUTED BY MATH MODEL

APPROACH VELOCITIES (PROTOTYPE)
DISCHARGE - 600,000 CFS

TRAPEZOIDAL

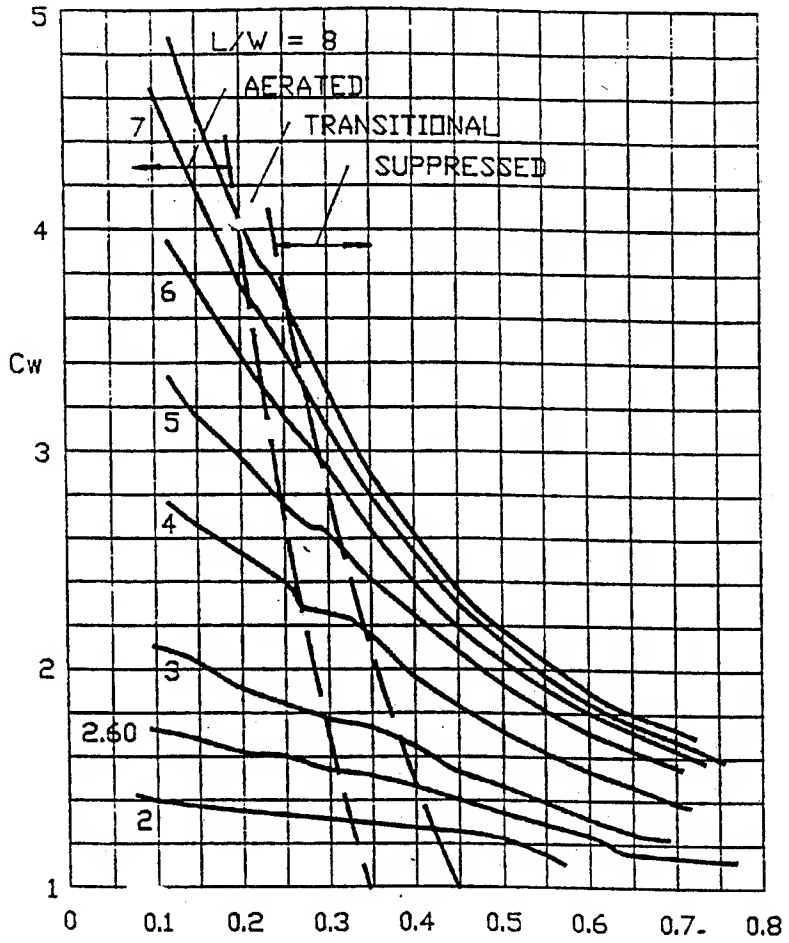

ROUNDED CREST DESIGN CURVES

$$Q = Cw \left(\frac{W/P}{W/P+K} \right) nWH\sqrt{gH}$$

W - CYCLE WIDTH, FT
P - APPROACH DEPTH, FT
K - 0.1
L - CREST LENGTH/CYCLE
n - NUMBER OF CYCLES
H - TOTAL HEAD ON CREST, FT
g - ACCELERATION DUE TO GRAVITY, FT/SEC^2

DESIGN AND CONSTRUCTION OF LABYRINTH WEIRS', LUX AND HINCHLIFF (1985)

Plate 5

Plate 6

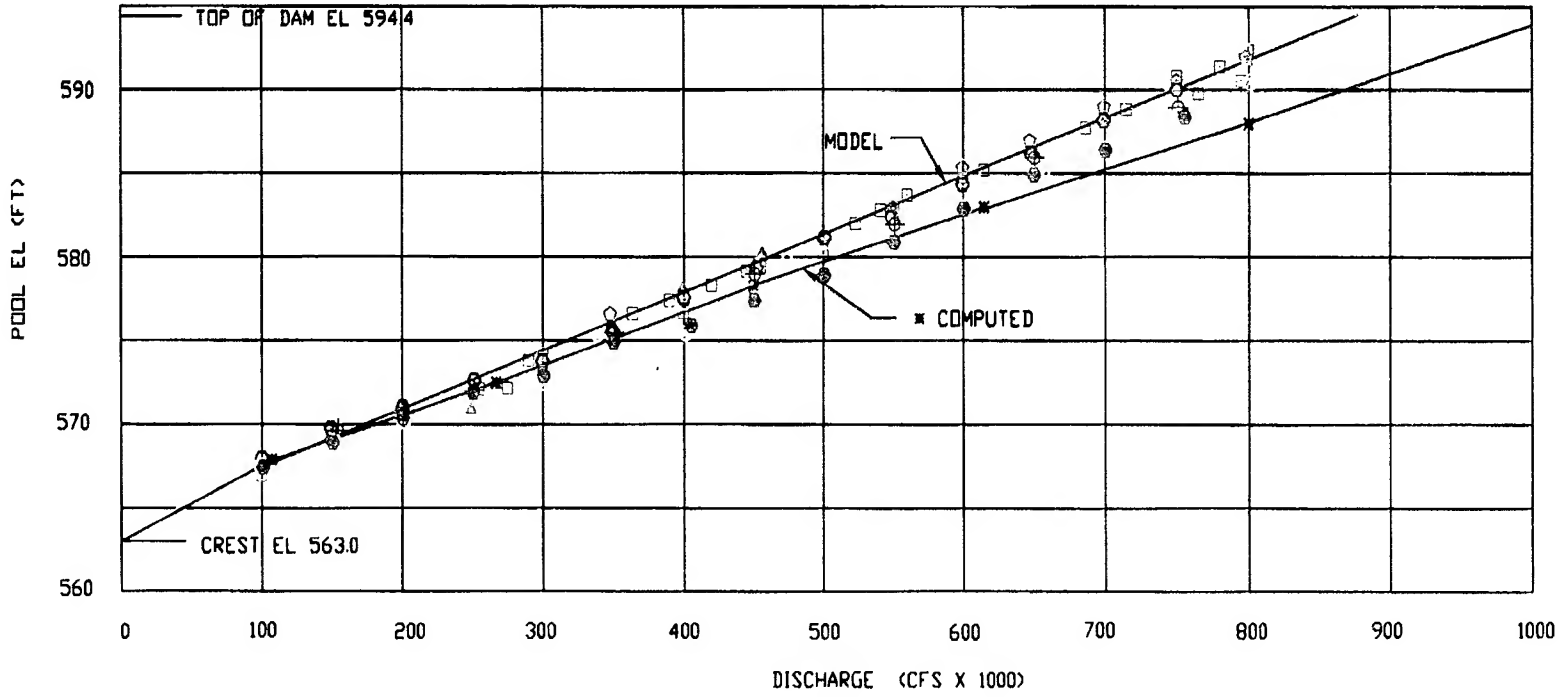

□ TYPE 1 DESIGN

△ TYPE 3 DESIGN
⬠ TYPE 4 DESIGN
○ TYPE 5 DESIGN
⊕ TYPE 6 DESIGN
TYPE 8 DESIGN
◉ TYPE 9 DESIGN
✱ 'DESIGN AND CONSTRUCTION OF LABYRINTH WEIRS',
JUNE 1985 ICOLD CONFERENCE, LUX AND HINCHLIFF

TYPE 1-9 DESIGNS
RATING CURVES

TYPE 1

Q (CFS)	POOL EL (FT)	Q (CFS)	POOL EL (FT)
255,000	572.15	765,000	589.85
290,000	573.85	795,000	590.60
364,000	576.65	200,000	570.10
390,000	577.45	100,000	567.40
420,000	578.35	500,000	580.55
445,000	579.20	400,000	576.85
455,000	579.45	300,000	573.40
523,000	582.05	600,000	584.85
541,000	582.85	750,000	590.50
560,000	583.75	800,000	592.70
615,000	585.25	780,000	591.75
687,000	587.80		
715,000	588.90		

TYPE 2

Q (CFS)	POOL EL (FT)	Q (CFS)	POOL EL (FT)
42,000	565.60	474,000	579.85
69,000	566.60	501,000	580.90
96,000	567.70	528,000	582.30
123,000	568.55	555,000	582.95
150,000	569.50	582,000	583.95
177,000	570.10	609,000	585.00
204,000	570.85	636,000	586.10
231,000	571.90	663,000	587.10
258,000	572.60	690,000	588.30
285,000	573.55	717,000	589.05
312,000	574.10	744,000	590.05
339,000	575.35	771,000	591.45
366,000	576.30	798,000	592.30
393,000	577.10		
447,000	578.55		

TYPE 3

Q (CFS)	POOL EL (FT)	Q (CFS)	POOL EL (FT)
100,000	567.55	500,000	581.35
150,000	569.15	550,000	583.30
200,000	570.20	600,000	584.95
250,000	571.05	650,000	586.90
300,000	573.90	700,000	588.50
350,000	575.80	750,000	590.40
400,000	578.35	800,000	592.10
450,000	580.25		

TYPE 4

Q (CFS)	POOL EL (FT)	Q (CFS)	POOL EL (FT)
100,000	567.50	550,000	583.30
200,000	570.75	600,000	585.45
300,000	574.45	650,000	587.60
350,000	576.30	700,000	589.20
400,000	577.85	750,000	590.85
450,000	579.80	800,000	592.65
500,000	581.15		

TYPE 5

Q (CFS)	POOL EL (FT)	Q (CFS)	POOL EL (FT)
100,000	568.00	500,000	581.20
150,000	569.80	550,000	582.85
200,000	571.25	600,000	584.60
250,000	572.50	650,000	586.55
300,000	573.80	700,000	588.25
350,000	575.65	750,000	590.00
400,000	577.70		
450,000	579.40		

TYPE 6

Q (CFS)	POOL EL (FT)	Q (CFS)	POOL EL (FT)
150,000	569.65	450,000	578.85
200,000	570.85	550,000	582.35
250,000	572.25	650,000	586.00
350,000	575.45	750,000	589.35

TYPE 8

Q (CFS)	POOL EL (FT)	Q (CFS)	POOL EL (FT)
100,000	567.4	450,000	577.70
150,000	569.05	600,000	583.30
200,000	570.25	650,000	585.00
250,000	571.60	700,000	586.45
300,000	572.55	750,000	588.60
350,000	574.15	800,000	590.75
400,000	575.65		

TYPE 9

Q (CFS)	POOL EL (FT)	Q (CFS)	POOL EL (FT)
100,000	567.40	450,000	577.90
150,000	569.10	500,000	579.35
200,000	570.45	550,000	581.35
250,000	571.90	600,000	582.85
300,000	573.25	650,000	584.80
350,000	574.85	700,000	586.65
400,000	576.35	750,000	588.65

BASIC DATA

Plate 7

Plate 8

ELEV (FT)	TYPE 1
GAGE 1	DISCHARGE
570.25	43,000
571.15	51,000
572.30	60,000
573.65	68,000
575.05	78,000
576.30	86,000
577.55	94,000
578.60	100,000
584.60	140,000
586.90	160,000

ELEV (FT)	TYPE 2
GAGE 1	DISCHARGE
569.75	42,000
571.85	57,000
573.45	68,000
574.70	78,000
576.05	86,000
577.25	94,000
578.35	100,000
578.75	105,000
579.50	110,000
579.40	115,000
580.60	120,000
580.40	125,000
581.45	130,000
582.00	135,000
584.45	140,000
583.50	145,000
585.70	150,000
585.00	155,000
586.45	160,000

SCALE

0 200 400

GAGE

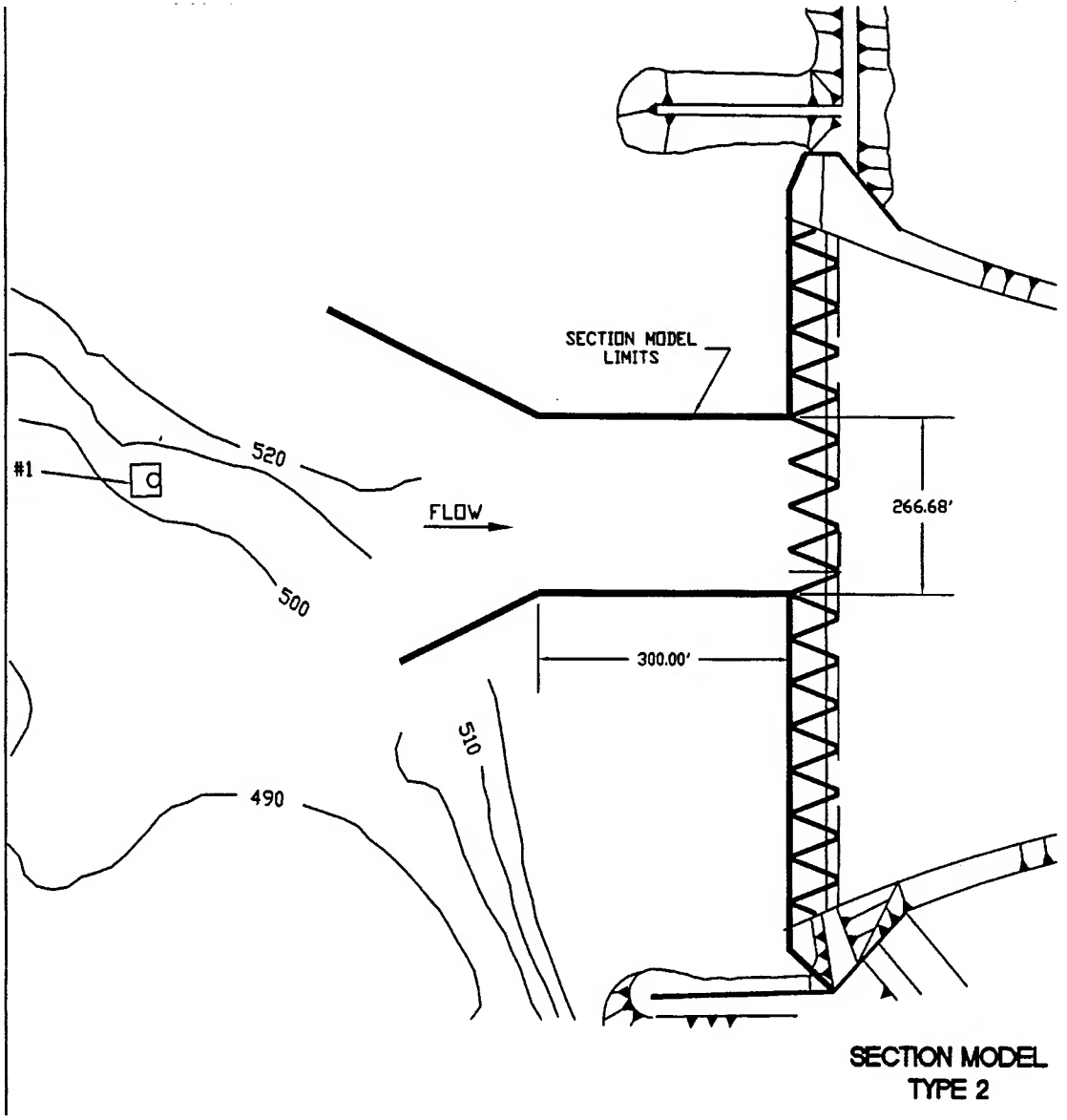

SECTION MODEL
TYPE 2

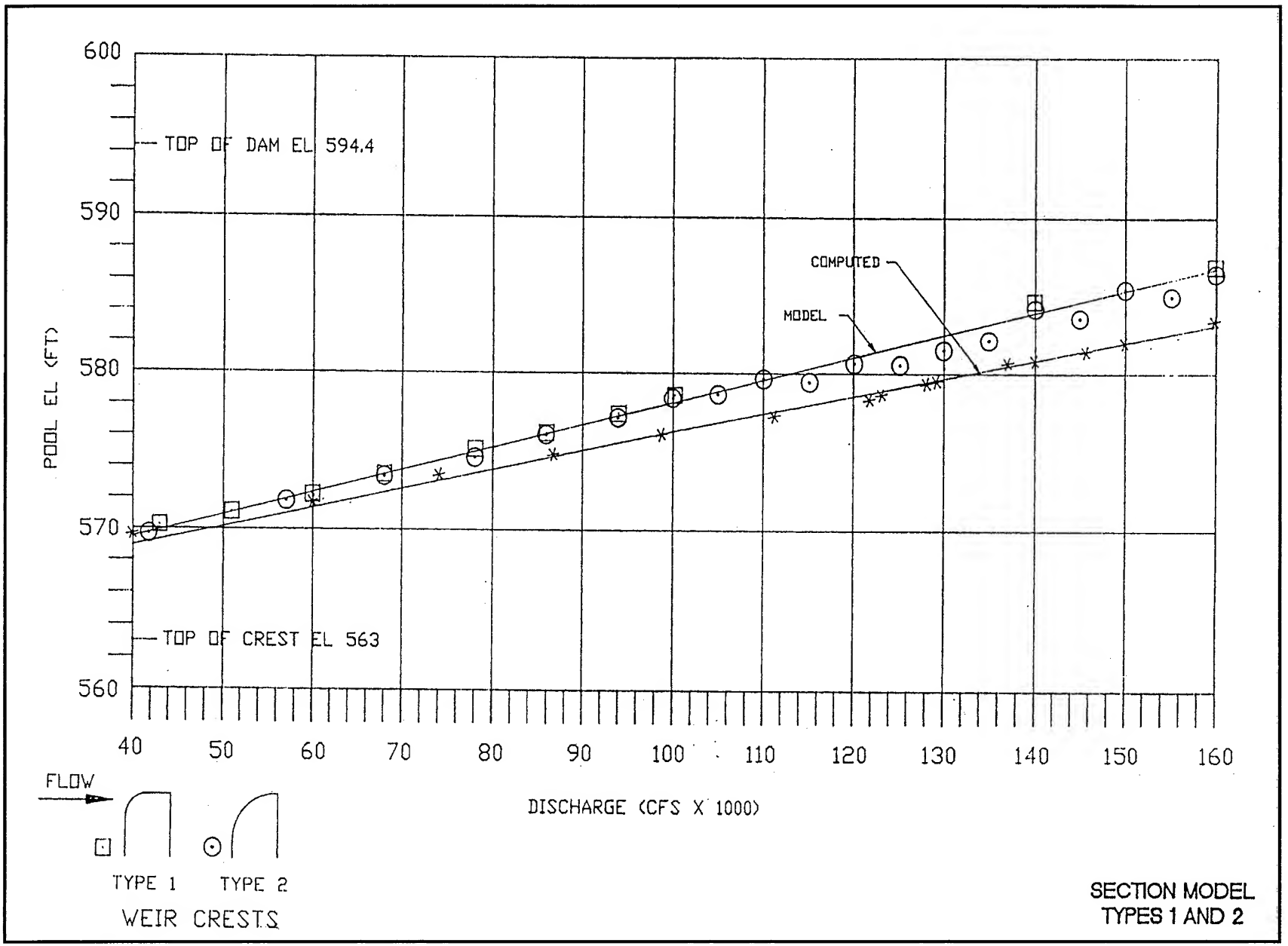

SECTION MODEL
TYPES 1 AND 2

Plate 9

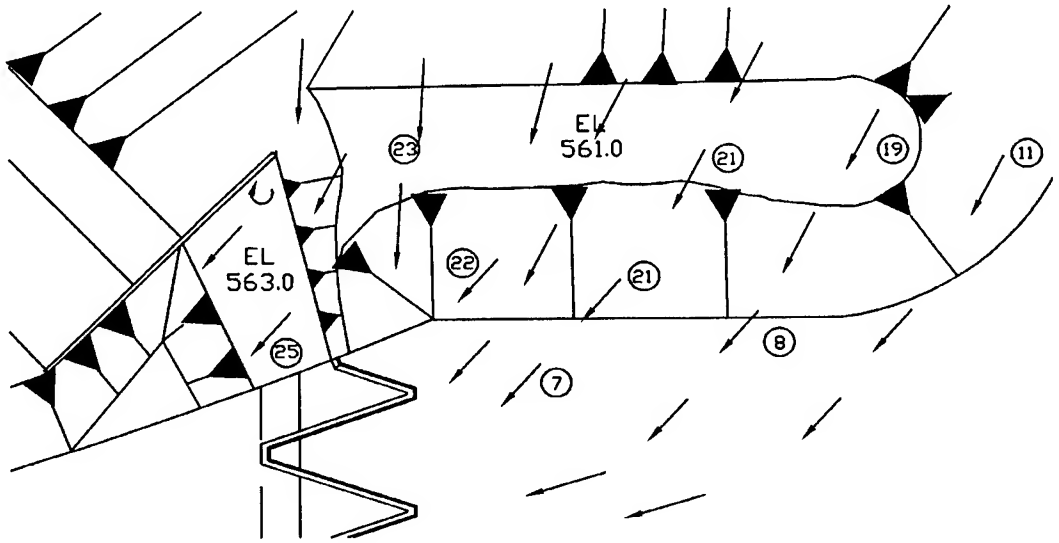

RIGHT OVERFLOW BERM

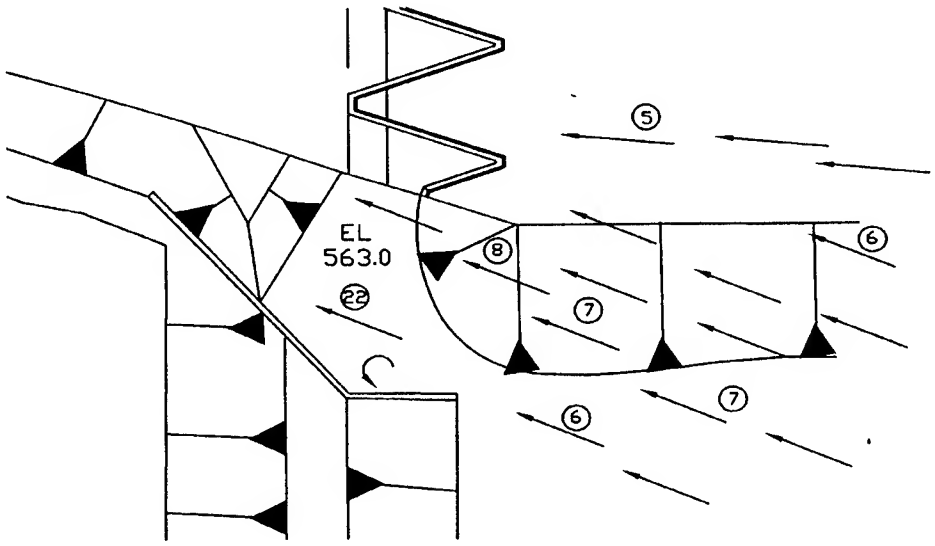

LEFT OVERFLOW BERM

NOTE: VELOCITIES ARE IN PROTOTYPE FT PER SEC AND WERE MEASURED 2 FT ABOVE THE BOTTOM

TYPE 4 DESIGN
DISCHARGE – 700,000 CFS
POOL EL – 589.0

Plate 10

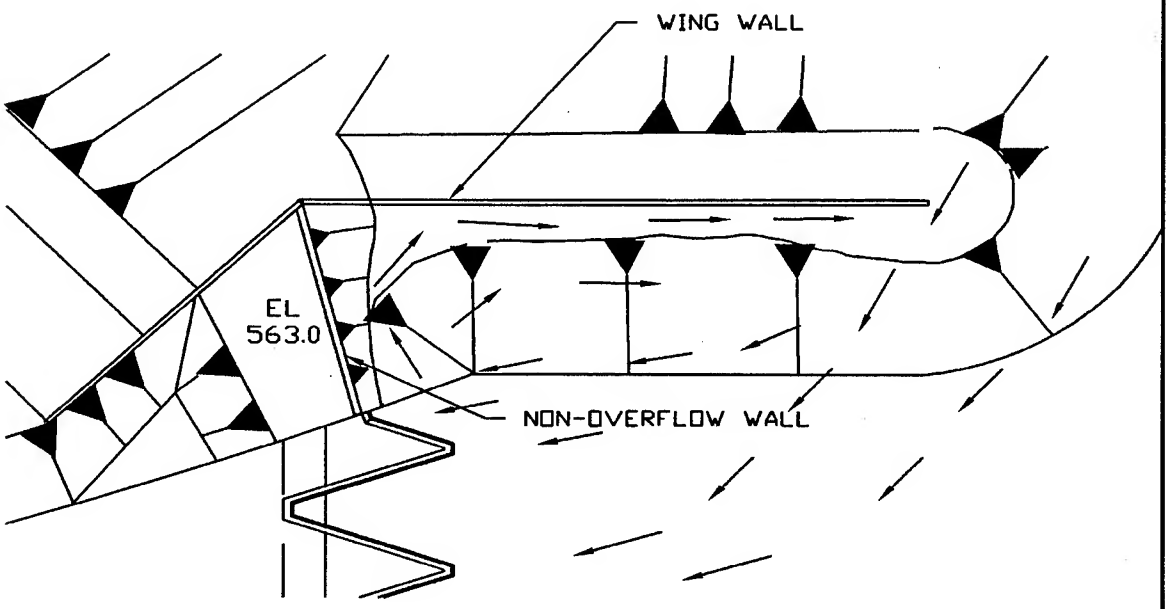

RIGHT OVERFLOW BERM

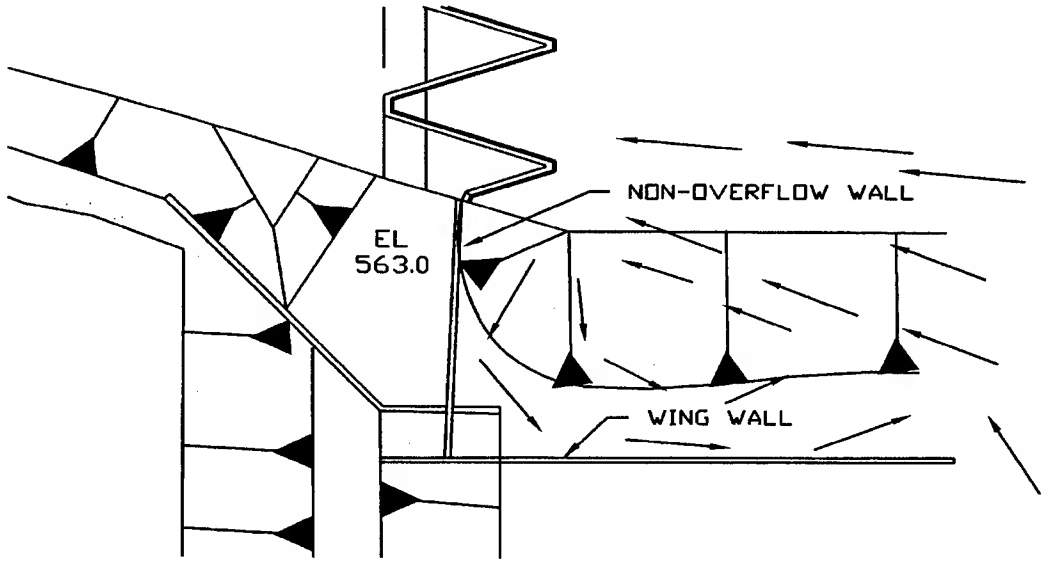

LEFT OVERFLOW BERM

TYPE 5 DESIGN
DISCHARGE – 700,000 CFS
POOL EL – 589.0

Plate 11

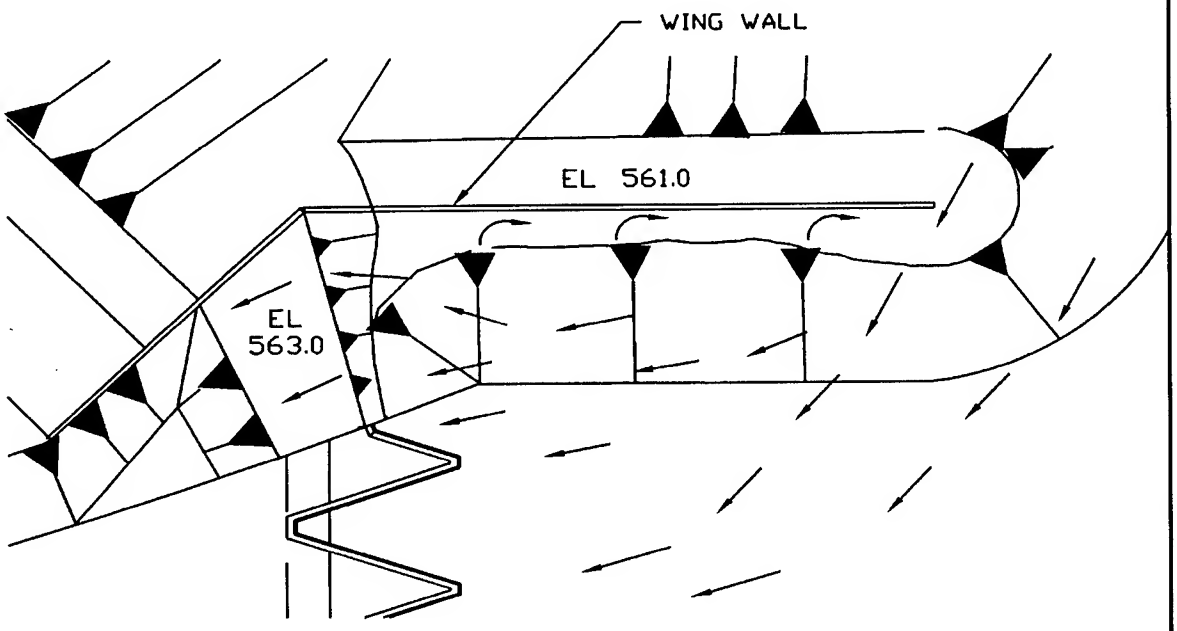

RIGHT OVERFLOW BERM

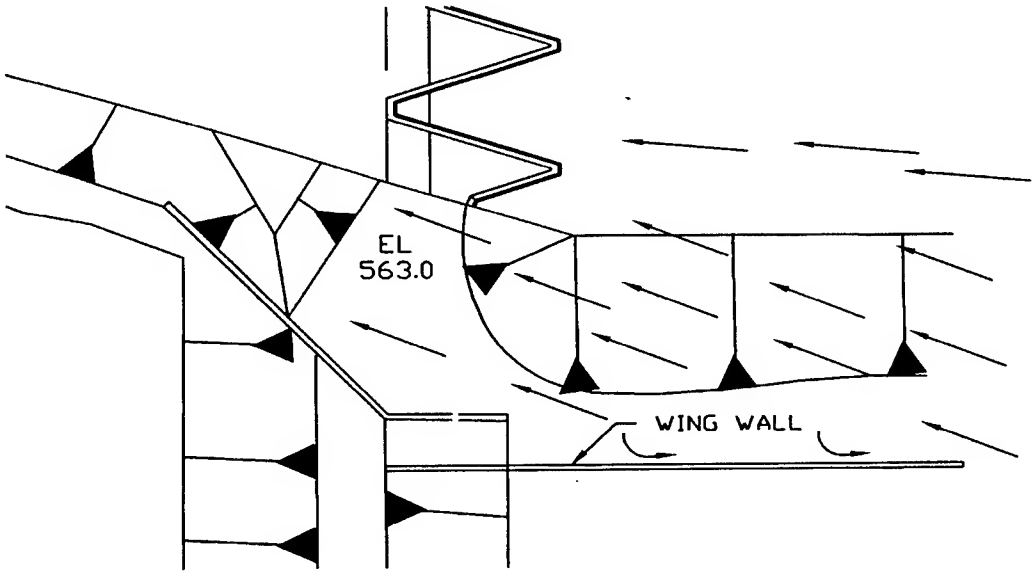

LEFT OVERFLOW BERM

TYPE 6 DESIGN
DISCHARGE – 700,000 CFS
POOL EL – 589.0

Plate 12

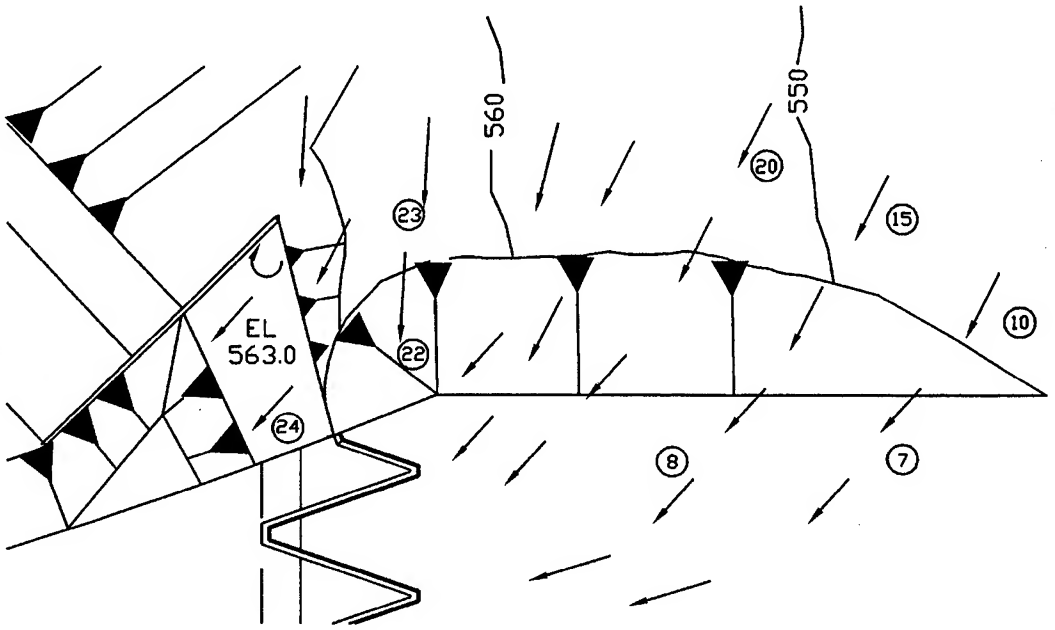

RIGHT OVERFLOW BERM

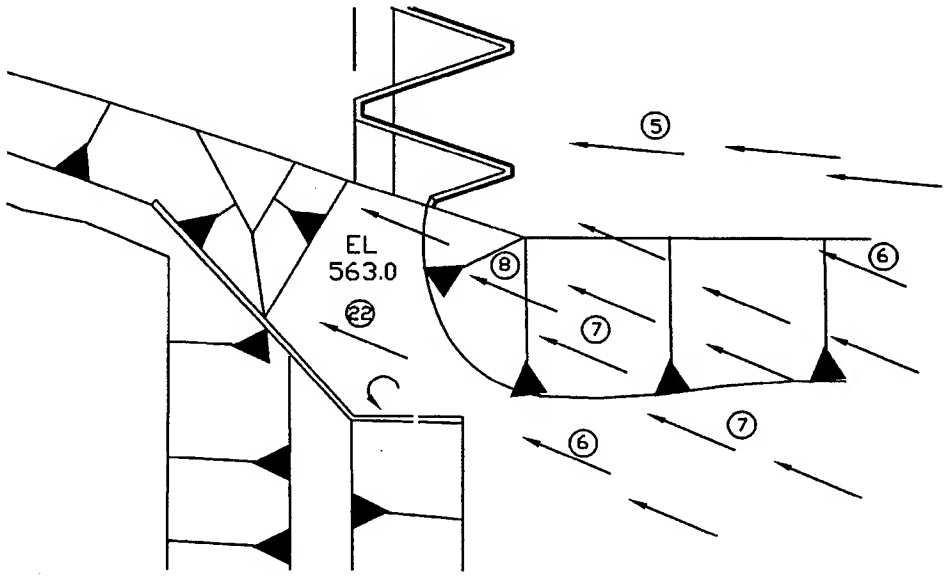

LEFT OVERFLOW BERM

VELOCITIES ARE IN PROTOTYPE FT PER SEC
AND WERE MEASURED 2 FT ABOVE THE BOTTOM

TYPE 7 DESIGN
DISCHARGE – 700,000 CFS
POOL EL – 589.0

Plate 13

Plate 14

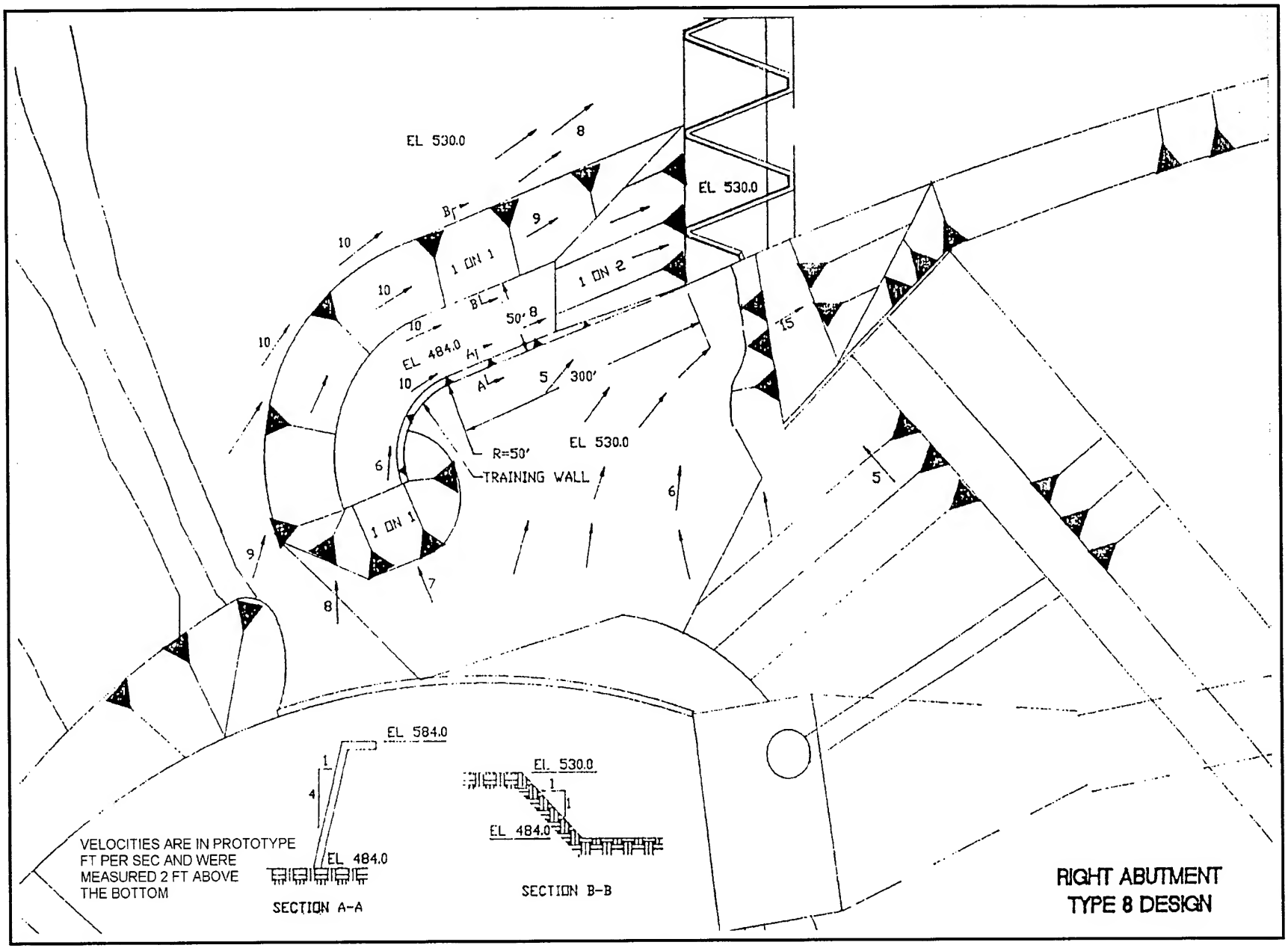
EL 530.0
8
EL 530.0
9
10
1 ON 1
1 ON 2
BL
50'
8
10
10
EL 484.0
10
AL
5
300'
15
EL 530.0
R=50'
TRAINING WALL
6
6
5
1 ON 1
9
8
7
EL 584.0
1
4
EL 484.0
SECTION A-A
EL. 530.0
1
1
EL 484.0
SECTION B-B
VELOCITIES ARE IN PROTOTYPE FT PER SEC AND WERE MEASURED 2 FT ABOVE THE BOTTOM
RIGHT ABUTMENT
TYPE 8 DESIGN

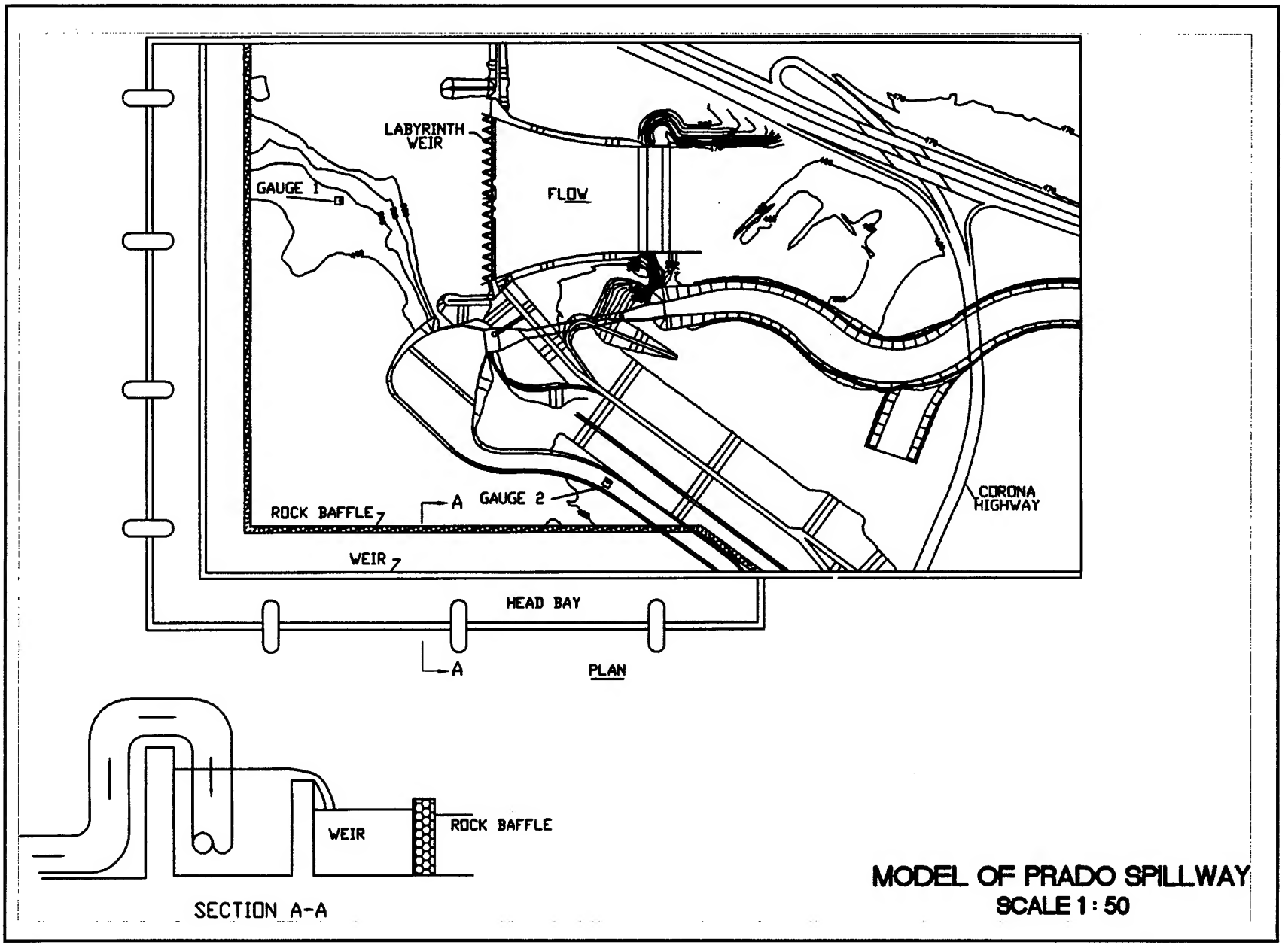

MODEL OF PRADO SPILLWAY
SCALE 1 : 50

Plate 15

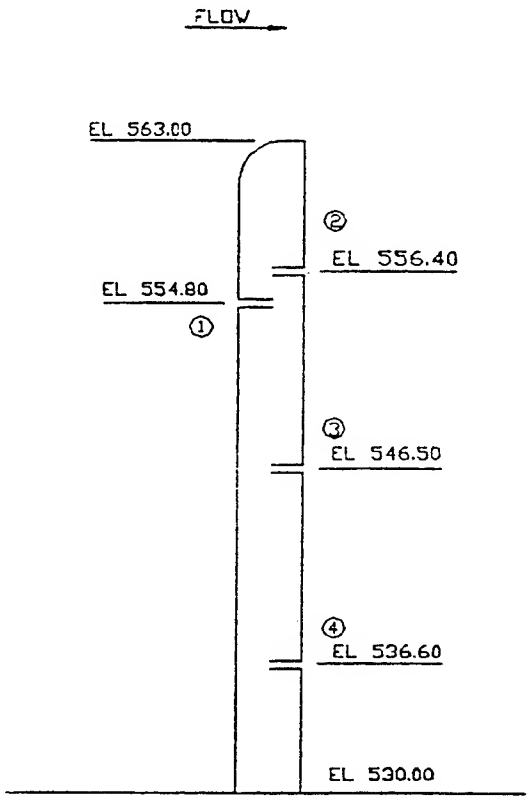

SECTION A-A

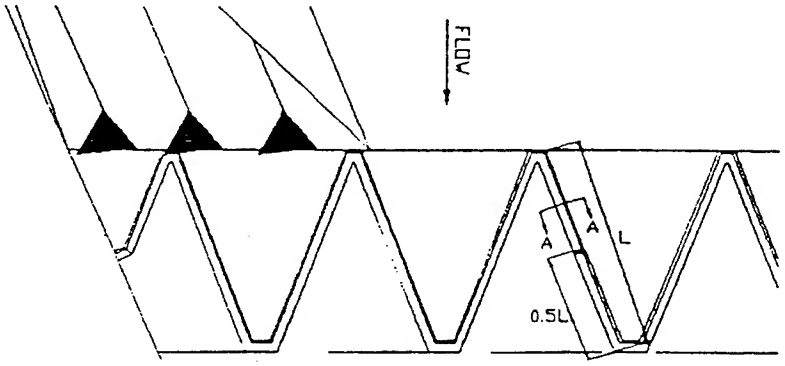

PLAN

TYPE 9 DESIGN
PIEZOMETER LOCATIONS

Plate 16

POOL EL.	DISCHARGE	PIEZOMETER		HYDRAULIC GRADIENT		HYDRAULIC PRESSURES	
		NO.	EL.	MIN.	MAX.	MIN.	MAX.
567.45	100,000	1	554.8	567.4	567.4	12.6	12.6
567.45	100,000	2	556.4	556.3	556.3	-0.1	-0.1
567.45	100,000	3	546.5	548.8	548.8	2.3	2.3
567.45	100,000	4	536.6	544.3	544.3	7.7	7.7

POOL EL.	DISCHARGE	PIEZOMETER		HYDRAULIC GRADIENT		HYDRAULIC PRESSURES	
		NO.	EL.	MIN.	MAX.	MIN.	MAX.
571.60	250,000	1	554.8	571.5	571.5	16.7	16.7
571.60	250,000	2	556.4	556.3	556.3	-0.1	-0.1
571.60	250,000	3	546.5	548.3	549.3	1.8	2.8
571.60	250,000	4	536.6	553.8	554.8	17.2	18.2

POOL EL.	DISCHARGE	PIEZOMETER		HYDRAULIC GRADIENT		HYDRAULIC PRESSURES	
		NO.	EL.	MIN.	MAX.	MIN.	MAX.
574.35	340,000	1	554.8	574.3	574.3	19.5	19.5
574.35	340,000	2	556.4	545.5	550.8	-10.9	-5.6
574.35	340,000	3	546.5	552.8	562.3	6.3	15.8
574.35	340,000	4	536.6	563.3	568.8	26.7	32.2

TYPE 9 DESIGN
HYDRAULIC GRADIENTS AND PRESSURES

Plate 17

POOL EL.	DISCHARGE	PIEZOMETER		HYDRAULIC GRADIENT		HYDRAULIC PRESSURES	
		NO.	EL.	MIN.	MAX.	MIN.	MAX.
580.75	530,000	1	554.8	578.8	579.8	24.0	25.0
580.75	530,000	2	556.4	545.8	552.3	-10.6	-4.1
580.75	530,000	3	546.5	568.8	570.3	22.3	23.8
580.75	530,000	4	536.6	573.3	573.8	36.7	37.2

POOL EL.	DISCHARGE	PIEZOMETER		HYDRAULIC GRADIENT		HYDRAULIC PRESSURES	
		NO.	EL.	MIN.	MAX.	MIN.	MAX.
583.90	630,000	1	554.8	581.3	582.3	26.5	27.5
583.90	630,000	2	556.4	553.8	557.8	-2.6	1.4
583.90	630,000	3	546.5	571.3	572.8	24.8	26.3
583.90	630,000	4	536.6	574.8	577.3	38.2	40.7

POOL EL.	DISCHARGE	PIEZOMETER		HYDRAULIC GRADIENT		HYDRAULIC PRESSURES	
		NO.	EL.	MIN.	MAX.	MIN.	MAX.
590.90	800,000	1	554.8	586.8	587.8	32.0	33.0
590.90	800,000	2	556.4	559.8	570.8	3.4	14.4
590.90	800,000	3	546.5	568.3	576.3	21.8	29.8
590.90	800,000	4	536.6	575.3	580.8	38.7	44.2

TYPE 9 DESIGN
HYDRAULIC GRADIENTS AND PRESSURES

Plate 18

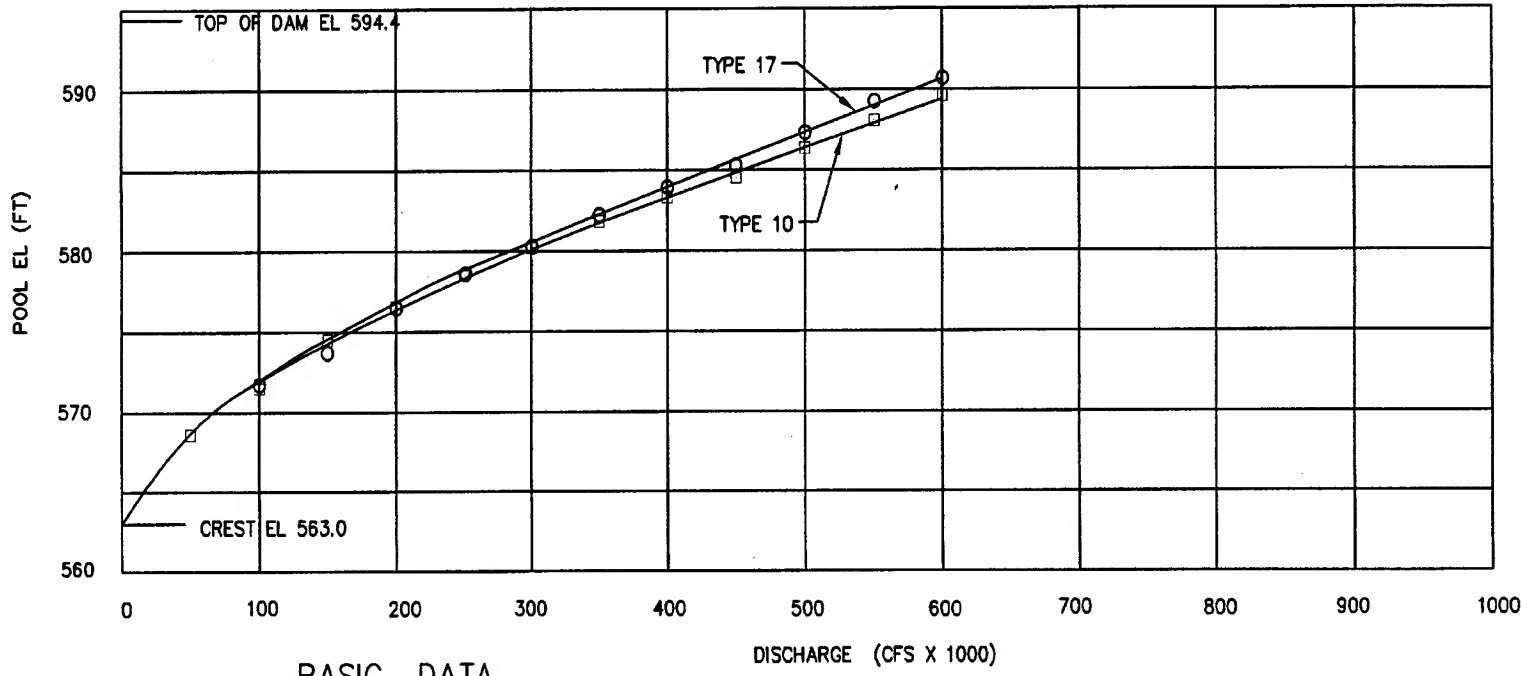

BASIC DATA

TYPE 10 □		TYPE 17 O	
POOL EL (FT)	DISCHARGE (CFS)	POOL EL (FT)	DISCHARGE (CFS)
50,000	568.60	100,000	571.80
100,000	571.55	150,000	573.80
150,000	574.50	200,000	576.45
200,000	576.55	250,000	578.65
250,000	578.50	300,000	580.35
300,000	580.20	350,000	582.20
350,000	581.85	400,000	583.95
400,000	583.35	450,000	585.25
450,000	584.55	500,000	587.25
500,000	586.35	550,000	589.20
550,000	588.05	600,000	590.80
600,000	589.60		

TYPE 10 AND 17
RATING CURVES

Plate 19

Plate 20

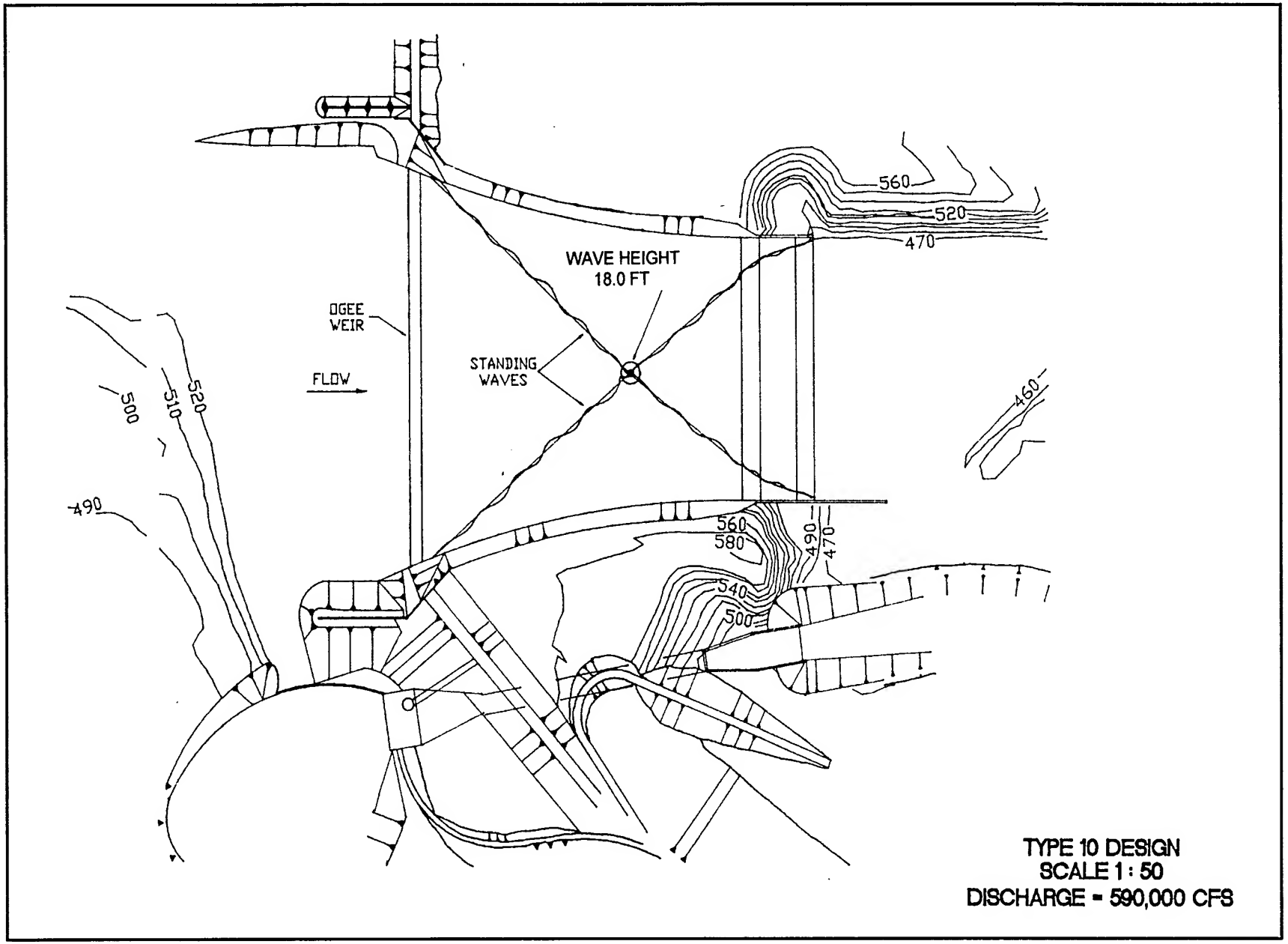
WAVE HEIGHT
18.0 FT
OGEE
WEIR
FLOW
STANDING
WAVES
560
520
470
460
500
510
520
490
560
580
490
470
540
500
TYPE 10 DESIGN
SCALE 1 : 50
DISCHARGE = 590,000 CFS

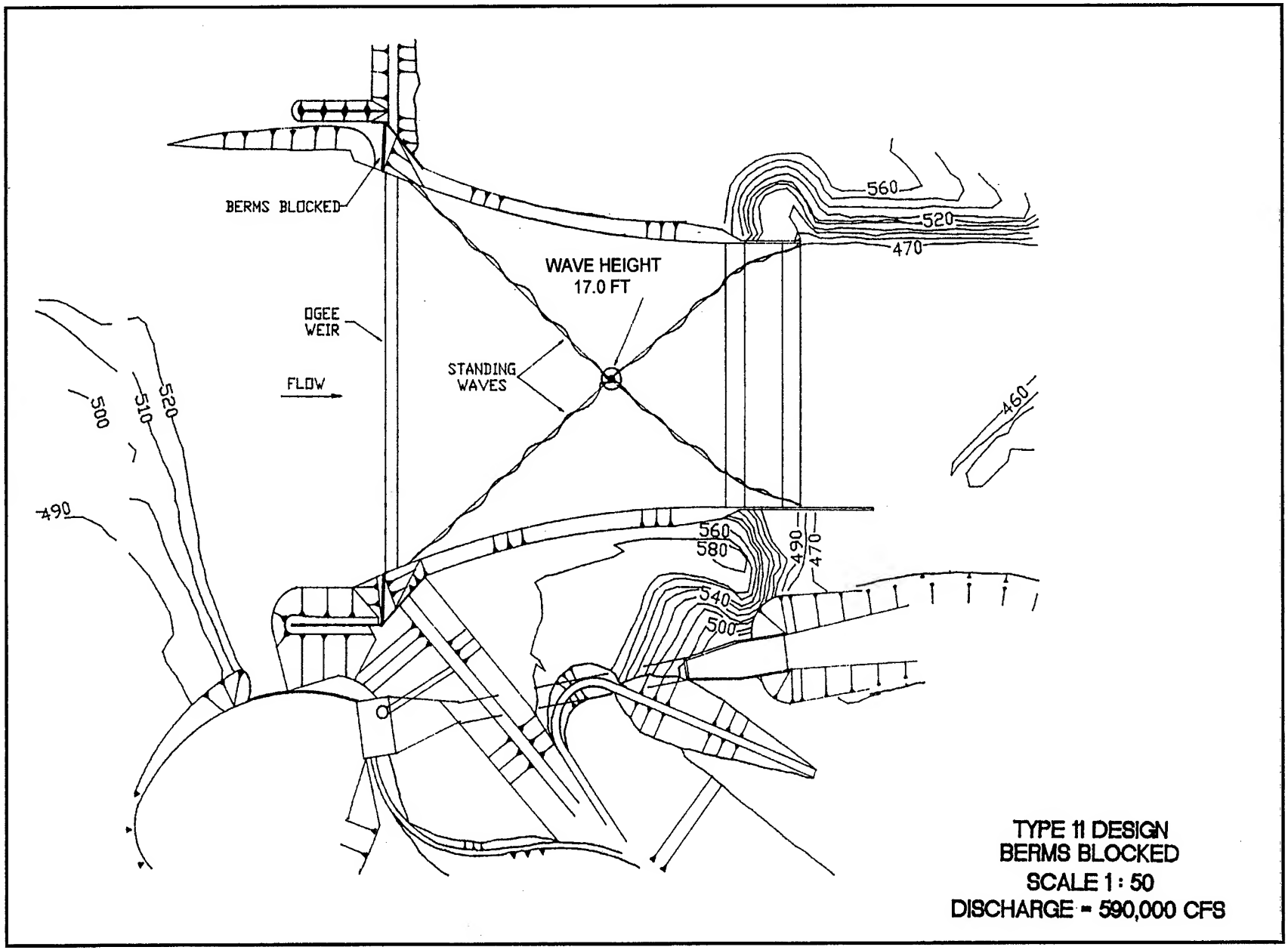
BERMS BLOCKED
WAVE HEIGHT
17.0 FT
OGEE
WEIR
FLOW
STANDING
WAVES
560
520
470
500
510
520
490
460
560
580
490
470
540
500
TYPE 11 DESIGN
BERMS BLOCKED
SCALE 1 : 50
DISCHARGE = 590,000 CFS

Plate 21

Plate 22

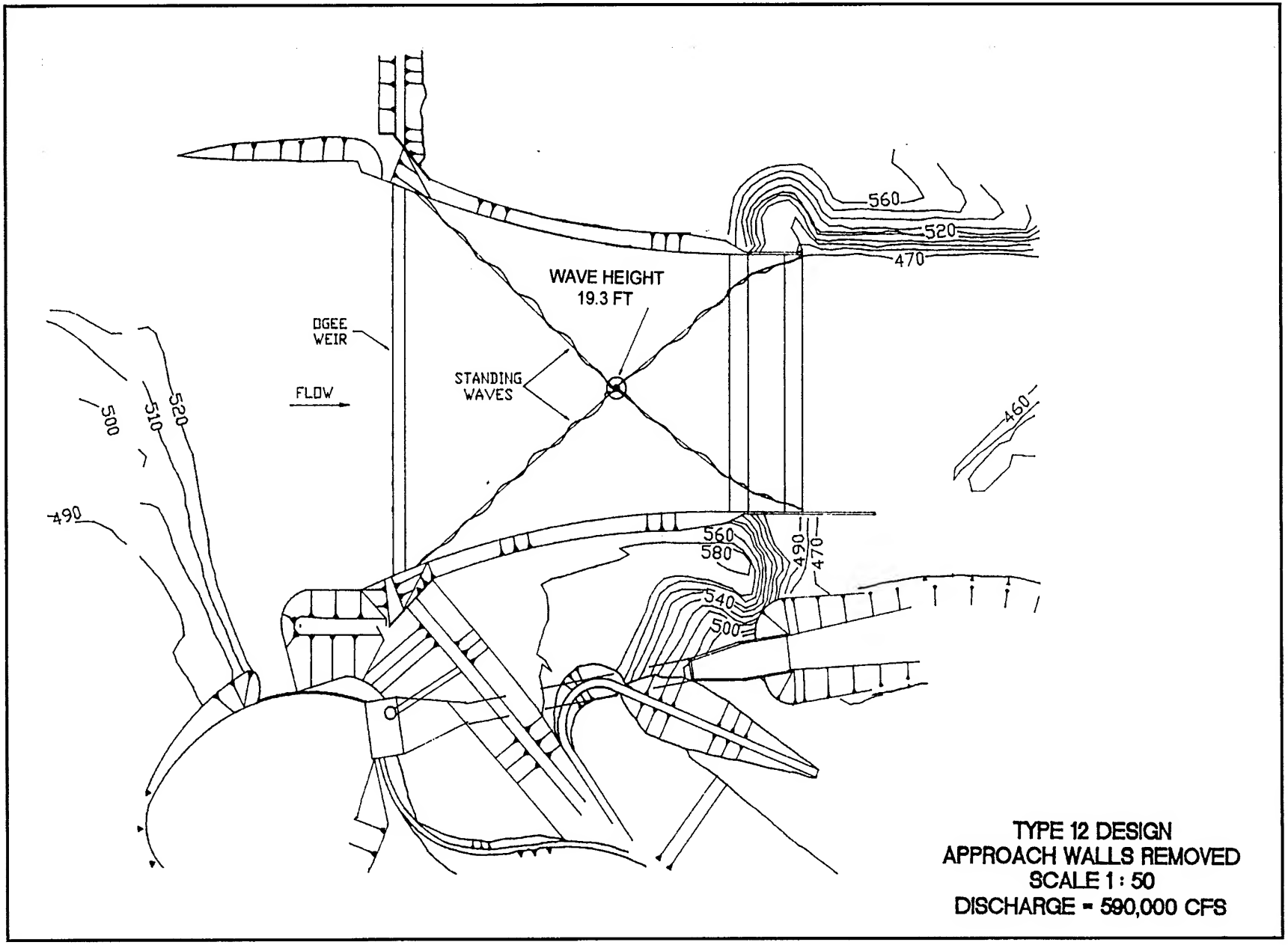

TYPE 12 DESIGN
APPROACH WALLS REMOVED
SCALE 1 : 50
DISCHARGE = 590,000 CFS

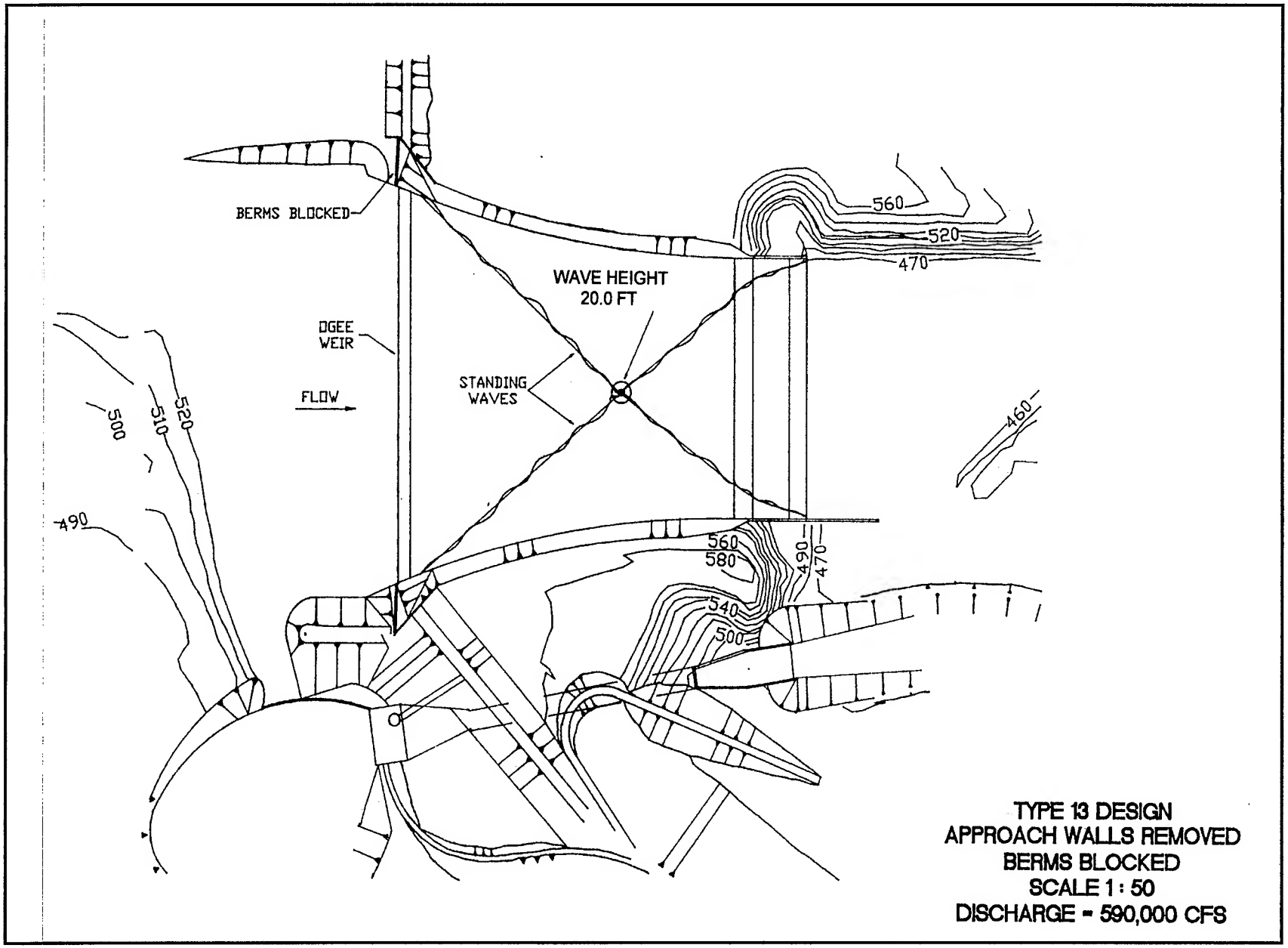
BERMS BLOCKED
WAVE HEIGHT
20.0 FT
OGEE
WEIR
FLOW
STANDING
WAVES
560
520
470
460
500
510
520
490
560
580
490
470
540
500
TYPE 13 DESIGN
APPROACH WALLS REMOVED
BERMS BLOCKED
SCALE 1 : 50
DISCHARGE = 590,000 CFS

Plate 23

Plate 24

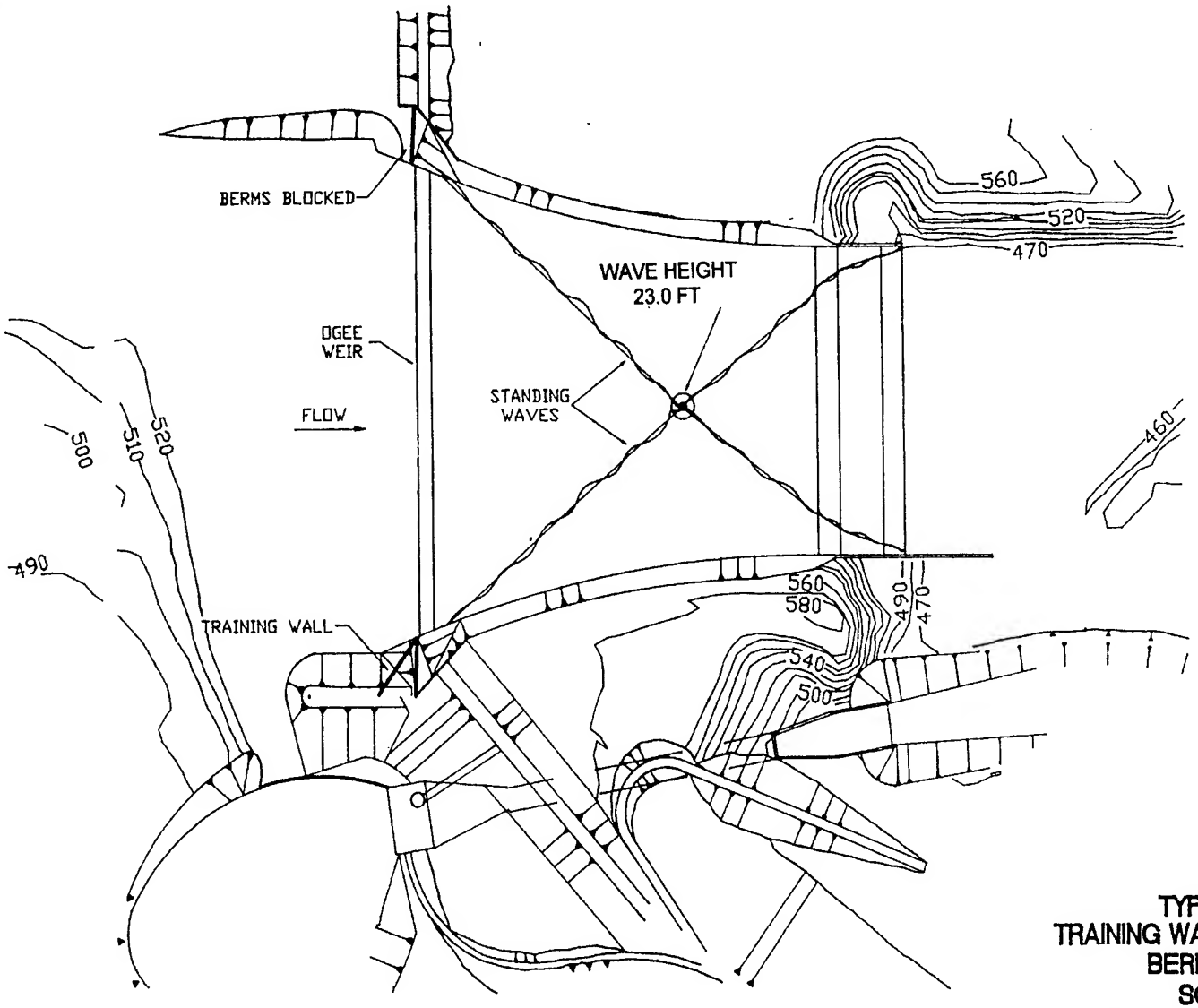

TYPE 14 DESIGN
TRAINING WALL RIGHT ABUTMENT
BERMS BLOCKED
SCALE 1 : 50
DISCHARGE = 590,000 CFS

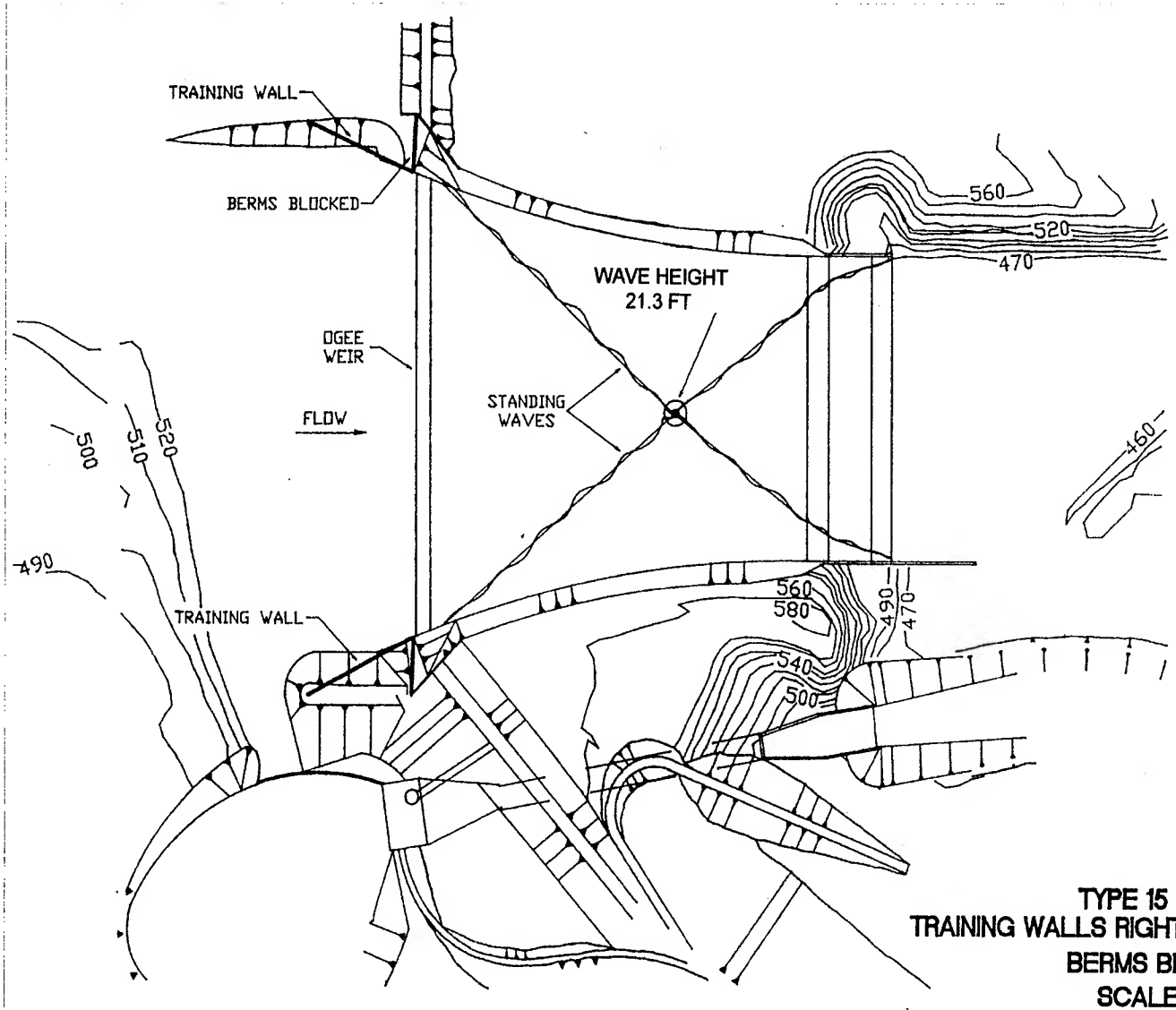

TYPE 15 DESIGN
TRAINING WALLS RIGHT + LEFT ABUTMENTS
BERMS BLOCKED
SCALE 1 : 50
DISCHARGE = 590,000 CFS

Plate 25

Plate 26

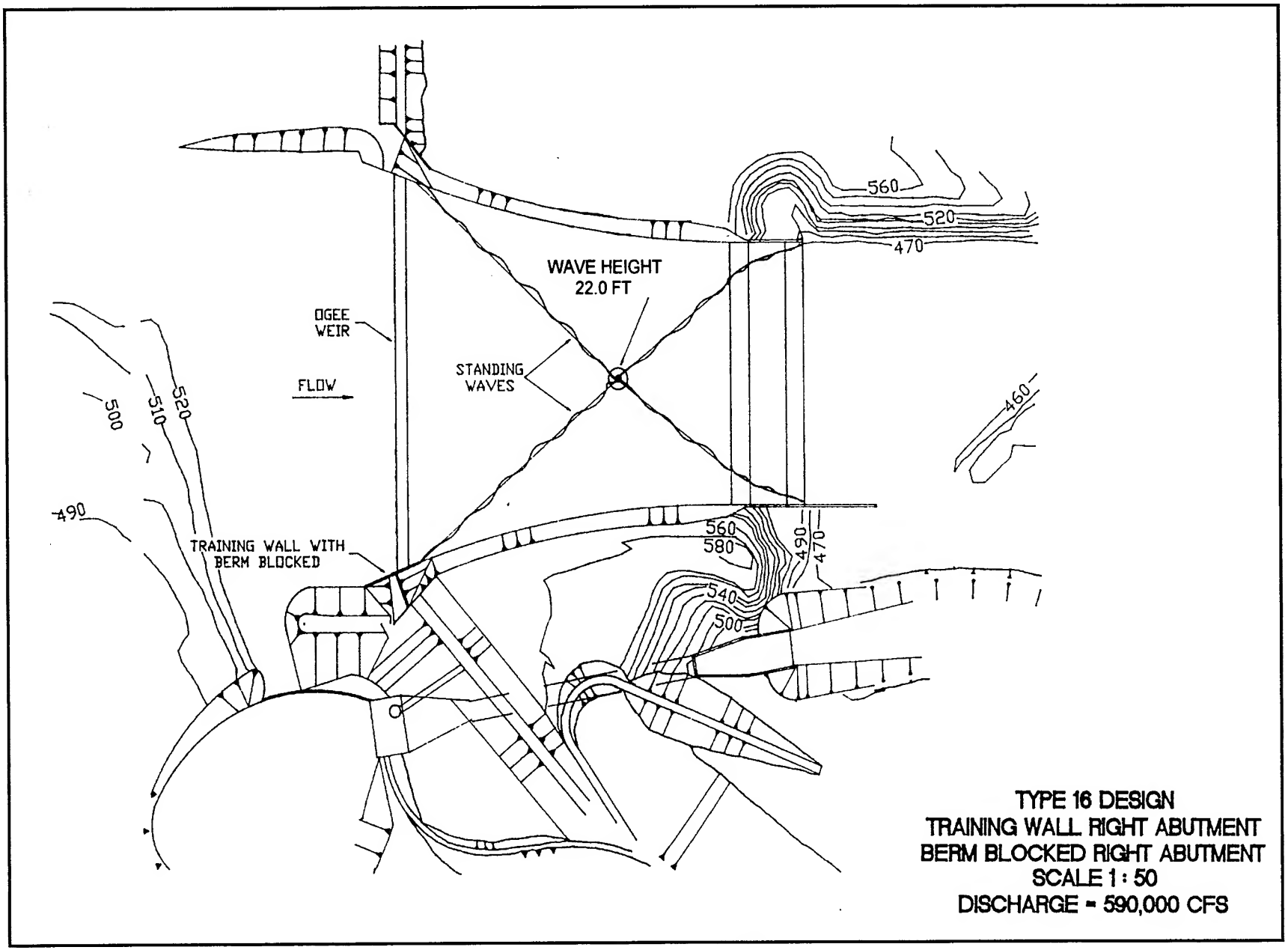
560
520
470
WAVE HEIGHT
22.0 FT
OGEE
WEIR
FLOW
STANDING
WAVES
500
510
520
490
460
TRAINING WALL WITH
BERM BLOCKED
560
580
490
470
540
500
TYPE 16 DESIGN
TRAINING WALL RIGHT ABUTMENT
BERM BLOCKED RIGHT ABUTMENT
SCALE 1 : 50
DISCHARGE = 590,000 CFS

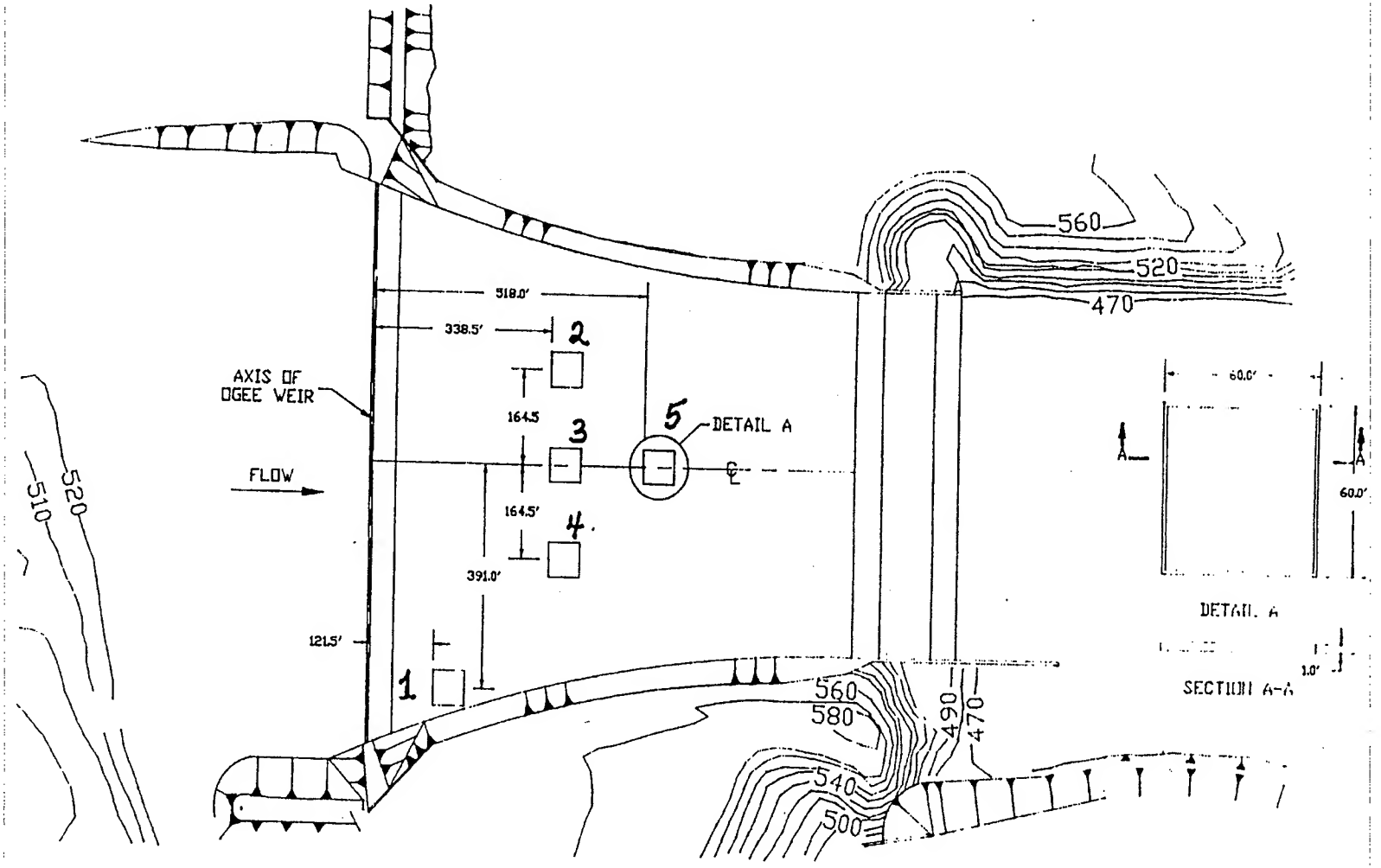

TYPE 12 DESIGN
60 FT SQ BLOCKS
SCALE 1 : 50

Plate 27

Plate 28

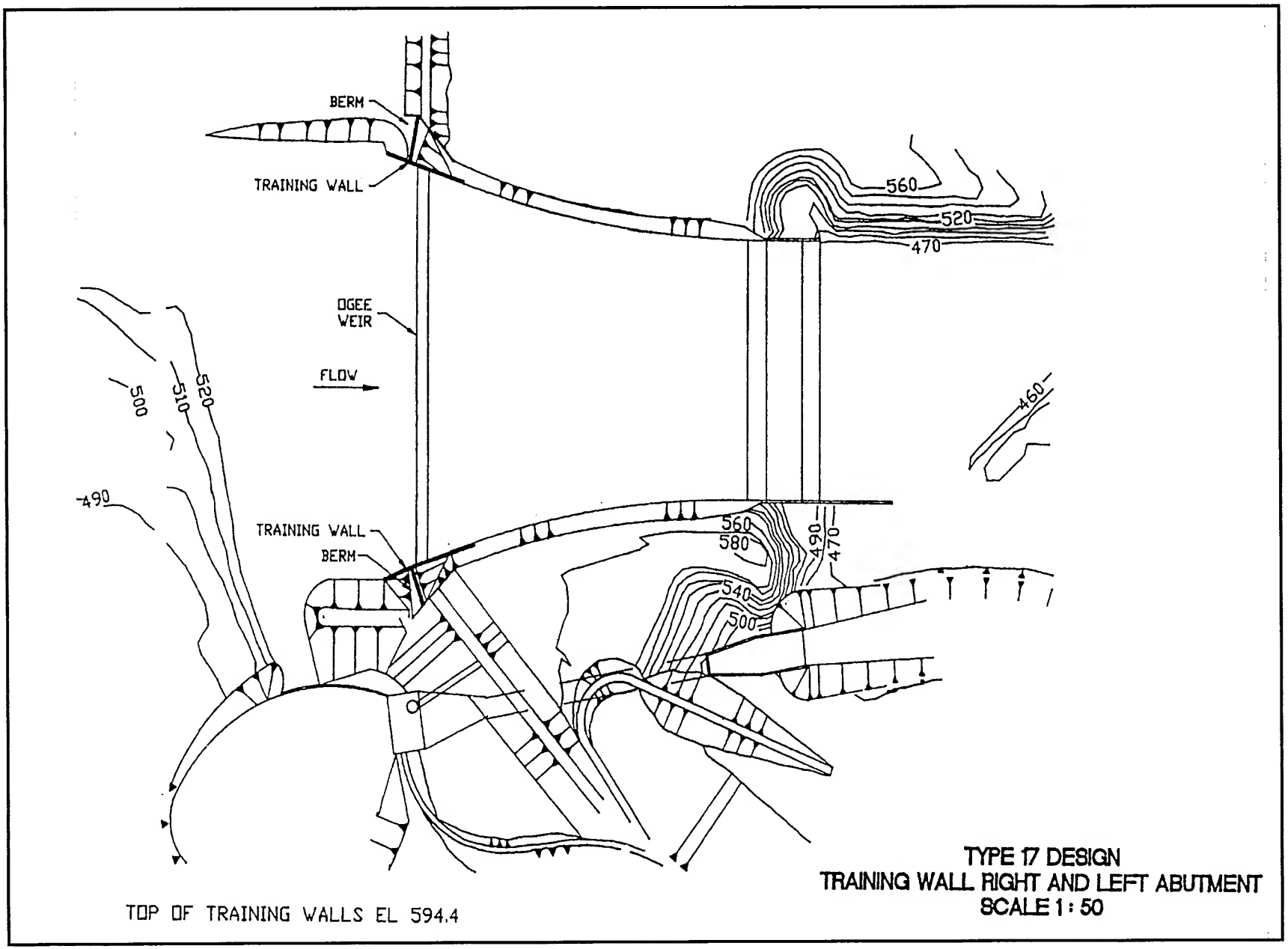
BERM
TRAINING WALL
560
520
470
OGEE
WEIR
FLOW
500
510
520
490
460
TRAINING WALL
BERM
560
580
490
470
540
500
TOP OF TRAINING WALLS EL 594.4
TYPE 17 DESIGN
TRAINING WALL RIGHT AND LEFT ABUTMENT
SCALE 1 : 50

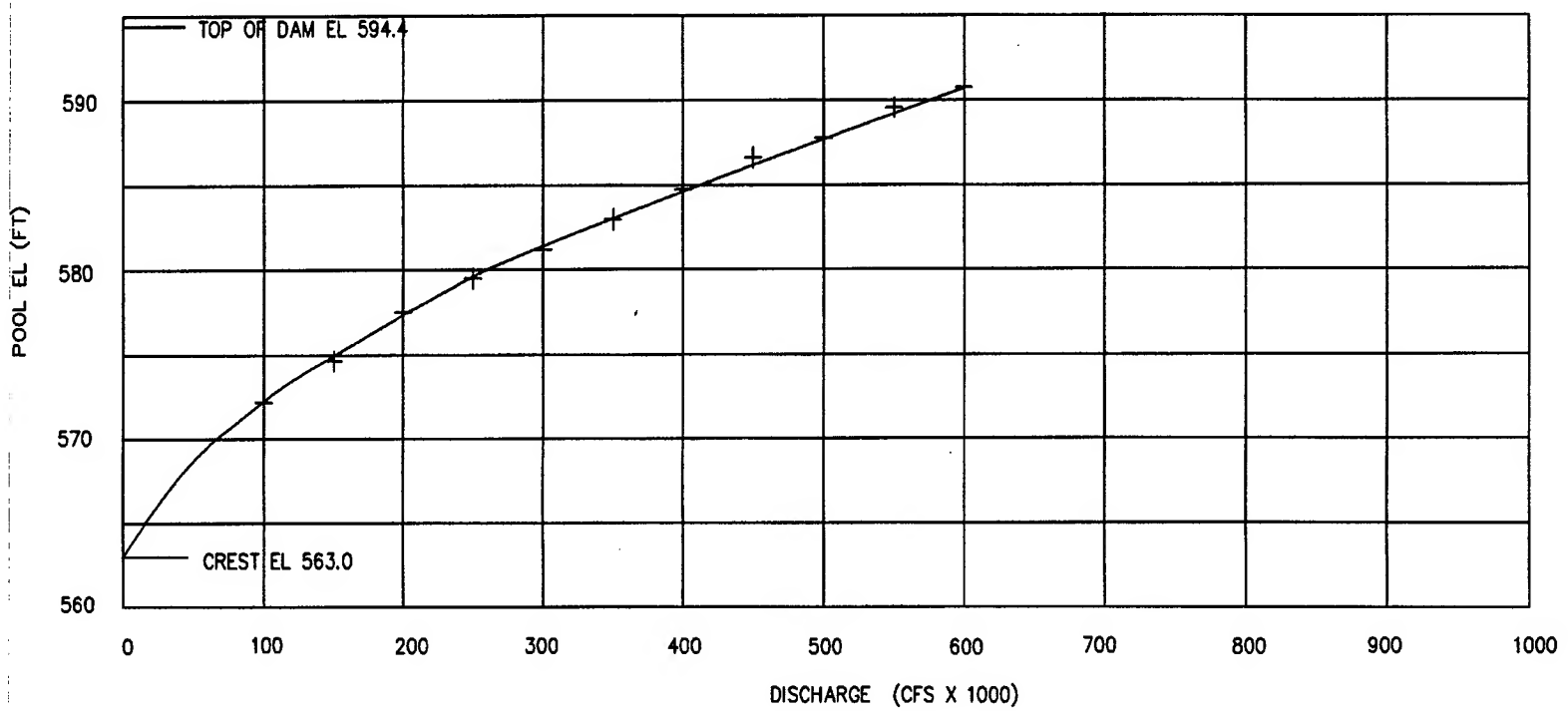

BASIC DATA

DISCHARGE	POOL EL
100,000	572.20
150,000	574.65
200,000	577.50
250,000	579.50
300,000	581.20
350,000	583.00
400,000	584.75
450,000	586.60
500,000	587.75
550,000	589.55
600,000	590.75

TYPE 18 DESIGN
RATING CURVE

Plate 29

Plate 30

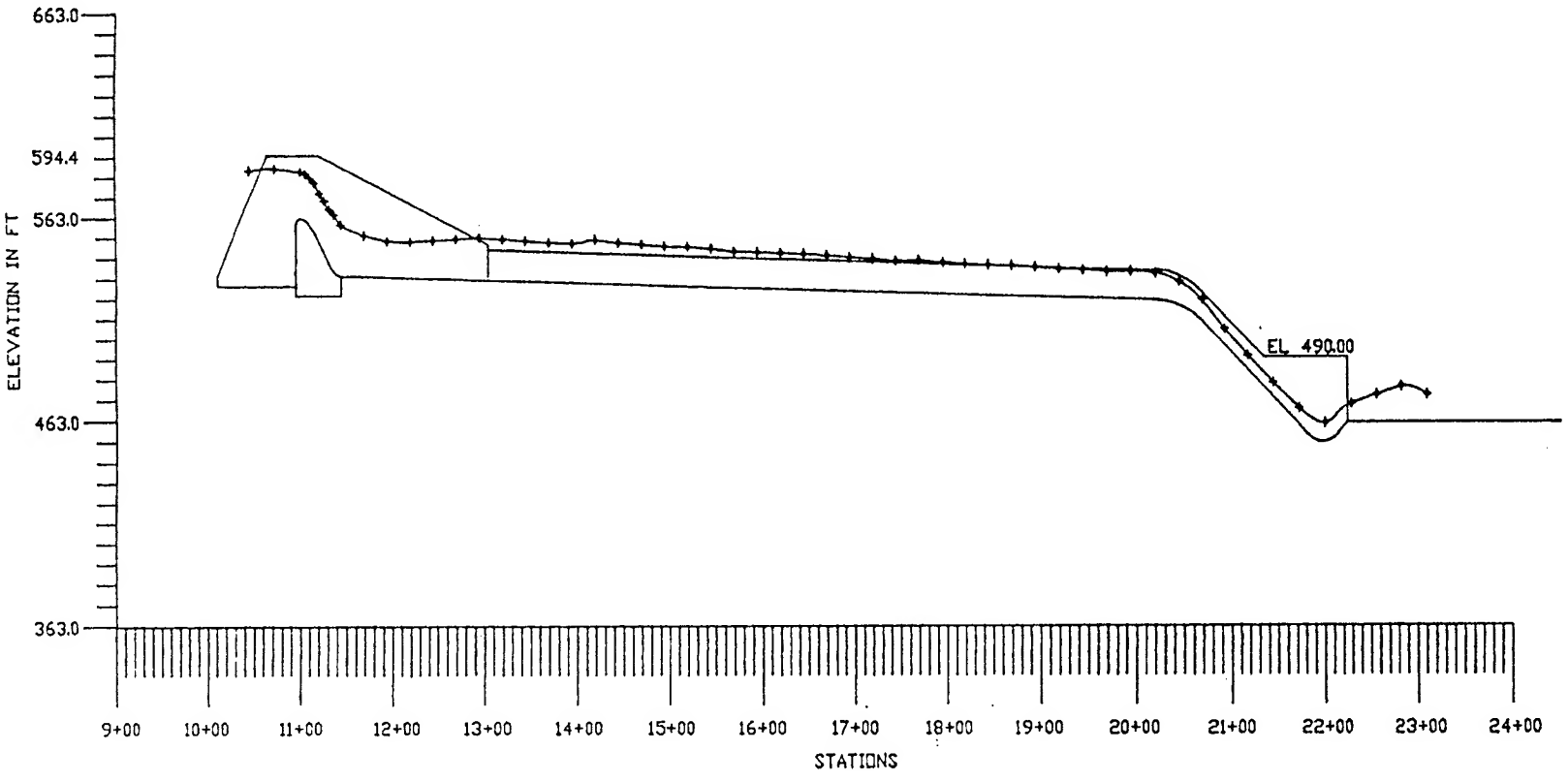

NOTE: STA 11+00 = CENTERLINE OF CREST

WATER SURFACE PROFILE-LEFT WALL
TYPE 18 DESIGN
Q = 481,000 CFS

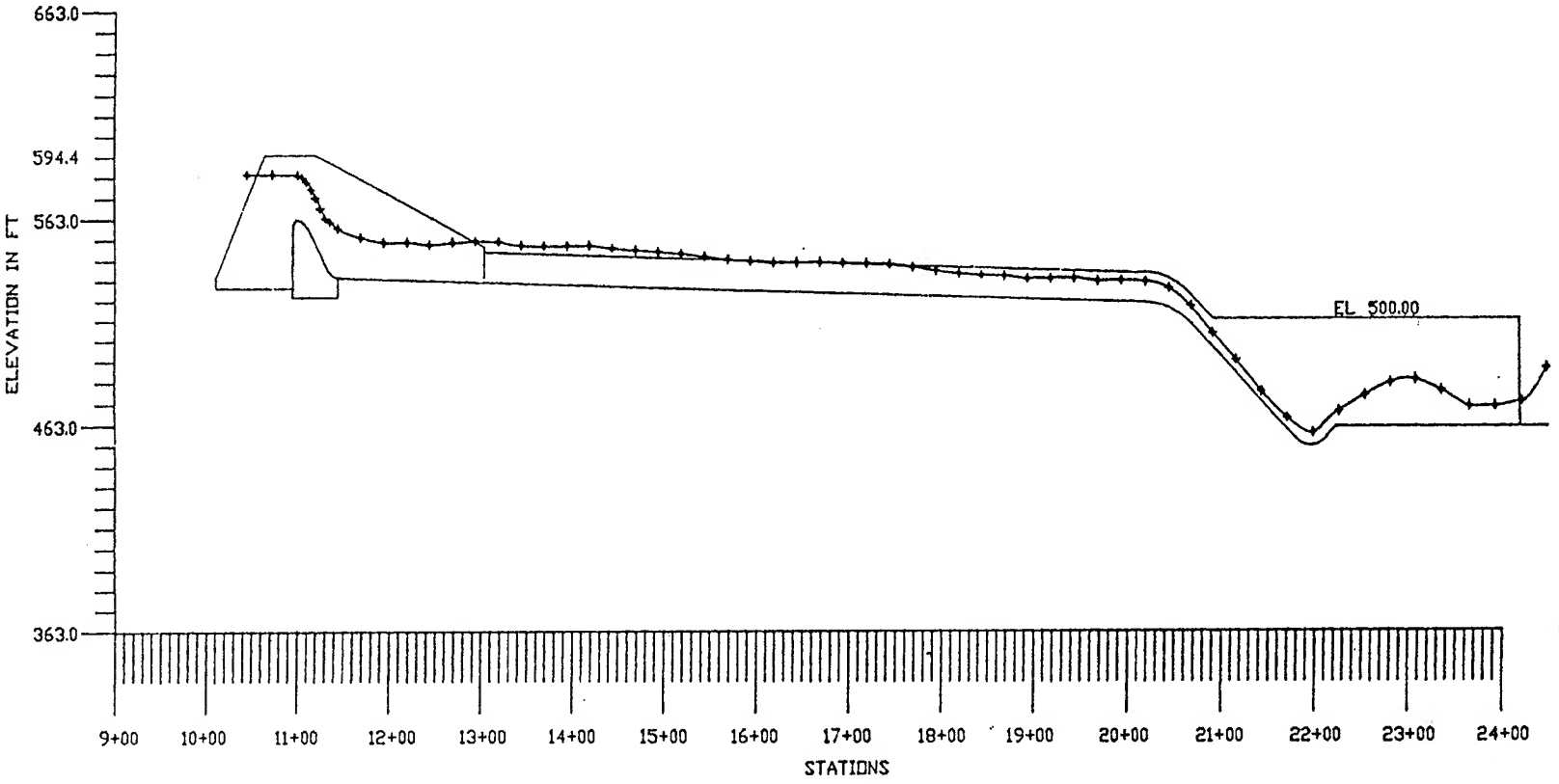

STA 11+00 = CENTER LINE OF CREST

WATER SURFACE PROFILE-RIGHT WALL
TYPE 18 DESIGN
Q = 481,000 CFS

Plate 31

Q = 481,000 CFS

STATION	LEFT WALL	RIGHT WALL
STA 10+45	588.00	585.00
STA 10+72	588.00	585.00
STA 11+00	586.00	584.50
STA 11+05	585.45	583.95
STA 11+11	583.35	581.35
STA 11+16	580.85	577.85
STA 11+22	575.72	573.72
STA 11+27	572.00	568.50
STA 11+33	567.78	563.78
STA 11+38	565.06	562.06
STA 11+45	559.99	558.99
STA 11+70	554.26	554.26
STA 11+95	551.42	551.92
STA 12+20	568.72	552.07
STA 12+45	551.72	550.72
STA 12+70	552.37	551.87
STA 12+95	553.02	552.52
STA 13+20	552.17	552.17
STA 13+45	551.32	550.32
STA 13+70	550.47	549.97
STA 13+95	550.12	550.12
STA 14+20	551.77	550.27
STA 14+45	550.42	548.92
STA 14+70	549.58	548.08
STA 14+95	548.73	547.23
STA 15+20	548.38	546.38
STA 15+45	547.53	545.03
STA 15+70	546.18	543.68
STA 15+95	545.83	542.83
STA 16+20	545.48	541.98
STA 16+45	545.14	542.14
STA 16+70	544.28	542.28
STA 16+95	543.44	541.94
STA 17+20	542.59	541.59
STA 17+45	541.74	541.24
STA 17+70	542.19	540.19
STA 17+95	541.04	538.04
STA 18+20	540.19	536.69
STA 18+45	539.84	535.84
STA 18+70	539.49	535.49
STA 18+95	538.64	534.14
STA 19+20	537.80	534.30
STA 19+45	537.45	534.45
STA 19+70	536.60	533.10
STA 19+95	536.75	533.25
STA 20+20	535.90	532.90
STA 20+45	531.66	529.66
STA 20+68	522.68	520.68
STA 20+93	507.	506.83
STA 21+17	494.57	493.57
STA 21+44	481.36	478.86
STA 21+71	468.66	466.16
STA 21+99	461.46	458.96
STA 22+27	470.97	469.47
STA 22+54	475.47	476.97
STA 22+82	479.47	482.97
STA 23+09	475.47	484.47
STA 23+37		479.47
STA 23+64		471.97
STA 23+92		471.97
STA 24+19		474.47
STA 24+47		489.47

STA 11+00 = CENTER LINE OF CREST

BASIC DATA
WATER SURFACE ELEVATIONS
TYPE 18 DESIGN

Plate 32

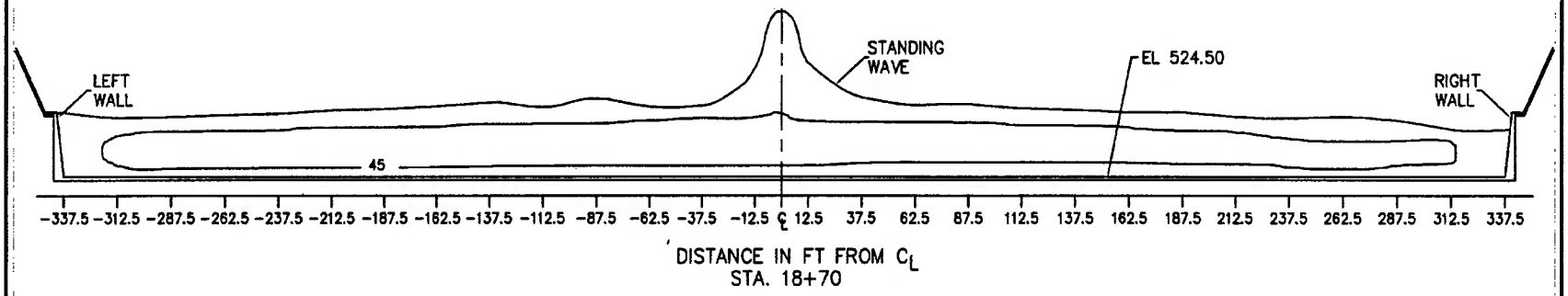

NOTE: MAXIMUM HEIGHT STANDING WAVE DEVELOPED AT STATION 18+70, ISOVEL IS IN FT PER SEC

Q = 481,000 CFS

DISTANCE FROM ℄	ELEVATION	DISTANCE FROM ℄	ELEVATION
-337.5	539.49	12.5	550.84
-312.5	538.29	37.5	542.99
-287.5	538.44	62.5	541.14
-262.5	538.89	87.5	541.29
-237.5	539.19	112.5	540.39
-212.5	539.99	137.5	540.04
-187.5	540.24	162.5	539.49
-162.5	540.89	187.5	539.44
-137.5	541.74	212.5	538.39
-112.5	540.74	237.5	538.04
-87.5	542.74	262.5	538.44
-62.5	540.84	287.5	537.54
-37.5	541.04	312.5	535.49
-12.5	548.44	337.5	535.49
0.0	562.84		

TYPE 18 DESIGN
CROSS SECTION VIEWED
FROM UPSTREAM
Q = 481,000 CFS

Plate 33

Plate 34

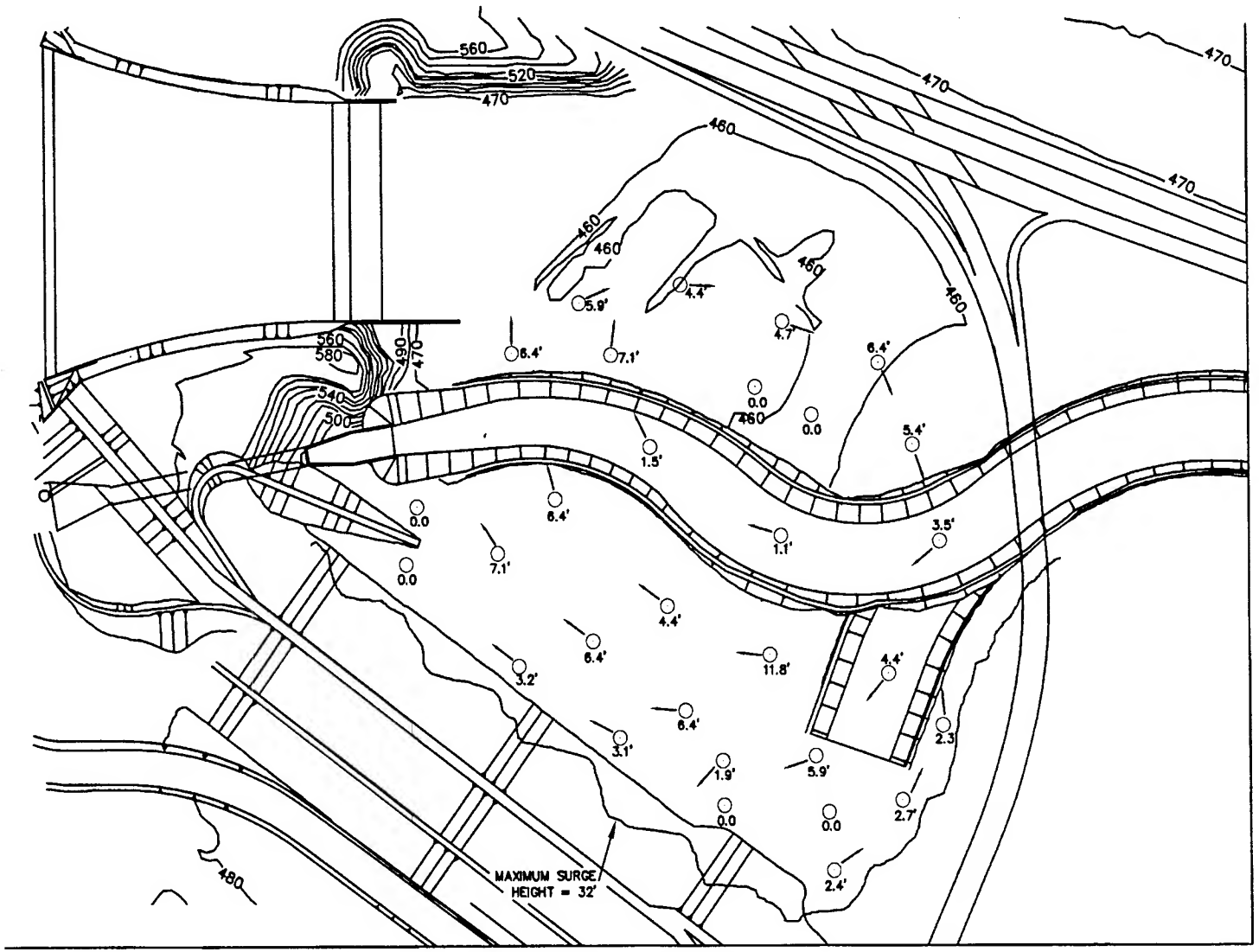

LEGEND
⊙— VELOCITIES

NOTE: VELOCITIES ARE IN FEET PER SECOND
MEASURED 1 FT ABOVE THE BOTTOM
Q = 481,000 CFS
TAILWATER EL = 501.00

TYPE 18 DESIGN
VELOCITIES

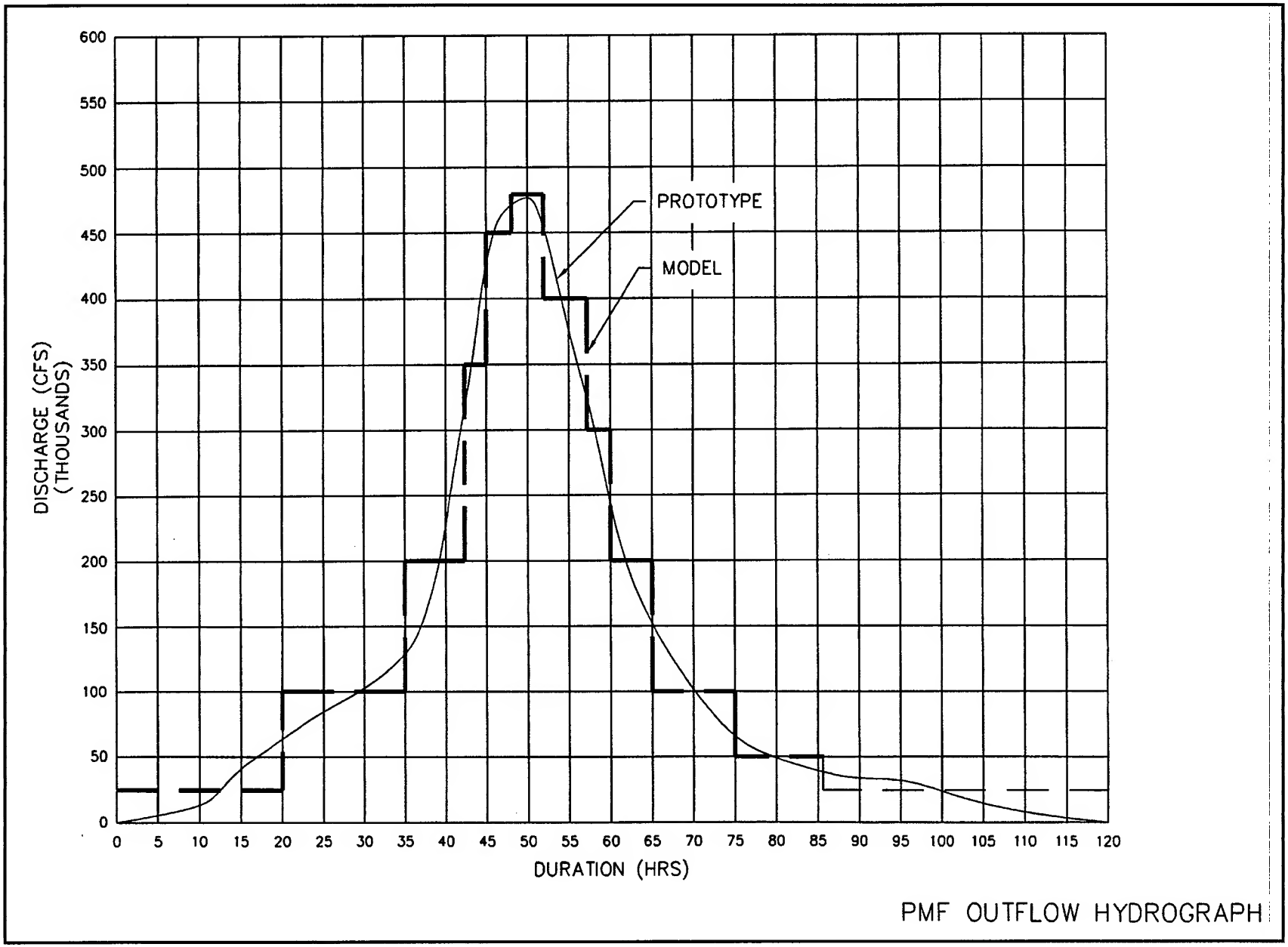

PMF OUTFLOW HYDROGRAPH

Plate 35

Plate 36

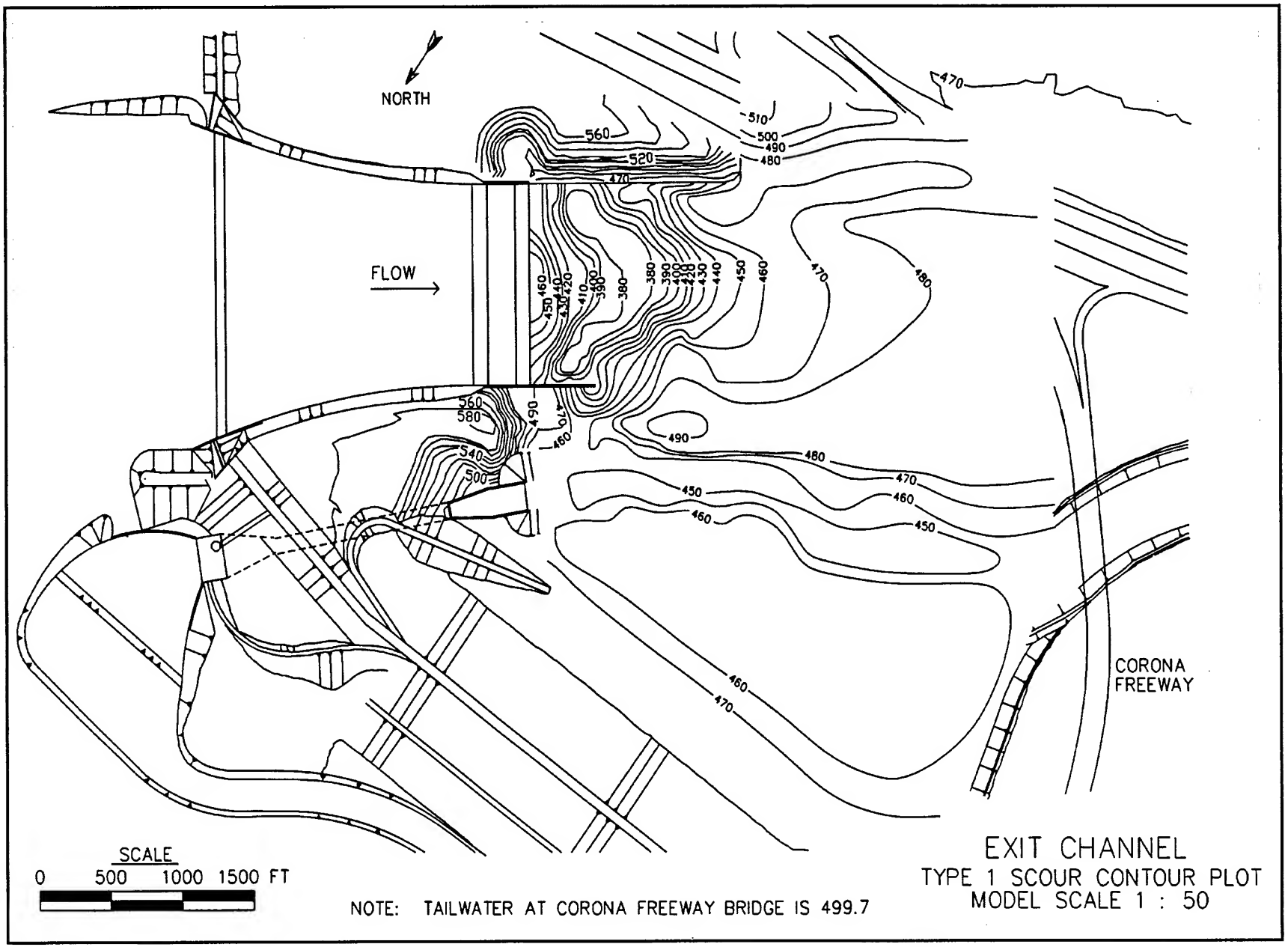
NORTH
FLOW
CORONA FREEWAY
SCALE
0 500 1000 1500 FT
NOTE: TAILWATER AT CORONA FREEWAY BRIDGE IS 499.7
EXIT CHANNEL
TYPE 1 SCOUR CONTOUR PLOT
MODEL SCALE 1 : 50

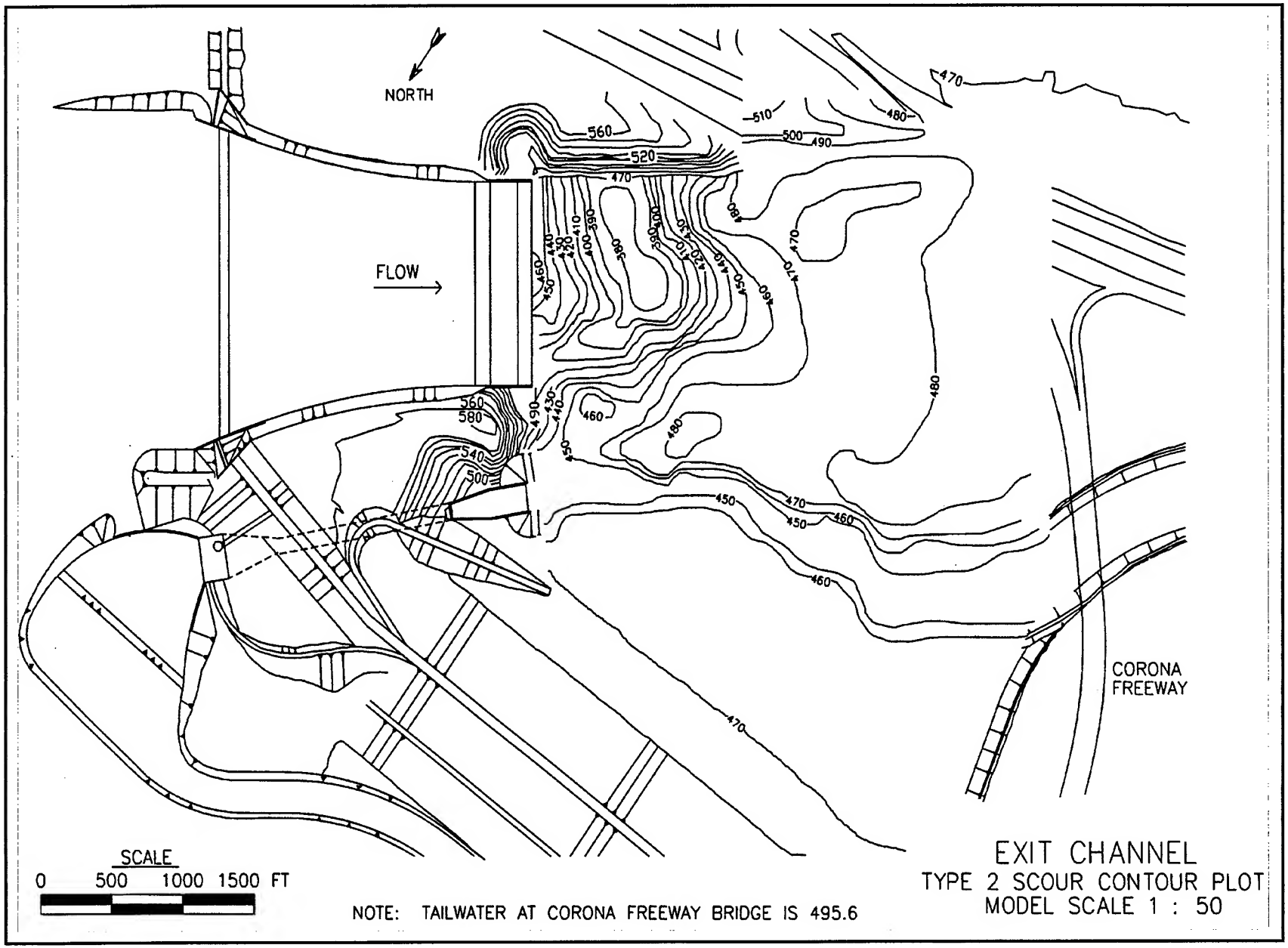
NORTH
FLOW
CORONA
FREEWAY
SCALE
0 500 1000 1500 FT
NOTE: TAILWATER AT CORONA FREEWAY BRIDGE IS 495.6
EXIT CHANNEL
TYPE 2 SCOUR CONTOUR PLOT
MODEL SCALE 1 : 50

Plate 37

Plate 38

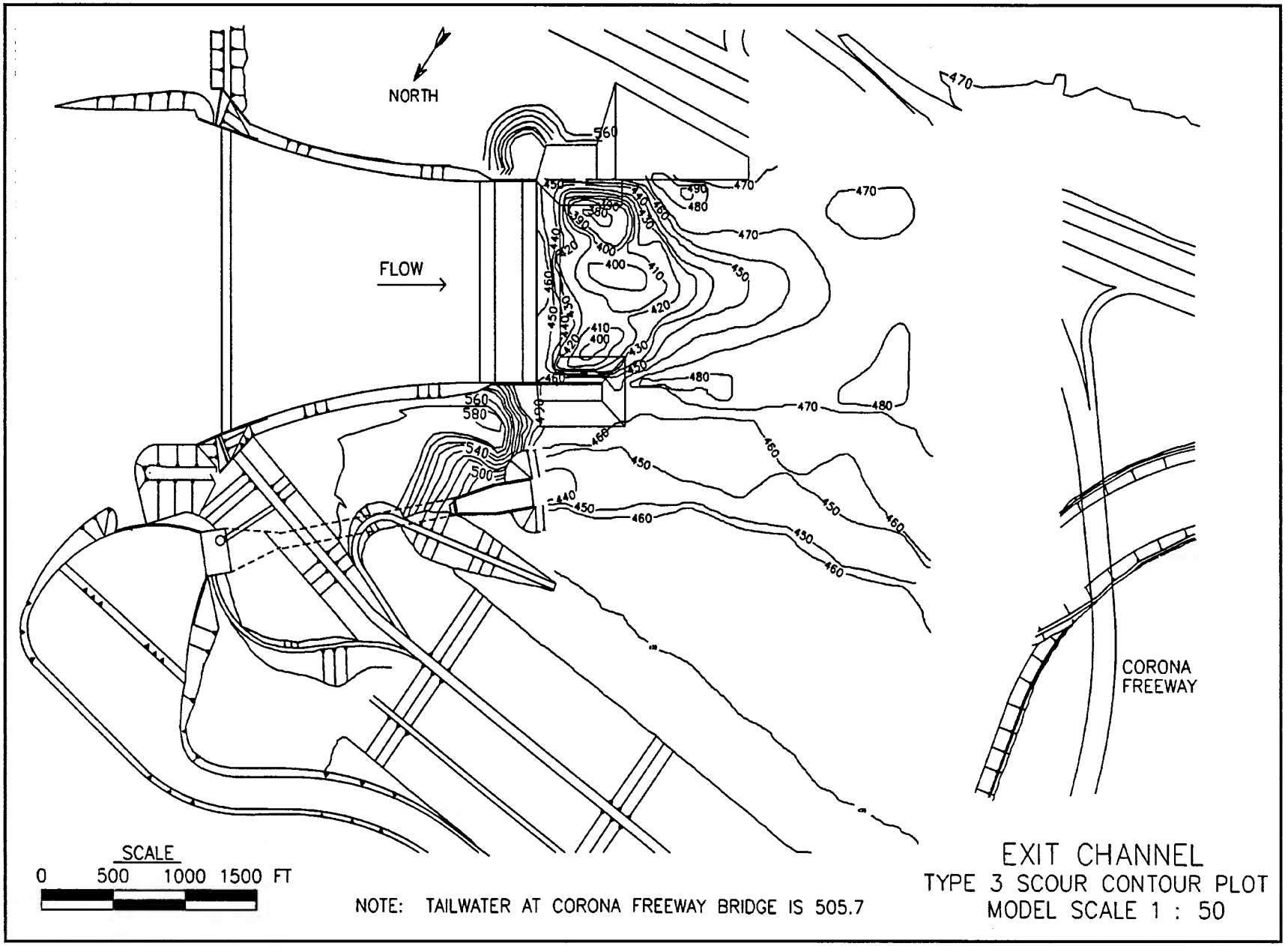
NORTH
FLOW
CORONA FREEWAY
SCALE
0 500 1000 1500 FT
NOTE: TAILWATER AT CORONA FREEWAY BRIDGE IS 505.7
EXIT CHANNEL
TYPE 3 SCOUR CONTOUR PLOT
MODEL SCALE 1 : 50

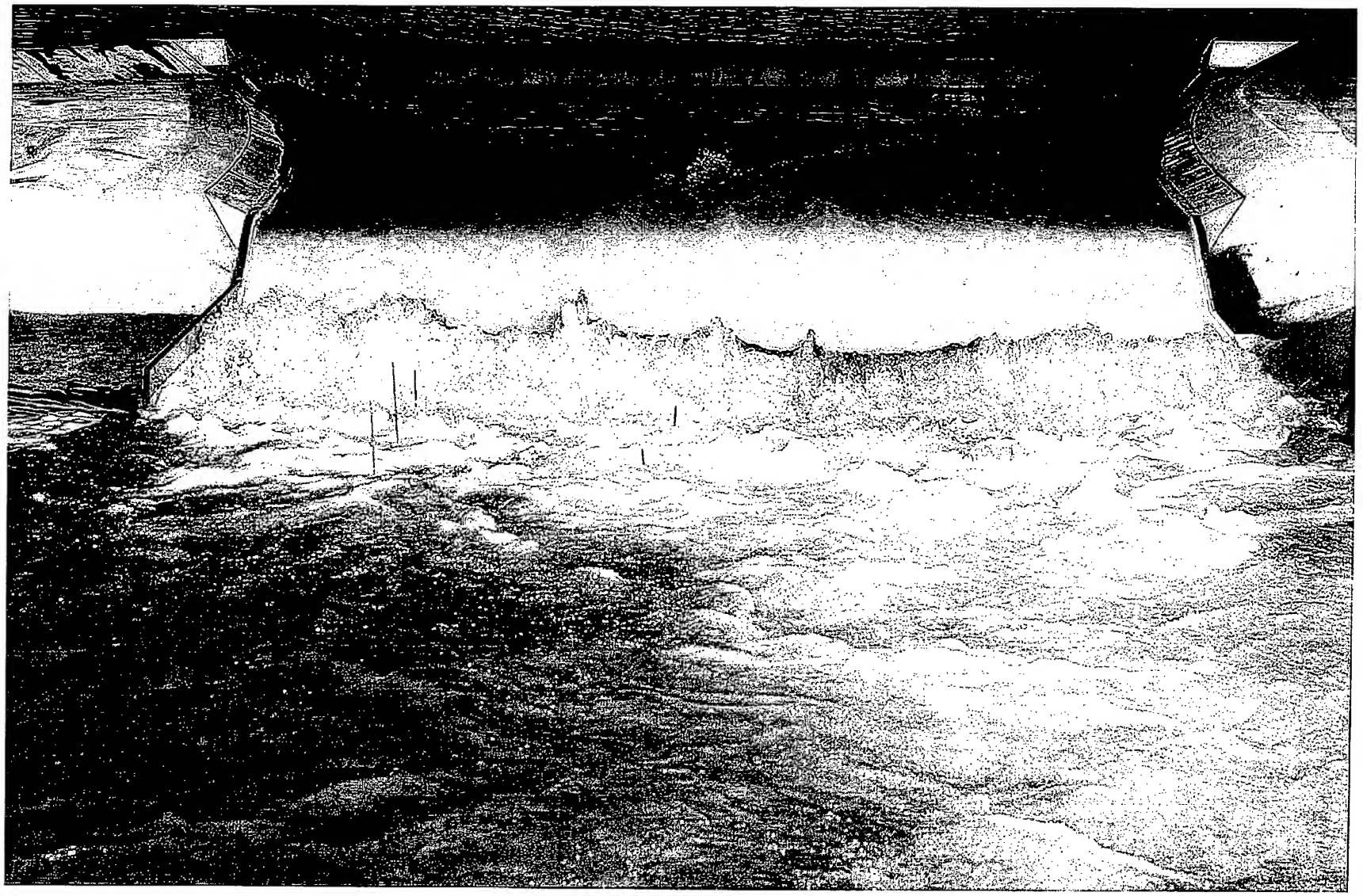

Figure 14. Hydraulic performance of type 19 spillway and type 6 exit channel looking upstream

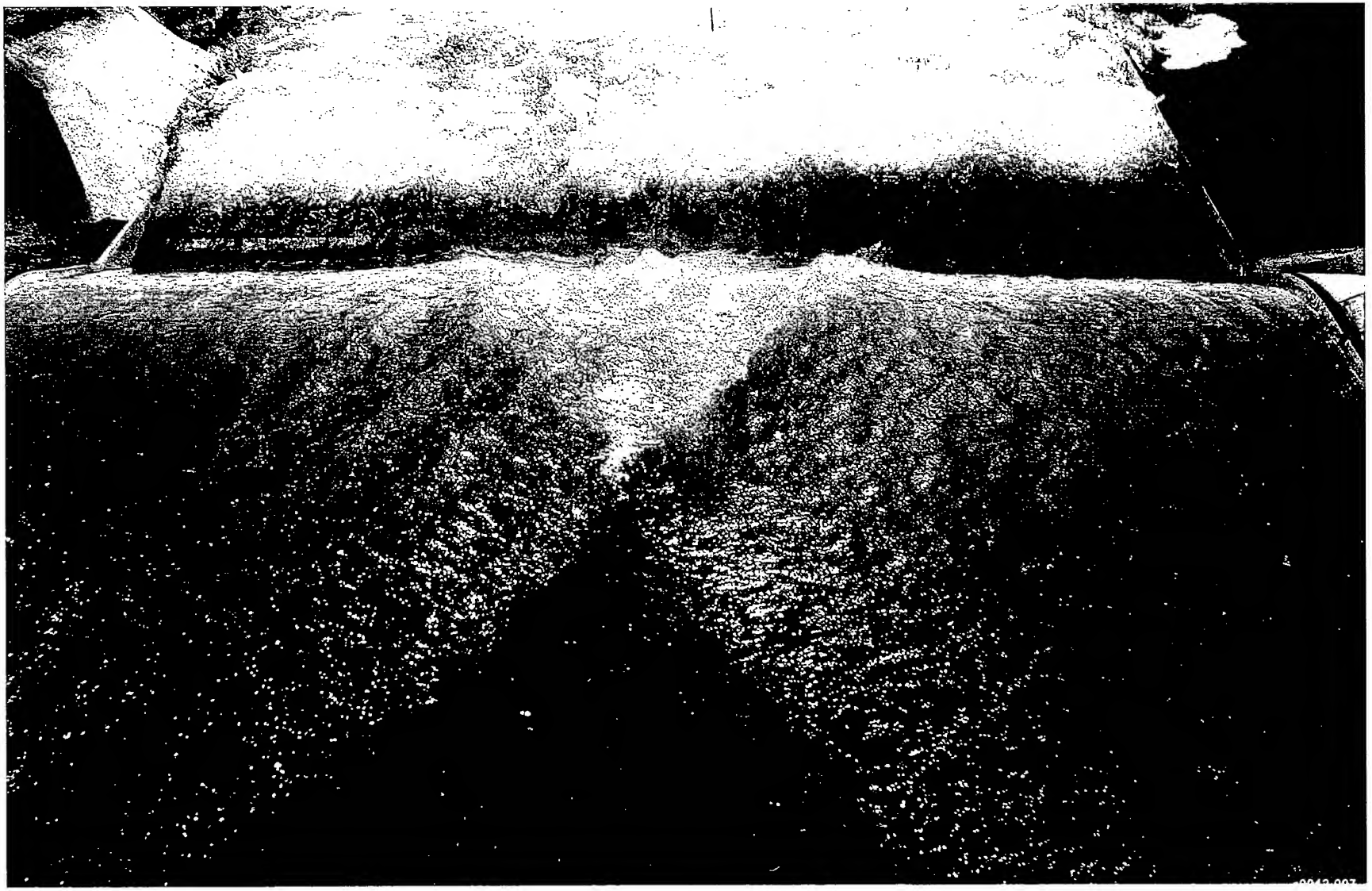

Figure 15. Hydraulic performance of type 19 spillway and type 6 exit channel looking downstream

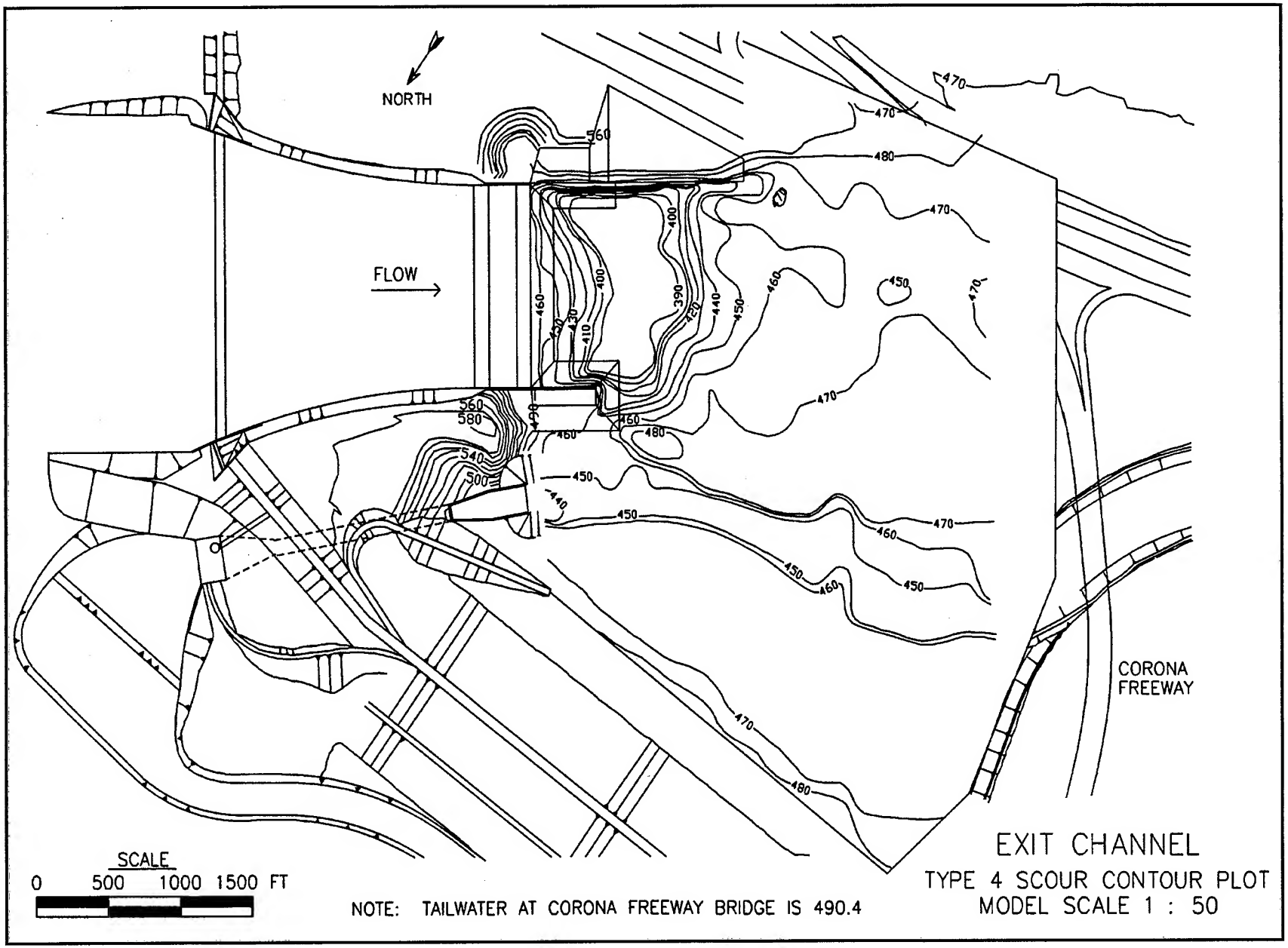
NORTH
FLOW
CORONA
FREEWAY
SCALE
0 500 1000 1500 FT
NOTE: TAILWATER AT CORONA FREEWAY BRIDGE IS 490.4
EXIT CHANNEL
TYPE 4 SCOUR CONTOUR PLOT
MODEL SCALE 1 : 50

Plate 41

Plate 42

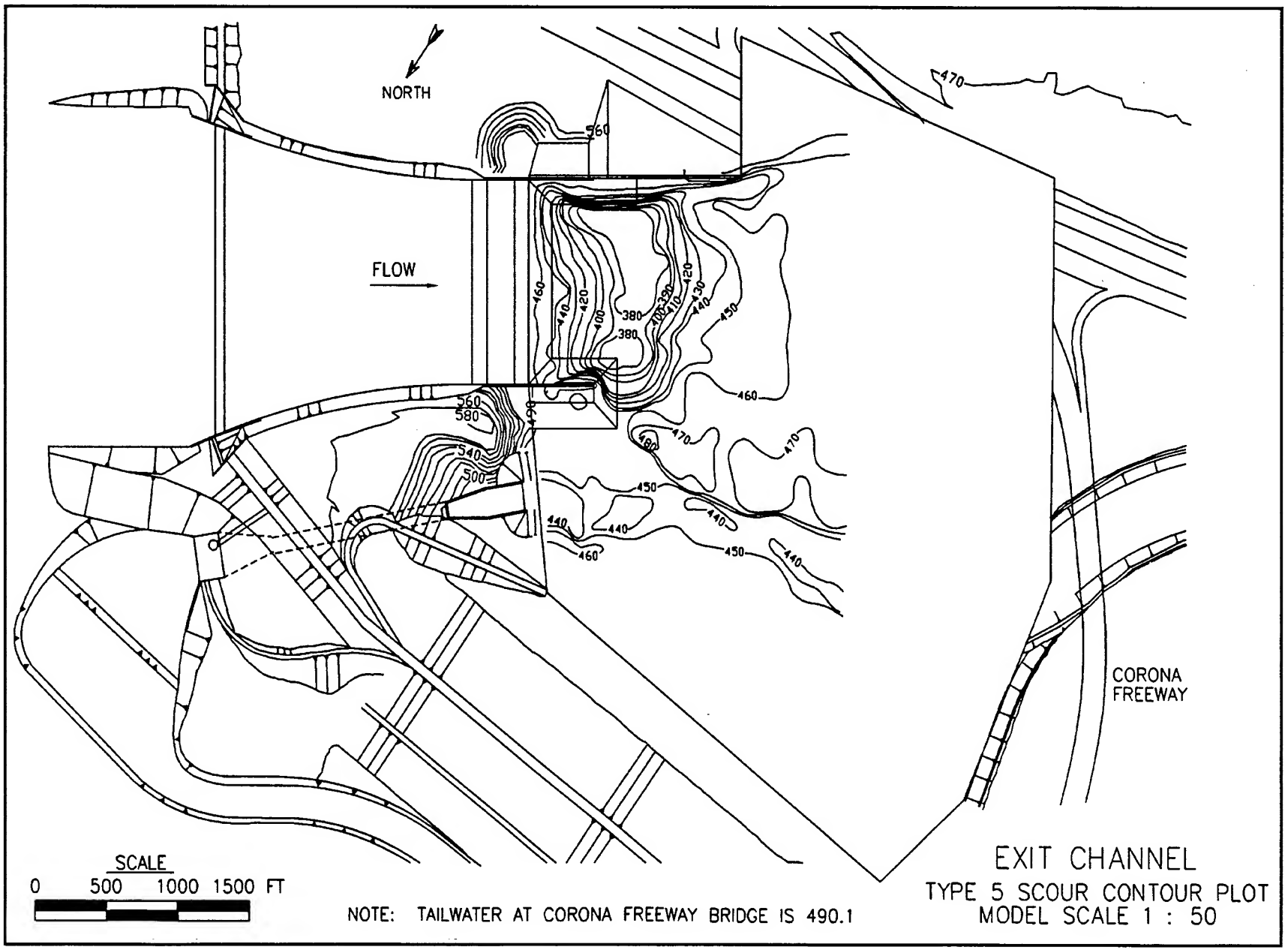
NORTH
FLOW
560
470
460
440
420
400
380
360
340
320
310
430
450
580
540
500
490
480
CORONA
FREEWAY
SCALE
0 500 1000 1500 FT
NOTE: TAILWATER AT CORONA FREEWAY BRIDGE IS 490.1
EXIT CHANNEL
TYPE 5 SCOUR CONTOUR PLOT
MODEL SCALE 1 : 50

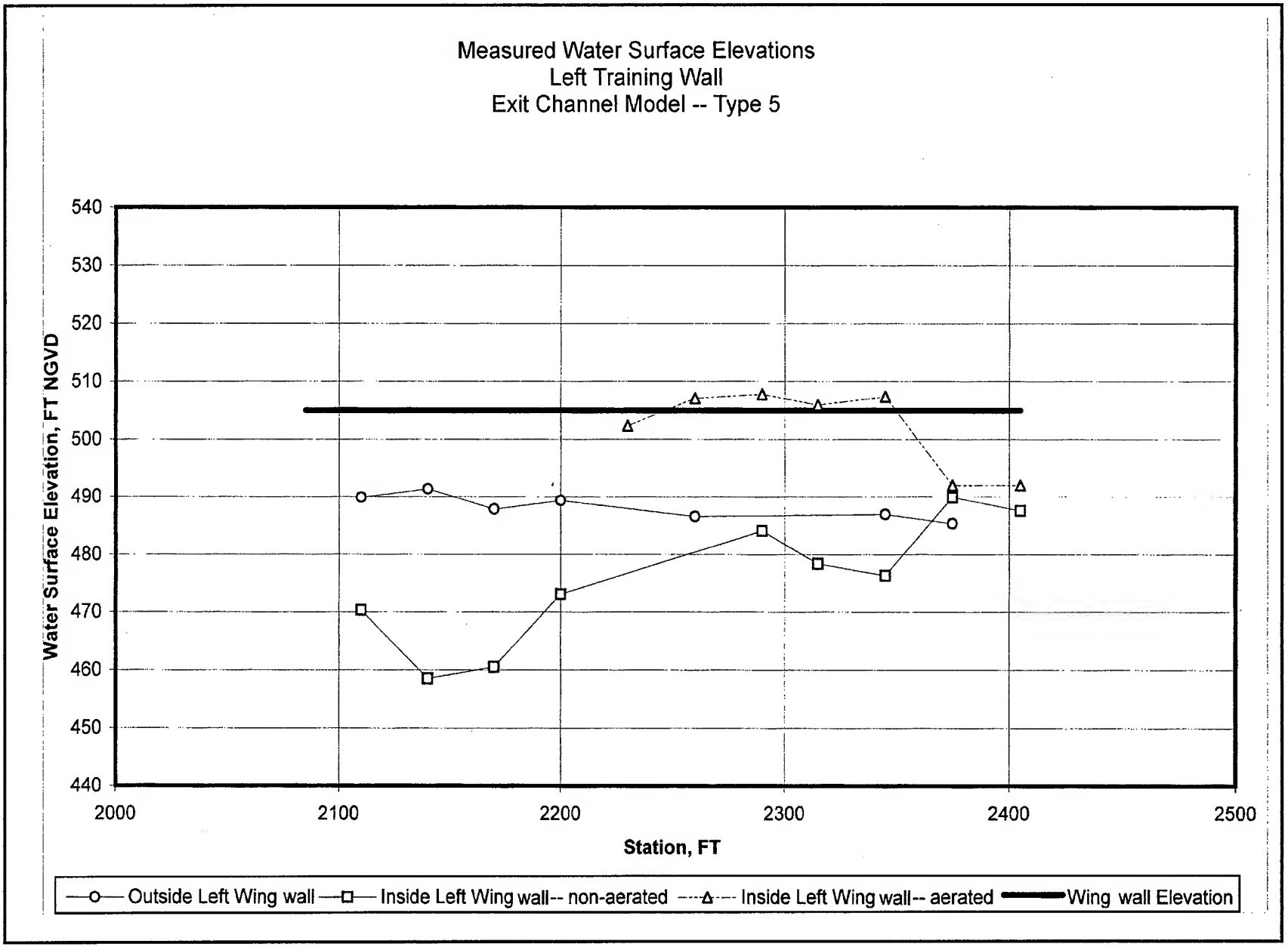
Measured Water Surface Elevations
Left Training Wall
Exit Channel Model -- Type 5
Water Surface Elevation, FT NGVD
540
530
520
510
500
490
480
470
460
450
440
2000
2100
2200
2300
2400
2500
Station, FT
Outside Left Wing wall
Inside Left Wing wall-- non-aerated
Inside Left Wing wall-- aerated
Wing wall Elevation

Plate 43

Plate 44

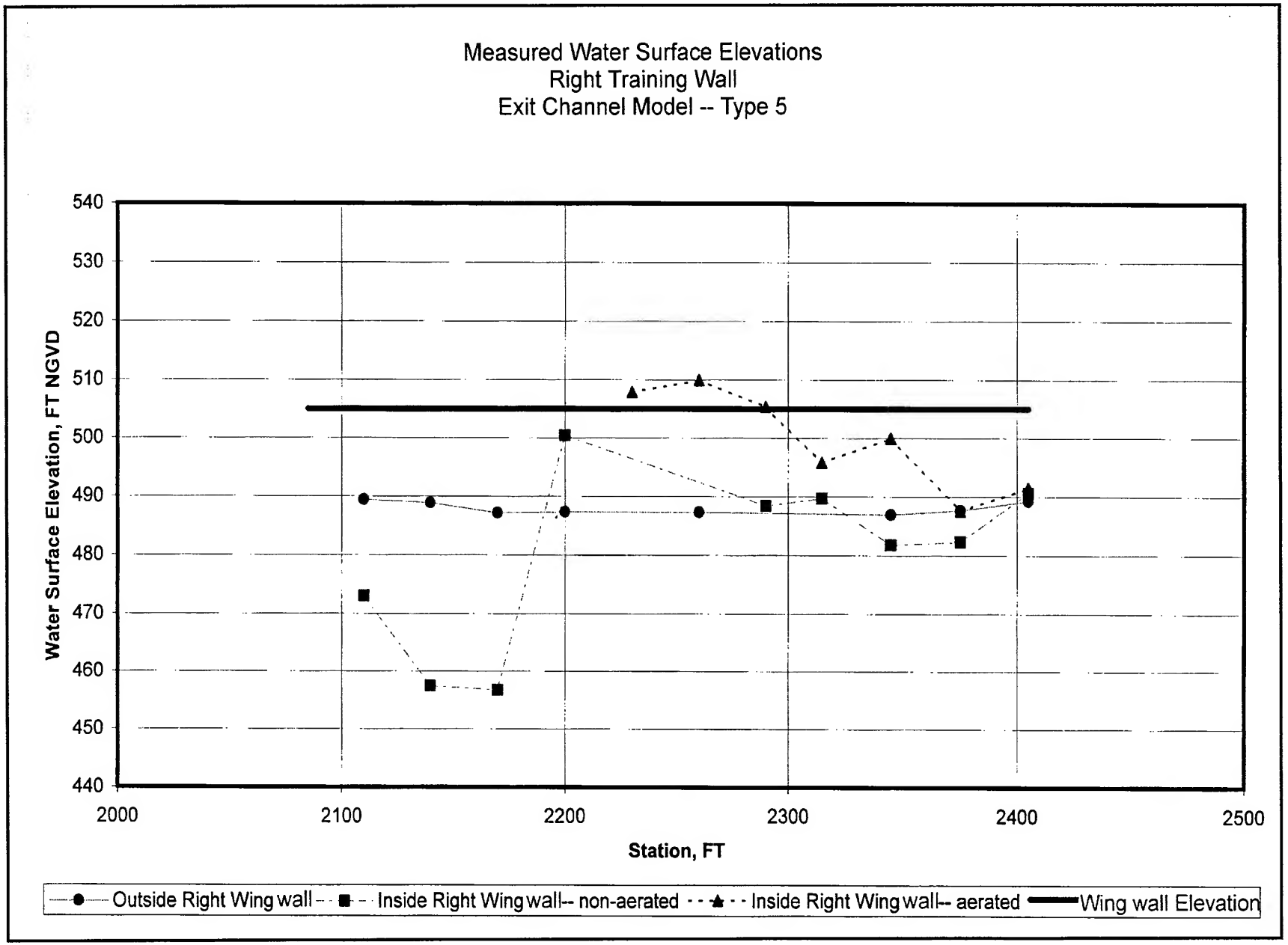
Measured Water Surface Elevations
Right Training Wall
Exit Channel Model -- Type 5
Water Surface Elevation, FT NGVD
540
530
520
510
500
490
480
470
460
450
440
2000
2100
2200
2300
2400
2500
Station, FT
Outside Right Wing wall
Inside Right Wing wall-- non-aerated
Inside Right Wing wall-- aerated
Wing wall Elevation

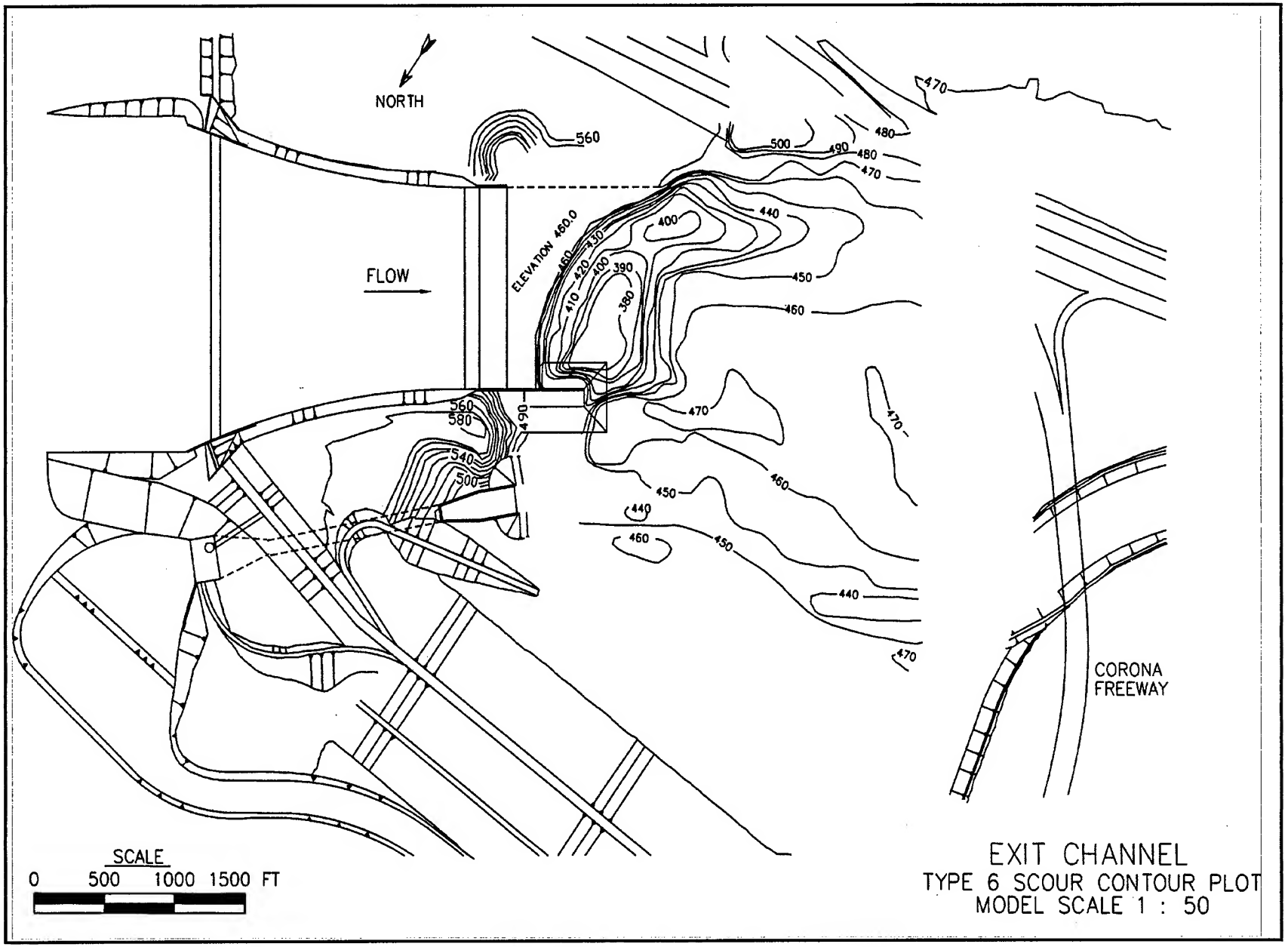

EXIT CHANNEL
TYPE 6 SCOUR CONTOUR PLOT
MODEL SCALE 1 : 50

Plate 45

REPORT DOCUMENTATION PAGE

Form Approved
OMB No. 0704-0188

1. REPORT DATE *(DD-MM-YYYY)*	2. REPORT TYPE	3. DATES COVERED *(From - To)*
September 2000	Final Report	

4. TITLE AND SUBTITLE

Model Study of Prado Spillway, California
Hydraulic Model Investigation

5a. CONTRACT NUMBER

5b. GRANT NUMBER

5c. PROGRAM ELEMENT NUMBER

6. AUTHOR(S)

Ronald R. Copeland and Bobby P. Fletcher

5d. PROJECT NUMBER

5e. TASK NUMBER

5f. WORK UNIT NUMBER

7. PERFORMING ORGANIZATION NAME(S) AND ADDRESS(ES) AND ADDRESS(ES)

U.S. Army Engineer Research and Development Center
Coastal and Hydraulics Laboratory
3909 Halls Ferry Road
Vicksburg, MS 39180-6199

8. PERFORMING ORGANIZATION REPORT NUMBER

ERDC/CHL TR-00-17

9. SPONSORING / MONITORING AGENCY NAME(S) AND ADDRESS(ES)

Headquarters, U.S. Army Corps of Engineers
Washington, DC 20314-1000

10. SPONSOR/MONITOR'S ACRONYM(S)

11. SPONSOR/MONITOR'S REPORT NUMBER(S)

12. DISTRIBUTION / AVAILABILITY STATEMENT

Approved for public release; distribution is unlimited.

13. SUPPLEMENTARY NOTES

14. ABSTRACT

A 1:50-scale hydraulic model was used to evaluate hydraulic performance of proposed modifications to the Prado Dam Spillway. Prado Dam is located about 40 miles southeast of Los Angeles, CA, on the Santa Ana River and was completed in 1941. Urbanization in the dam's watershed and an increase in the Probable Maximum Flood design rainfall resulted in a significant increase in design discharges for the flood control project, making it necessary to increase both the dam's storage capacity and the spillway discharge capacity. Spillway rating curves were determined for labyrinth and ogee-crested weirs. Several abutment and approach channel designs were considered. Velocities were measured in the spillway approach channel and in the downstream exit channel. The model was used to determine water-surface elevations in the spillway channel and chute, velocities and surges against the downstream dam embankment, scour potential against the downstream spillway training wall and cutoff wall, and to design toe protection for these downstream features.

15. SUBJECT TERMS

Hydraulic models
Prado Dam
Santa Ana River
Spillways
Labyrinth

16. SECURITY CLASSIFICATION OF:			17. LIMITATION OF ABSTRACT	18. NUMBER OF PAGES	19a. NAME OF RESPONSIBLE PERSON
a. REPORT	b. ABSTRACT	c. THIS PAGE			19b. TELEPHONE NUMBER *(include area code)*
UNCLASSIFIED	UNCLASSIFIED	UNCLASSIFIED		132	